

Bant: Byzantine Antidote via Trial Function and Trust Scores

Gleb Molodtsov^{1*}, Daniil Medyakov^{1*}, Sergey Skorik², Nikolas Khachaturov³, Shahane Tigranyan⁴, Vladimir Aletov¹, Aram Avetisyan², Martin Takáč⁵, Aleksandr Beznosikov¹

¹Basic Research of Artificial Intelligence Laboratory (BRAIn Lab)

²Trusted AI Research Center, RAS

³Russian-Armenian University

⁴Institute for Informatics and Automation Problems, NAS RA

⁵Mohamed bin Zayed University of Artificial Intelligence
gleb.molodcov@gmail.com

Abstract

Recent advancements in machine learning have improved performance while also increasing computational demands. While federated and distributed setups address these issues, their structures remain vulnerable to malicious influences. In this paper, we address a specific threat: Byzantine attacks, wherein compromised clients inject adversarial updates to derail global convergence. We combine the concept of trust scores with trial function methodology to dynamically filter outliers. Our methods address the critical limitations of previous approaches, allowing operation even when Byzantine nodes are in the majority. Moreover, our algorithms adapt to widely used scaled methods such as ADAM and RMSPROP, as well as practical scenarios, including local training and partial participation. We validate the robustness of our methods by conducting extensive experiments on both public datasets and private ECG data collected from medical institutions. Furthermore, we provide a broad theoretical analysis of our algorithms and their extensions to the aforementioned practical setups. The convergence guarantees of our methods are comparable to those of classical algorithms developed without Byzantine interference.

Code — <https://github.com/brain-lab-research/Bant>

1 Introduction

As the field of machine learning expands, researchers are confronted with challenges stemming from increasingly complex models and larger computational demands. To address these issues, distributed and federated learning scenarios have been developed (Kairouz et al. 2021; Konečný et al. 2016; Li et al. 2020). These approaches are crucial for a wide range of tasks (Smith et al. 2017; McMahan et al. 2017; Verbraeken et al. 2020), yet, they introduce several complications. Making the training process multi-node leads to threats related to data storage and transmission. These vulnerabilities manifest as device malfunctions, incorrect data relays, or even initial data corruption (Biggio, Nelson, and Laskov 2012). (Wang et al. 2023) demonstrated how adversarial attacks on data integrity

compromise training. In the midst of them are Byzantine attacks. They occur in networks where certain workers, known as Byzantines, may corrupt data (Blanchard et al. 2017).

This paper specifically examines the threat of Byzantine attacks. We highlight the limitations of existing protection mechanisms, particularly their reliance on strong assumptions. In response, we propose an approach that leverages diverse concepts to develop a universal method, free from these constraints and applicable to practical scenarios.

Setup. We examine the problem often encountered in distributed machine learning, with \mathcal{D}_i representing an unknown distribution of the training sample data on the i -th device:

$$\min_{x \in \mathbb{R}^d} [f(x)] = \frac{1}{n} \sum_{i=1}^n \mathbb{E}_{\xi_i \sim \mathcal{D}_i} [f_{\xi_i}(x)]. \quad (1)$$

We consider a setup involving n workers connected to a central server. These workers are divided into two categories: Good (or Honest) workers, indicated by \mathcal{G} , and Byzantines, indicated by \mathcal{B} . At each iteration t , the sets $\mathcal{G}(t)$ and $\mathcal{B}(t)$ are redefined. This allows the composition of honest and Byzantine workers to vary dynamically over time. At every step, we assume that the set of honest workers $\mathcal{G}(t)$ is nonempty, i.e., $G(t) := |\mathcal{G}(t)| \geq 1$. During training, the number of Byzantines at each iteration remains unknown. This number is used only in the theoretical analysis of the worst-case scenario.

2 Related work

Sophisticated attacks. Methods resistant to Byzantine attacks are crucial for solving optimization problems. Classical methods for distributed optimization, such as SGD (Robbins and Monro 1951; Bottou 2012; Recht and Ré 2013; McMahan et al. 2017), ADAM (Kingma and Ba 2014; Reddi et al. 2020), and SCAFFOLD (Karimireddy et al. 2020), average the received gradients or models. However, they *cease to operate when even a single Byzantine worker appears in the network* (Blanchard et al. 2017). Given the critical importance of this problem, numerous publications have addressed it (Feng, Xu, and Mannor 2014; Damaskinos et al. 2019). Initial approaches proposed robust aggregation rules for data from devices, such as COORDINATE-WISE MEDIAN, TRIMMED MEAN (Yin et al. 2018), KRUM (Blanchard et al. 2017),

*These authors contributed equally.

BULYAN (Mhamdi, Guerraoui, and Rouault 2018). However, sophisticated attacks, such as ALIE (Baruch, Baruch, and Goldberg 2019) or INNER PRODUCT MANIPULATION (Xie, Koyejo, and Gupta 2020), managed to *circumvent these aggregation rules* by shifting the mean they sought to find.

Clipping, Momentum, and Variance Reduction. Aggregation rules are *non-robust even in the absence of attacks*. For example, this occurs in cases of imbalanced classes. This issue was addressed in (Karimireddy, He, and Jaggi 2021b), where CENTERED CLIP (CC) technique was revealed. Additionally, the authors highlighted that the aforementioned Byzantine-robust methods cannot converge with any predetermined accuracy. Given the importance of this issue, they added client momentum, effectively addressing the problem. Another approach to combat the Byzantines is the application of the variance reduction technique. Originally introduced to eliminate irreducible errors in stochastic methods, it was subsequently proposed as an effective way to mitigate the presence of noise in computing stochastic gradient estimators (Gorbunov et al. 2023). Then this idea was developed in (Malinovsky et al. 2023).

These methods demonstrated significant improvements in resilience against Byzantine attacks. However, they also contain notable limitations. First, variance reduction methods exhibit *moderate convergence* in deep learning applications and are prone to *overfitting* (Defazio and Bottou 2019). Additionally, all aforementioned approaches *suffer from the requirement that the majority of devices must be honest*.

Validation tests. Another approach to achieving solutions with any specified accuracy involves techniques such as validation tests (Alistarh, Allen-Zhu, and Li 2018; Allen-Zhu et al. 2020) or computation checks (Gorbunov et al. 2022). Nevertheless, they still require a *majority of honest devices* and rely on *strict assumptions* in the analysis (Alistarh, Allen-Zhu, and Li 2018; Allen-Zhu et al. 2020).

Heterogeneous setup. While much work on the Byzantines focused on the distributed case with homogeneous data, a different series of papers allowed for data heterogeneity (Wu et al. 2020; El-Mhamdi et al. 2021; Data and Diggavi 2021; Nguyen et al. 2022). This corresponds, for example, to the federated setting. Methods were primarily built around robust aggregation (Karimireddy, He, and Jaggi 2021a; Chang et al. 2019; Data and Diggavi 2021; Allouah et al. 2024c; Dorfman, Yehya, and Levy 2024; Allouah et al. 2024b), and variance reduction techniques (Allouah et al. 2023). One of the most advanced approaches assigned coefficients (TRUST SCORES) to clients based on their reliability, using these scores to perform gradient steps (Cao et al. 2021; Yan et al. 2024). These studies provided a foundation for Byzantine-robust optimization in the federated setup, yet suffered from *the aforementioned drawbacks*.

Majority of attackers – trial function. To avoid requiring a majority of honest workers, several methods leverage server-held ground-truth data to filter compromised updates. ZENO (Xie, Koyejo, and Gupta 2019) implements this idea by maintaining a small validation set on the server and scoring each incoming gradient against the gradient computed on that set. We define the function evaluated on the validation set as the TRIAL FUNCTION. As for ZENO, it uses the

trial function to compute trust scores but primarily aggregates updates through simple averaging, down-weighting or excluding devices with very low trust. As a result, its performance depends strongly on the devices that are treated as trusted. (Cao and Lai 2019) proposed an alternative that filters updates by comparing them to a noisy gradient approximation computed on a small dataset, which is effectively equivalent to using a validation set as in ZENO. The idea of using a small server-side dataset to validate local updates was also utilized in SAGEFLOW (Park et al. 2021), which handles majority adversarial clients. However, this method *performs poorly* under an attack ratio of 60%. Moreover, all aggregation schemes that discard clients based on trust scores remain *sensitive to hyperparameters*, as they require threshold choices to label devices as malicious. It requires tuning, and we discuss such instability regarding ZENO in Appendix, Table 7.

The authors of (Xie, Koyejo, and Gupta 2019; Cao and Lai 2019; Park et al. 2021) extended their results to address data heterogeneity by requiring the server to possess a representative sample of all device data. However, this assumption is *unrealistic* in real-world scenarios, undermining the fundamental achievements of federated learning with respect to privacy. Approaches (Guo et al. 2021, 2024) also *accumulate user data* on the server, raising doubts about applicability.

Other shortcomings of previous research. In addition to aforementioned limitations, many studies in this field are predominantly *heuristic and lack rigorous theoretical analysis* (Yan et al. 2024; Guo et al. 2021, 2024; Chang et al. 2019; Xu and Lyu 2020; Rodríguez-Barroso et al. 2022; Nguyen et al. 2022; Zhang et al. 2022; Huang et al. 2024). Moreover, in some studies, the *practical component seems flawed* due to the absence of experiments assessing test accuracy (Gorbunov et al. 2023). Furthermore, theoretical settings often do not align with practical aspects. For instance, in (Cao et al. 2021), *homogeneous data sampling is assumed* while focusing on the federated learning. Besides, the analysis of SAGEFLOW is confined to an *unrealistic strongly convex setup*.

Furthermore, when addressing problems in the distributed or federated setups, local methods (Woodworth, Patel, and Srebro 2020; Khaled, Mishchenko, and Richtárik 2020; Gorbunov, Hanzely, and Richtárik 2021; Nguyen et al. 2022), as well as the partial participation scenario (Yang, Fang, and Liu 2021; Kairouz et al. 2021; Sadiev et al. 2022; Nguyen et al. 2022), is typically assumed. While these options improve computational efficiency and reduce data transmission overhead, only a few studies (Data and Diggavi 2021; Malinovsky et al. 2023; Allouah et al. 2024a; Dorfman, Yehya, and Levy 2024) address these aspects, whereas the majority of works do not. In addition, research is often limited to SGD-like methods, *neglecting adaptive algorithms* such as ADAM (Kingma and Ba 2014) and RMSPROP (Tieleman and Hinton 2012), which are widely used in machine learning. Given the challenges and gaps identified in the existing literature, we aim to advance the trust score methodology and trial function concept to enhance defense mechanisms.

Contributions

Our main results are summarized as follows.

- **Combine trust scores with the trial function approach.**

Trial loss is based on a subset of the training data stored on the server. Weights are assigned to the gradients sent from each device based on the extent to which these gradients reduce the trial function in each iteration. In real networks, honest stochastic gradients may increase the target loss. We account for this by incorporating weights from the previous epoch and a momentum parameter for more stable convergence.

- **Milder assumptions.** Unlike most existing studies, our approach requires only one reliably honest worker instead of a majority. Moreover, unlike previous trial function-based methods that assume data homogeneity (Cao et al. 2021; Gorbunov et al. 2022), our algorithms operate under the more realistic assumption of data similarity in federated learning.

- **Extensions.** We adapt our algorithms to important scenarios that are often overlooked in research.

- (a) **Local methods.** In our work, we propose utilizing Local SGD to address the high communication costs typically associated with distributed training.
- (b) **Partial participation.** Our algorithms incorporate the option for partial participation. Thus, devices may not participate in every learning step, and the attackers may vary across iterations.
- (c) **Adaptive methods.** In this work, we extend our analysis to adaptive algorithms (e.g., ADAM and RMSPROP), which are widely used in machine learning.

- **Convergence guarantees.** We prove upper bounds on the convergence rates of the main methods and extensions presented for the smooth problem under various assumptions regarding the convexity of the target function (strong convexity, convexity, non-convexity).

- **Experiments.** We demonstrate the superiority of our method in both previously studied attacks and scenarios where alternative methods fail. Our experiments are performed on the CIFAR-10 dataset and real ECG data, utilizing RESNET-18 and RESNET-1D18 neural networks, respectively. Additionally, we validate our approach to Learning-to-Rank tasks by training a Transformer-based ranking model.

3 Methodology

To tackle Byzantine attacks, we introduce a pivotal component of our methodology – a trial loss function \hat{f} . In the homogeneous setting (1) with $\mathcal{D}_i = \mathcal{D}$, we take a separate sample from \mathcal{D} , but in a smaller volume than the entire dataset. The trial function calculated on this data forms \hat{f} . Under the heterogeneous data scenario, we sample from the distribution \mathcal{D}_1 on the server to obtain delayed data for \hat{f} (indexing the server does not violate generality; we further consider it a device with index 1). Formally, we can write the trial function as $\hat{f}(x) = \frac{1}{N} \sum_{i=1}^N f_1(x, \xi_i)$, where N is the number of samples in \hat{f} . This function is stored on the server (obviously, an honest device). The sample distribution of the trial function is similar to the entire distribution \mathcal{D} due to the property of data similarity. Besides, in practical scenarios, a server may not

be able to share the entire dataset, providing only a sample of size N . Depending on the size of this sample, f_1 may differ from \hat{f} . Nevertheless, the larger the volume of this delayed sample, the closer \hat{f} approximates the function f_1 (discussed in Lemma C.1 in Appendix). A small public or synthetic trial dataset is a practical assumption in Byzantine-robust federated learning. Methods such as FLTrust (Cao et al. 2021) and Zeno (Xie, Koyejo, and Gupta 2019) utilize such datasets. Here we outline the assumptions under which we establish the convergence rates.

Assumption 3.1. The function \hat{f} is L -smooth, i.e., $\|\nabla \hat{f}(x) - \nabla \hat{f}(y)\| \leq L\|x - y\|$ for any $x, y \in \mathbb{R}^d$.

Assumption 3.2. The function \hat{f} is:

- (a) **μ -strongly convex** if for all $x, y \in \mathbb{R}^d$, it satisfies: $\hat{f}(y) \geq \hat{f}(x) + \langle \nabla \hat{f}(x), y - x \rangle + \frac{\mu}{2}\|y - x\|^2$.
- (b) **convex** if for all $x, y \in \mathbb{R}^d$, it satisfies: $\hat{f}(y) \geq \hat{f}(x) + \langle \nabla \hat{f}(x), y - x \rangle$.
- (c) **non-convex** if it has at least one (not necessarily unique) minimum, i.e., $\hat{f}(\hat{x}^*) = \inf_{x \in \mathbb{R}^d} \hat{f}(x) > -\infty$.

Assumption 3.3. Each worker $i \in \mathcal{G}(t)$ has access to an independent and unbiased stochastic gradient with $\mathbb{E}[g_i(x, \xi_i)] = \nabla f_i(x)$ and its variance is bounded by σ^2 :

$$\mathbb{E}\|g_i(x, \xi_i) - \nabla f_i(x)\|^2 \leq \sigma^2, \quad \text{for all } x \in \mathbb{R}^d.$$

We also assume data similarity – a common premise for ensuring convergence in Byzantine literature (Karimireddy, He, and Jaggi 2021a; Gorbunov et al. 2023; Yan et al. 2024).

Assumption 3.4. We assume data similarity in the following way: good clients possess (δ_1, δ_2) -heterogeneous local loss functions for some $\delta_1 \geq 0$ and $\delta_2 \geq 0$, such that for all $x \in \mathbb{R}^d$, the following holds:

$$\|\nabla f_i(x) - \nabla f(x)\|^2 \leq \delta_1 + \delta_2 \|\nabla f(x)\|^2 \quad \forall i \in \mathcal{G}(t).$$

In over-parameterized models, introducing a positive δ_2 can sometimes reduce the value of δ_1 . Several studies have explored heterogeneous scenarios in which honest workers handle distinct local functions (Wu et al. 2020; Karimireddy, He, and Jaggi 2021a). Note that achieving a predefined accuracy becomes feasible in the presence of Byzantines only when heterogeneity is limited to δ_2 -bounded settings ($\delta_1 = 0$) (Karimireddy, He, and Jaggi 2021a). Under a more general assumption, which we utilize, the term with δ_1 inadvertently appears in the estimate.

Assumption 3.5. Byzantine workers are assumed to be omniscient, i.e., they have access to the computations performed by the other workers.

4 Algorithms and Convergence Analysis

4.1 First method: Bant

In this section, we introduce our method, termed Byzantine ANTidote (Bant) – Algorithm 1. Our method relies on the core idea of assigning trust scores to devices. We integrate this with the concept of a trial function by aggregating the stochastic gradients g_i^t of devices with their respective

Algorithm 1 Bant

```

1: Input: Starting point  $x^0 \in \mathbb{R}^d, \omega_i^0 = 1/n \forall i$ 
2: Parameters: Stepsize  $\gamma > 0$ , momentum  $\beta \in (0, 1]$ 
3: for  $t = 0, 1, 2, \dots, T - 1$  do
4:   Server sends  $x^t$  to each worker
5:   for all workers  $i = 1, 2, \dots, n$  in parallel do
6:     Generate  $\xi_i^t$  independently
7:     Compute stochastic gradient  $g_i^t = g_i(x^t, \xi_i^t)$ 
8:     Send  $g_i^t$  to server
9:   end for
10:   $\omega_i^t = (1 - \beta)\omega_i^{t-1} + \beta \frac{[\hat{f}(x^t) - \hat{f}(x^t - \gamma g_i^t)]_0}{\sum_{j=1}^n [\hat{f}(x^t) - \hat{f}(x^t - \gamma g_j^t)]_0}$ 
11:  if each  $[\hat{f}(x^t) - \hat{f}(x^t - \gamma g_i^t)]_0 = 0$  then
12:     $\omega_i^t = (1 - \beta)\omega_i^{t-1} + \beta \frac{1}{n}$ 
13:  end if
14:   $x^{t+1} = x^t - \gamma \sum_{i=1}^n \mathbb{I}_{[\hat{f}(x^t) - \hat{f}(x^t - \gamma g_i^t)]_0 > 0} \omega_i^t g_i^t$ 
15: end for
16: Output:  $\frac{1}{T} \sum_{t=0}^{T-1} x^t$ 

```

weights w_i^t . To find the latter, we first calculate the contribution coefficients for each worker i at each step: $\theta_i^t = \hat{f}(x^t) - \hat{f}(x^t - \gamma g_i^t)$. These coefficients demonstrate how the i -th device affects convergence. If $\theta_i^t > 0$, the stochastic gradient minimizes trial loss and is assigned a weight. Otherwise, it is assigned a weight of zero (Line 10 in Algorithm 1). We ensure non-negativity with $[\theta_i^t]_0 = \max\{\theta_i^t, 0\}$ and normalize to provide a total weight of 1.

To address stochastic gradient instability, which can increase the loss function, we introduce a momentum parameter for the weights (Line 10). If all gradients increase the loss, they are assigned zero weights, thereby stopping the minimization process even in the absence of Byzantine devices in the network.

By adding momentum, we achieve a more stable convergence in practice. This allows previous favorable gradients to influence current weights, even if a device receives a small or zero weight in the current iteration. An indicator in the step (Line 14) ensures that gradients maximizing trial loss are ignored, thereby guaranteeing minimization at each step. We also define $G = \min_t G(t)$ as the minimum, taken over all iterations, of the number of honest workers at each iteration. Now we are ready to proceed with the theoretical results.

Theorem 4.1. *Under Assumptions 3.1, 3.2(b), 3.3, 3.4 with $\delta_2 \leq \frac{1}{12}$, 3.5, for solving the problem (1), after T iterations of Algorithm 1 with $\gamma \leq \frac{1}{13L}$, the following holds:*

$$\frac{1}{T} \sum_{t=0}^{T-1} \mathbb{E} \|\nabla f(x^t)\|^2 \leq \frac{\mathbb{E}[\hat{f}(x^0) - \hat{f}(\hat{x}^*)]}{\gamma T} \cdot \frac{4n}{\beta G} + 6L\gamma\sigma^2 + 3\delta_1 + 4\zeta(N).$$

The first two terms in the result of Theorem 4.1 replicate the findings from the standard SGD analysis, up to constant factors. The last term, which depends on $\zeta(N)$, is of special interest. The function $\zeta(N)$ reflects the relationship between f_1 and the trial loss \hat{f} and represents an approximation error. The dependence of $\zeta(N)$ on N is natural: the larger

N , the smaller the error becomes. More precisely, for our function f , this error is $\zeta(N) = \tilde{\mathcal{O}}\left(\frac{1}{N}\right)$ (see Lemma C.1 in Appendix). Although this error degrades convergence, it is common in machine learning tasks. In particular, the original learning problem, like (1), is often replaced by its Monte Carlo approximation (Johnson and Zhang 2013; Defazio, Bach, and Lacoste-Julien 2014; Allen-Zhu 2018), and the resulting problem is commonly referred to as empirical risk minimization (Shalev-Shwartz and Ben-David 2014). This replacement also leads to an error. Finally, δ_1 is a typical term that represents data similarity (Assumption 3.4) and is unavoidable in the presence of Byzantines (Wu et al. 2020; Karimireddy, He, and Jaggi 2021a; Gorbunov et al. 2022). Since our approach resembles ZENO (Xie, Koyejo, and Gupta 2019) in its use of the trial function, we should mention that we found some issues in their proofs. In Theorem 1 of (Xie, Koyejo, and Gupta 2019), the authors incorrectly apply the expectation operator when deriving their recursion. They sample a trial function from the full dataset and use $\mathbb{E}[\hat{f}^t(x)] = f(x)$, which is valid for a random point. However, in the case of point x^{t+1} , a mistake was made. Since they sample \hat{f}^t in every iteration, the point x^{t+1} depends on the sample \hat{f}^t , leading to $\mathbb{E}[\hat{f}^t(x^{t+1}) \mid x^t] \neq f(x^{t+1})$. By carrying the conditional expectation without considering the full expectation, it becomes impossible to enter the recursion and achieve convergence regarding the function f itself. In turn, we explicitly bound the gradient discrepancy $|\nabla f_1(x^t) - \nabla \hat{f}(x^t)|$, leveraging trial function sampling to ensure convergence as the sample size increases. This difference in Theorem 4.1 is represented by the discussed $\zeta(N)$.

Corollary 4.2. *Under the assumptions of Theorem 4.1, for solving the problem (1), after T iterations of Algorithm 1 with*

$\gamma \leq \min\left\{\frac{1}{13L}, \frac{\sqrt{2\mathbb{E}[\hat{f}(x^0) - \hat{f}(\hat{x}^*)]n}}{\sigma\sqrt{3LG\beta T}}\right\}$, *the following holds:*

$$\frac{1}{T} \sum_{t=1}^{T-1} \mathbb{E} \|\nabla f(x^t)\|^2 = \mathcal{O}\left(\frac{\mathbb{E}[\hat{f}(x^0) - \hat{f}(\hat{x}^*)]Ln}{\beta GT} + \frac{\sigma \cdot \sqrt{\mathbb{E}[\hat{f}(x^0) - \hat{f}(\hat{x}^*)] \cdot Ln}}{\sqrt{\beta GT}} + \delta_1 + \zeta(N)\right).$$

If we consider the first two terms in the convergence estimates from Corollary 4.2, the only difference from the classical SGD convergence results (Moulines and Bach 2011; Stich 2019) is the additional factor $\frac{n}{G}$, however, the rate is asymptotically optimal. The proofs and results for the strongly-convex objective can be found in Appendix D.

4.2 Improving theoretical estimates: AutoBant

Despite practical advantages of Bant, it has some theoretical imperfections related to the mechanism of assigning trust scores. While parameter β helps honest clients maintain trust scores despite occasional bad gradients, it also enables Byzantine devices to retain their weights during attacks. To combat this, we add an indicator for the trial function reduction (the indication of the device being Byzantine at the considered iteration). However, this limits the theoretical applicability of the method to non-convex problems prevalent in modern

Algorithm 2 AutoBant

```

1: Input: Starting point  $x^0 \in \mathbb{R}^d$ 
2: Parameters: Stepsize  $\gamma > 0$ , error accuracy  $\delta$ 
3: for  $t = 0, 1, 2, \dots, T - 1$  do
4:   Server sends  $x^t$  to each worker
5:   for all workers  $i = 0, 1, 2, \dots, n$  in parallel do
6:     Generate  $\xi_i^t$  independently
7:     Compute stochastic gradient  $g_i^t = g_i(x^t, \xi_i^t)$ 
8:     Send  $g_i^t$  to server
9:   end for
10:   $\omega^t \approx \arg \min_{\omega \in \Delta_1^n} \hat{f}(x^t - \gamma \sum_{i=1}^n \omega_i g_i^t)$ 
11:   $x^{t+1} = x^t - \gamma \sum_{i=1}^n \omega_i^t g_i^t$ 
12: end for
13: Output:  $\frac{1}{T} \sum_{t=0}^{T-1} x^t$ 

```

machine learning. To resolve these limitations, we present our second method, called AUxiliary Trial Optimization for Byzantines ANTidote (AutoBant), Algorithm 2.

The idea of assigning weights to devices as part of the optimization process has gained popularity in federated learning. For instance, in many works, it leads to improved solution quality (Li et al. 2023; Tupitsa et al. 2024), or it is used in more specific settings, such as personalized learning (Mishchenko et al. 2023). We propose adapting this to Byzantine-robust learning by optimizing \hat{f} regarding weights calculated after each algorithmic step (Line 10).

To solve the minimization problem, we can use various methods, e.g., Mirror Descent (Beck and Teboulle 2003; Allen-Zhu and Orecchia 2014):

$$\omega^{k+1} = \arg \min_{\omega \in \Delta_1^n} \left\{ \eta \left\langle \nabla_{\omega} \hat{f} \left(x^t - \gamma \sum_{i=1}^n \omega_i^k g_i^t \right), \omega \right\rangle + \mathcal{KL}(\omega \| \omega^k) \right\},$$

where $\mathcal{KL}(\cdot \| \cdot)$ denotes the Kullback-Leibler divergence. The error in solving this is bounded by δ :

$$\left| \min_{\omega \in \Delta_1^n} \hat{f} \left(x^t - \gamma \sum_{i=1}^n \omega_i g_i^t \right) - \hat{f} \left(x^t - \gamma \sum_{i=1}^n \omega_i^t g_i^t \right) \right| \leq \delta.$$

After solving this auxiliary problem, we produce an actual model update using the optimized weights (Line 11). In light of the proposed method, the question of the cost of implementing such an optimal scheme comes to the forefront. Note that the computational complexity of solving this subproblem at each iteration is only $\mathcal{O}(\log n / \delta^2)$ (Beck and Teboulle 2003), which is not critical. For the following theoretical analysis, we assume the minimization subproblem can be solved to arbitrary precision, neglecting errors in our estimates. In practice, however, the convergence rate is directly influenced by the accuracy of this solution. A numerical study of this effect is presented in Table 6 in Appendix. Now we are ready to present the main theoretical result of this section.

Theorem 4.3. *Under Assumptions 3.1, 3.2(c), 3.3, 3.4 with $\delta_2 < \frac{1}{12}$, 3.5, for solving the problem 1, after T iterations of*

Algorithm 2 with $\gamma \leq \frac{1}{13L}$, the following holds:

$$\frac{1}{T} \sum_{t=0}^{T-1} \mathbb{E} \|\nabla f(x^t)\|^2 \leq \frac{4\mathbb{E}[\hat{f}(x^0) - \hat{f}(\hat{x}^*)]}{\gamma T} + 3\delta_1 + \frac{6L\gamma}{G} \sigma^2 + 2\zeta(N).$$

Corollary 4.4. *Under assumptions of Theorem 4.3, for solving the problem (1), after T iterations of Algorithm 2 with*

$$\gamma \leq \min \left\{ \frac{1}{13L}, \frac{\sqrt{2\mathbb{E}[\hat{f}(x^0) - \hat{f}(\hat{x}^*)]G}}{\sigma\sqrt{3LT}} \right\}, \text{ the following holds:}$$

$$\frac{1}{T} \sum_{t=0}^{T-1} \mathbb{E} \|\nabla f(x^t)\|^2 = \mathcal{O} \left(\frac{\mathbb{E}[\hat{f}(x^0) - \hat{f}(\hat{x}^*)]L}{T} + \delta_1 + \zeta(N) + \frac{\sigma\sqrt{\mathbb{E}[\hat{f}(x^0) - \hat{f}(\hat{x}^*)]L}}{\sqrt{TG}} \right).$$

Detailed proofs are presented in Appendix E. In the first and second terms, we observe that the method converges in the same pace as the standard SGD only with honest workers (Ghadimi and Lan 2013; Ghadimi, Lan, and Zhang 2016). It turns out that we throw out all Byzantines, and this result is nearly optimal and unimprovable. As in Algorithm 1, a term responsible for the approximation error $\zeta(N)$ appears. Compared with the result of Corollary 4.2, we improve the rate through a more advanced aggregation mechanism. We remove the factor $\frac{n}{\beta G}$ from the main term and achieve a decrease in variance by a factor of G . However, an additional error δ is incurred, which can be viewed as a trade-off for solving the subproblem. Furthermore, our approach applies to a broader class of non-convex functions. Addressing the dependence of the stepsize on the number of Byzantines, this choice is based on the theoretical analysis of the worst-case scenario, considering the number of Byzantines. If this number is unknown, setting the minimum possible value of 1 eliminates this dependency.

5 Extensions

Byzantine robust optimization, as discussed earlier, lacks a solid theoretical foundation in several real-world settings. We address this gap. This section provides a brief overview of the scenarios to which we extend our analysis.

5.1 Local methods

The main idea is that each device performs a predefined number of local steps. Then the aggregation of gradients and the mutual updates of model parameters, initialized by the server, take place. This reduces the number of communication rounds. However, it affects the convergence proportionally to the length of the communication round. Complete updates are performed only at specific iterations: $t = t_{k,l}$ for some $k = 0, \lfloor T/l \rfloor$. During the remaining iterations, we perform local updates using the rule $x_i^{t+1} = x_i^t - \gamma g_i^t$. This approach ensures that communication overhead is minimized while maintaining efficient convergence.

Algorithm 3 Scaled AutoBant (part)

10: $\omega^t \approx \arg \min_{\omega \in \Delta_1^n} \hat{f} \left(x^t - \gamma (\hat{P}^t)^{-1} \sum_{i=1}^n \omega_i g_i^t \right)$
 11: $x^{t+1} = x^t - \gamma (\hat{P}^t)^{-1} \sum_{i=1}^n \omega_i^t g_i^t$

Algorithm 4 SimBant (part)

10: $\omega_i^t = (1 - \beta) \omega_i^{t-1} + \beta \frac{\text{sim}(m(x^t - \gamma g_i^t, \hat{D}), m(x^t - \gamma g_1^t, \hat{D}))}{\sum_{j=1}^n \text{sim}(m(x^t - \gamma g_j^t, \hat{D}), m(x^t - \gamma g_1^t, \hat{D}))}$
 11: $x^{t+1} = x^t - \gamma \sum_{i=1}^n \omega_i^t g_i^t$

5.2 Partial participation

It occurs when only a subset of clients actively participates in the training process during each communication round (Yang, Fang, and Liu 2021), allowing clients to join or leave the system. This approach is beneficial in scenarios such as mobile edge computing. However, it poses challenges such as incomplete model updates and potential degradation in model performance due to missed contributions from inactive clients (Wang and Ji 2022; Li et al. 2022). Our methods adapt to the scenario of partial participation by assigning trust scores to devices explicitly participating in training during the considered iteration. Furthermore, it is crucial to account for the minimum number of nodes participating in training across all iterations. Specifically, we analyze $\tilde{G}(t) = \min_{t \leq T} G(t)$, where $G(t)$ denotes the set of active honest workers at iteration t .

5.3 Scaled methods

Adaptive methods such as ADAM (Kingma and Ba 2014) and RMSPROP (Tieleman and Hinton 2012) have become widely popular due to their superior performance compared to standard SGD-like methods. We propose corresponding methods that utilize a diagonal preconditioner $(\hat{P}^t)^{-1}$, which scales a gradient to $(\hat{P}^t)^{-1} g_i^t$, and the step is executed using this scaled gradient. We present the part of Scaled AutoBant based on Algorithm 2. The estimates obtained are identical to those derived from the scaled methods in the non-Byzantine regime. All details can be found in Appendix F.

5.4 Finding scores from validation

Another interesting direction to obtain trust scores w_i is to calculate *similarity between the logits* obtained on the server and on the device. The trust score for the i -th device is the function $\alpha_i \rightarrow \text{sim}(m(x^t - \gamma g_i^t, \hat{D}), m(x^t - \gamma g_1^t, \hat{D}))$. Based on Algorithm 2, we present a part of the SimBant algorithm (see details in Appendix I).

6 Experiments

To evaluate the performance of the proposed methods, we conduct experiments on several benchmarks.

- **Classification Task:** We first validate our approach on the public dataset. We use RESNET-18 (He et al. 2016) for CIFAR-10 (Krizhevsky, Hinton et al. 2009) classification.

- **ECG Abnormality Detection:** In multi-hospital collaborations, labels are derived from expert annotations and automated pipelines, making attacks and subtle manipulations practical threats that can compromise patient safety. We obtain a proprietary dataset of 12-lead digital electrocardiograms (ECG) from five hospitals and train RESNET1D18 model for ECG abnormality detection.
- **Learning-to-Rank (Recommender Systems):** We conducted a series of experiments applied to the Learning-to-Rank (LTR) task, common in information retrieval and recommendation systems. We adopt the Transformer architecture (Vaswani et al. 2017), evaluating its performance on the dataset WEB30K (Qin and Liu 2013) under attacks.

We consider various Byzantine attacks to test our methods.

- **Label Flipping.** Attackers send gradients based on the loss calculated with randomly flipped labels.
- **Sign Flipping.** Attackers send the opposite gradient.
- **Random Gradients.** Attackers send random gradients.
- **IPM (Inner Product Manipulation).** Attackers send the average gradient of all honest clients multiplied by a factor of $-\kappa$ (we set κ to 0.5) (Xie, Koyejo, and Gupta 2020).
- **ALIE (A Little Is Enough).** Attackers average their gradients and scale the standard deviation to mimic the majority (Baruch, Baruch, and Goldberg 2019).

We define the number of Byzantine clients as a percentage of the total number of clients, and specify it in the attack name. We train Bant and AutoBant in the scaled version (see Section 5.3) with the ADAM preconditioner. We include SimBant, ADAM, and the existing methods: ZENO (Xie, Koyejo, and Gupta 2019), RECESS (Yan et al. 2024), CENTERED CLIP (Karimireddy, He, and Jaggi 2021b), SAFE-GUARD (Allen-Zhu et al. 2020), VR MARINA (Gorbunov et al. 2023) and FLTRUST (Cao et al. 2021). For CENTERED CLIP, we added techniques FIXING BY MIXING (Allouah et al. 2023) and BUCKETING (Karimireddy, He, and Jaggi 2021a). The methods were trained on the CIFAR-10 and ECG datasets for 200 and 150 rounds, respectively.

CIFAR-10 and ECG setups. For the CIFAR-10 dataset, we divide the data among 10 and 100 (see Appendix A.3) clients. We consider a homogeneous split with 5,000 images per client, as well as a Dirichlet split with $\alpha = 0.5$ and $\alpha = 1$. We use 500 separate samples to form \hat{f} . For the ECG dataset, we consider five clients, each representing a hospital with 10,000 and 20,000 records. To form \hat{f} on ECG, we use 100 samples from the publicly-available external PTB-XL dataset (Wagner et al. 2020). We solve the task of multiclass classification for CIFAR-10 and binary classification of 4 heart abnormalities for ECG: Atrial Fibrillation (AFIB), First-degree AV Block (1AVB), Premature Ventricular Complex (PVC), and Complete Left Bundle Branch Block (CLBBB). The accuracy for all considered attacks on the CIFAR-10 test dataset are illustrated in Figure 1. To further stress test the proposed methods, we consider the most strong Byzantine attacks under heterogeneous setups, as well as homogeneous split under 100 clients. Figure 2 shows the accuracy plots of the proposed methods with Dirichlet $\alpha = 0.5$ for the ALIE and Random Gradients attacks. More details are presented in the Appendix.

Algorithm	Without Attack		Label Flipping (60%)		Random Gradients (60%)		IPM (80%)		ALIE (40%)	
	G-mean	f1-score	G-mean	f1-score	G-mean	f1-score	G-mean	f1-score	G-mean	f1-score
ADAM	0.956±0.017	0.811±0.016	0.262±0.023	0.041±0.019	0.348±0.011	0.126±0.016	0.197±0.027	0.036±0.015	0.125±0.011	0.123±0.020
FLTRUST	0.952±0.020	0.800±0.019	0.952±0.016	0.753±0.011	0.617±0.020	0.174±0.019	0.061±0.017	0.125±0.015	0.017±0.013	0.123±0.018
RECESS	0.949±0.016	0.783±0.019	0.366±0.019	0.128±0.020	0.593±0.020	0.163±0.020	0.493±0.019	0.112±0.015	0.450±0.014	0.127±0.018
ZENO	0.921±0.012	0.787±0.014	0.014±0.017	0.110±0.015	0.163±0.010	0.089±0.014	0.102±0.012	0.066±0.018	0.010±0.009	0.091±0.011
CC	0.949±0.020	0.772±0.019	0.285±0.018	0.114±0.020	0.580±0.019	0.155±0.020	0.084±0.019	0.014±0.020	0.530±0.018	0.154±0.020
CC+FBM	0.954±0.016	0.808±0.020	0.840±0.019	0.716±0.014	0.562±0.011	0.151±0.020	0.027±0.018	0.123±0.015	0.876±0.017	0.594±0.013
CC+BUCKETING	0.947±0.013	0.790±0.018	0.829±0.011	0.708±0.020	0.570±0.012	0.164±0.018	0.035±0.020	0.118±0.012	0.870±0.019	0.587±0.014
SAFEGUARD	0.957±0.020	0.821±0.019	0.107±0.012	0.123±0.020	0.258±0.011	0.124±0.019	0.951±0.018	0.082±0.020	0.010±0.009	0.123±0.012
VR MARINA	0.010±0.014	0.120±0.010	0.027±0.018	0.123±0.020	0.176±0.012	0.103±0.013	0.127±0.013	0.079±0.019	0.012±0.010	0.108±0.013
Bant	0.953±0.017	0.830±0.020	0.956±0.016	0.777±0.020	0.948±0.018	0.809±0.020	0.946±0.020	0.676±0.015	0.947±0.018	0.770±0.020
AutoBant	0.953±0.019	0.781±0.020	0.790±0.020	0.276±0.020	0.946±0.019	0.748±0.018	0.942±0.020	0.690±0.020	0.892±0.016	0.585±0.020
SimBant	0.956±0.020	0.790±0.018	0.949±0.020	0.774±0.020	0.945±0.020	0.712±0.018	0.955±0.020	0.783±0.018	0.946±0.019	0.705±0.020

Table 1: RESNET1D18 on ECG (AFIB) for Byzantine-tolerance techniques under various attacks.

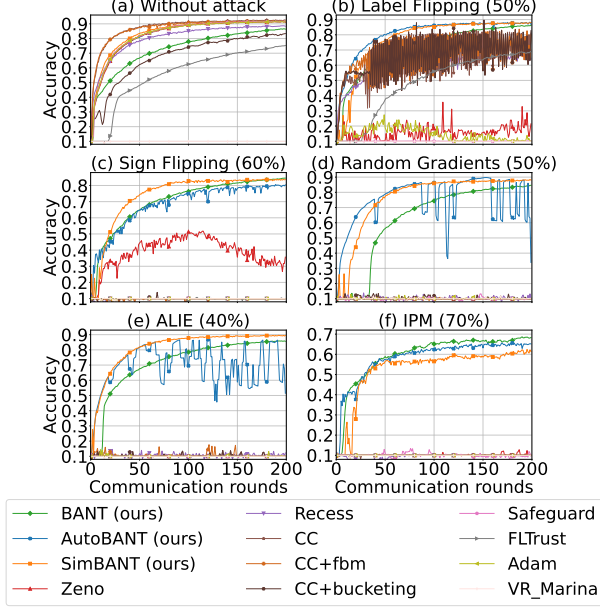


Figure 1: Test accuracy, ResNet18 on CIFAR-10.

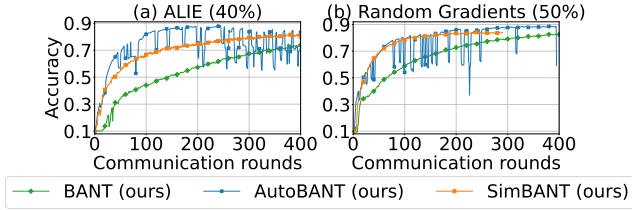


Figure 2: Test accuracy, ResNet18 on Dirichlet.

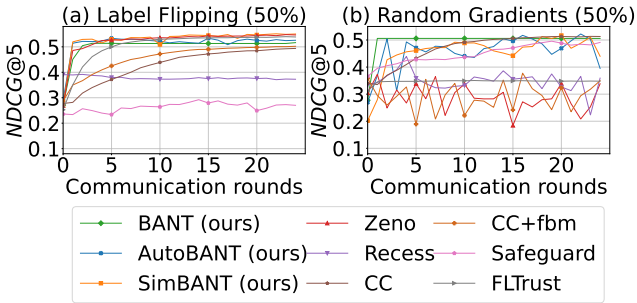


Figure 3: Test NDCG@5, Transformer on LTR task.

To assess model performance on the ECG data, we use the G-mean (the square root of sensitivity multiplied by specificity) and the f1-score metrics. Table 1 summarizes the results of the methods for the AFIB disease classification. Detailed results for all considered abnormalities across multiple metrics are presented in Tables 9-12 in Appendix.

Unlike previously established techniques, our methods exhibit robustness against all Byzantine attacks across different benchmarks. We note that AutoBant performs slightly worse than Bant and SimBant under Random Gradients and ALIE attacks. This occurs due to solving an auxiliary subproblem (Line 10 in Algorithm 2) using MIRROR DESCENT with KL-divergence. According to its properties, the algorithm assigns small but non-zero weights to Byzantines, contributing to unstable convergence, while Bant and SimBant lack this drawback. We analyze the required number of such iterations and the size of \hat{f} in Appendix A.4. RECESS and FLTRUST leverage the concept of trust scores but rely on a majority of honest devices. As a result, this leads to a significant decrease in the final quality under the majority of Byzantines in Random Gradients, IPM, and ALIE attacks that simulate a malicious majority. Similar behavior is observed for the CC and SAFEGUARD methods, which suffer from sensitivity to parameter tuning. FIXING BY MIXING and BUCKETING increase Label Flipping and ALIE metrics for ECG setup, but do not provide reliable convergence for all cases. ZENO exploits the trial function approach, however, it relies on the number of Byzantine clients. We address this in Appendix, Table 7.

Learning-to-Rank. In the LTR task, the goal is to learn a ranking function over query-document pairs. Each pair is represented using standard frequency-based feature vectors. The target labels correspond to human-assigned relevance scores, reflecting how well a document matches a given query. This setting provides a natural context for exploring Byzantine robustness. For example, label flipping attacks arise from this scenario. Annotators may provide inconsistent or biased relevance assessments. Such inconsistencies reflect real-world challenges in supervised learning from human-generated data. The quality of labeling is influenced by personal biases or mistakes. We compare our methods against the baselines from prior experiments – under the most severe attacks (Label Flipping 50%, Random Gradients 50%), see Figure 3.

References

- Alistarh, D.; Allen-Zhu, Z.; and Li, J. 2018. Byzantine stochastic gradient descent. *Advances in neural information processing systems*, 31.
- Allen-Zhu, Z. 2018. Katyusha: The first direct acceleration of stochastic gradient methods. *Journal of Machine Learning Research*, 18(221): 1–51.
- Allen-Zhu, Z.; Ebrahimiaghazani, F.; Li, J.; and Alistarh, D. 2020. Byzantine-Resilient Non-Convex Stochastic Gradient Descent. In *International Conference on Learning Representations*.
- Allen-Zhu, Z.; and Orecchia, L. 2014. Linear coupling: An ultimate unification of gradient and mirror descent. *arXiv preprint arXiv:1407.1537*.
- Allouah, Y.; Farhadkhani, S.; Guerraoui, R.; Gupta, N.; Pinot, R.; Rizk, G.; and Voitovych, S. 2024a. Byzantine-Robust Federated Learning: Impact of Client Subsampling and Local Updates. In *Forty-first International Conference on Machine Learning*. PMLR.
- Allouah, Y.; Farhadkhani, S.; Guerraoui, R.; Gupta, N.; Pinot, R.; and Stephan, J. 2023. Fixing by mixing: A recipe for optimal byzantine ml under heterogeneity. In *International Conference on Artificial Intelligence and Statistics*, 1232–1300. PMLR.
- Allouah, Y.; Guerraoui, R.; Gupta, N.; Jellouli, A.; Rizk, G.; and Stephan, J. 2024b. Boosting Robustness by Clipping Gradients in Distributed Learning. *arXiv preprint arXiv:2405.14432*.
- Allouah, Y.; Guerraoui, R.; Gupta, N.; Pinot, R.; and Rizk, G. 2024c. Robust distributed learning: tight error bounds and breakdown point under data heterogeneity. *Advances in Neural Information Processing Systems*, 36.
- Baruch, G.; Baruch, M.; and Goldberg, Y. 2019. A little is enough: Circumventing defenses for distributed learning. *Advances in Neural Information Processing Systems*, 32.
- Beck, A.; and Teboulle, M. 2003. Mirror descent and nonlinear projected subgradient methods for convex optimization. *Operations Research Letters*, 31(3): 167–175.
- Biggio, B.; Nelson, B.; and Laskov, P. 2012. Poisoning attacks against support vector machines. *arXiv preprint arXiv:1206.6389*.
- Blanchard, P.; El Mhamdi, E. M.; Guerraoui, R.; and Stainer, J. 2017. Machine learning with adversaries: Byzantine tolerant gradient descent. *Advances in neural information processing systems*, 30.
- Bottou, L. 2012. Stochastic gradient descent tricks. In *Neural Networks: Tricks of the Trade: Second Edition*, 421–436. Springer.
- Cao, X.; Fang, M.; Liu, J.; and Gong, N. Z. 2021. FLTrust: Byzantine-robust Federated Learning via Trust Bootstrapping. In *ISOC Network and Distributed System Security Symposium (NDSS)*.
- Cao, X.; and Lai, L. 2019. Distributed gradient descent algorithm robust to an arbitrary number of byzantine attackers. *IEEE Transactions on Signal Processing*, 67(22): 5850–5864.
- Chang, H.; Shejwalkar, V.; Shokri, R.; and Houmansadr, A. 2019. Cronus: Robust and heterogeneous collaborative learning with black-box knowledge transfer. *arXiv preprint arXiv:1912.11279*.
- Damaskinos, G.; El-Mhamdi, E.-M.; Guerraoui, R.; Guirguis, A.; and Rouault, S. 2019. Aggregathor: Byzantine machine learning via robust gradient aggregation. *Proceedings of Machine Learning and Systems*, 1: 81–106.
- Data, D.; and Diggavi, S. 2021. Byzantine-resilient high-dimensional SGD with local iterations on heterogeneous data. In *International Conference on Machine Learning*, 2478–2488. PMLR.
- Defazio, A.; Bach, F.; and Lacoste-Julien, S. 2014. SAGA: A fast incremental gradient method with support for non-strongly convex composite objectives. *Advances in neural information processing systems*, 27.
- Defazio, A.; and Bottou, L. 2019. On the ineffectiveness of variance reduced optimization for deep learning. *Advances in Neural Information Processing Systems*, 32.
- Dorfman, R.; Yehya, N. A.; and Levy, K. Y. 2024. Dynamic Byzantine-Robust Learning: Adapting to Switching Byzantine Workers. In *Forty-first International Conference on Machine Learning*. PMLR.
- El-Mhamdi, E. M.; Farhadkhani, S.; Guerraoui, R.; Guirguis, A.; Hoang, L.-N.; and Rouault, S. 2021. Collaborative learning in the jungle (decentralized, byzantine, heterogeneous, asynchronous and nonconvex learning). *Advances in neural information processing systems*, 34: 25044–25057.
- Feng, J.; Xu, H.; and Mannor, S. 2014. Distributed robust learning. *arXiv preprint arXiv:1409.5937*.
- Ghadimi, S.; and Lan, G. 2013. Stochastic first-and zeroth-order methods for nonconvex stochastic programming. *SIAM journal on optimization*, 23(4): 2341–2368.
- Ghadimi, S.; Lan, G.; and Zhang, H. 2016. Mini-batch stochastic approximation methods for nonconvex stochastic composite optimization. *Mathematical Programming*, 155(1): 267–305.
- Gorbunov, E.; Borzunov, A.; Diskin, M.; and Ryabinin, M. 2022. Secure distributed training at scale. In *International Conference on Machine Learning*, 7679–7739. PMLR.
- Gorbunov, E.; Hanzely, F.; and Richtárik, P. 2021. Local sgd: Unified theory and new efficient methods. In *International Conference on Artificial Intelligence and Statistics*, 3556–3564. PMLR.
- Gorbunov, E.; Horváth, S.; Richtárik, P.; and Gidel, G. 2023. Variance Reduction is an Antidote to Byzantine Workers: Better Rates, Weaker Assumptions and Communication Compression as a Cherry on the Top. In *11th International Conference on Learning Representations, ICLR 2023*.
- Guo, H.; Wang, H.; Song, T.; Hua, Y.; Lv, Z.; Jin, X.; Xue, Z.; Ma, R.; and Guan, H. 2021. Siren: Byzantine-robust federated learning via proactive alarming. In *Proceedings of the ACM Symposium on Cloud Computing*, 47–60.
- Guo, H.; Wang, H.; Song, T.; Ma, Y. H. R.; Jin, X.; Xue, Z.; and Guan, H. 2024. SIREN+: Robust Federated Learning with Proactive Alarming and Differential Privacy. *IEEE Transactions on Dependable and Secure Computing*.

- He, K.; Zhang, X.; Ren, S.; and Sun, J. 2016. Deep residual learning for image recognition. In *Proceedings of the IEEE conference on computer vision and pattern recognition*, 770–778.
- Huang, W.; Shi, Z.; Ye, M.; Li, H.; and Du, B. 2024. Self-Driven Entropy Aggregation for Byzantine-Robust Heterogeneous Federated Learning. In *Forty-first International Conference on Machine Learning*.
- Jahani, M.; Rusakov, S.; Shi, Z.; Richtárik, P.; Mahoney, M. W.; and Takáč, M. 2022. Doubly adaptive scaled algorithm for machine learning using second-order information. *ICLR*.
- Johnson, R.; and Zhang, T. 2013. Accelerating Stochastic Gradient Descent using Predictive Variance Reduction. In Burges, C.; Bottou, L.; Welling, M.; Ghahramani, Z.; and Weinberger, K., eds., *Advances in Neural Information Processing Systems*, volume 26. Curran Associates, Inc.
- Kairouz, P.; McMahan, H. B.; Avent, B.; Bellet, A.; Bennis, M.; Bhagoji, A. N.; Bonawitz, K.; Charles, Z.; Cormode, G.; Cummings, R.; et al. 2021. Advances and open problems in federated learning. *Foundations and trends® in machine learning*, 14(1–2): 1–210.
- Karimireddy, S. P.; He, L.; and Jaggi, M. 2021a. Byzantine-Robust Learning on Heterogeneous Datasets via Bucketing. In *International Conference on Learning Representations*.
- Karimireddy, S. P.; He, L.; and Jaggi, M. 2021b. Learning from history for byzantine robust optimization. In *International Conference on Machine Learning*, 5311–5319. PMLR.
- Karimireddy, S. P.; Kale, S.; Mohri, M.; Reddi, S.; Stich, S.; and Suresh, A. T. 2020. Scaffold: Stochastic controlled averaging for federated learning. In *International conference on machine learning*, 5132–5143. PMLR.
- Khaled, A.; Mishchenko, K.; and Richtárik, P. 2020. Tighter theory for local SGD on identical and heterogeneous data. In *International Conference on Artificial Intelligence and Statistics*, 4519–4529. PMLR.
- Kingma, D. P.; and Ba, J. 2014. Adam: A method for stochastic optimization. *arXiv preprint arXiv:1412.6980*.
- Koloskova, A.; Loizou, N.; Boreiri, S.; Jaggi, M.; and Stich, S. 2020. A unified theory of decentralized sgd with changing topology and local updates. In *International Conference on Machine Learning*, 5381–5393. PMLR.
- Konečný, J.; McMahan, H. B.; Ramage, D.; and Richtárik, P. 2016. Federated optimization: Distributed machine learning for on-device intelligence. *arXiv preprint arXiv:1610.02527*.
- Krizhevsky, A.; Hinton, G.; et al. 2009. Learning multiple layers of features from tiny images.
- Li, Q.; Diao, Y.; Chen, Q.; and He, B. 2022. Federated learning on non-iid data silos: An experimental study. In *2022 IEEE 38th international conference on data engineering (ICDE)*, 965–978. IEEE.
- Li, T.; Sahu, A. K.; Talwalkar, A.; and Smith, V. 2020. Federated learning: Challenges, methods, and future directions. *IEEE signal processing magazine*, 37(3): 50–60.
- Li, Z.; Lin, T.; Shang, X.; and Wu, C. 2023. Revisiting weighted aggregation in federated learning with neural networks. In *International Conference on Machine Learning*, 19767–19788. PMLR.
- Malinovsky, G.; Gorbunov, E.; Horváth, S.; and Richtárik, P. 2023. Byzantine robustness and partial participation can be achieved simultaneously: Just clip gradient differences. In *Privacy Regulation and Protection in Machine Learning*.
- McMahan, B.; Moore, E.; Ramage, D.; Hampson, S.; and y Arcas, B. A. 2017. Communication-efficient learning of deep networks from decentralized data. In *Artificial intelligence and statistics*, 1273–1282. PMLR.
- Mhamdi, E. M. E.; Guerraoui, R.; and Rouault, S. 2018. The hidden vulnerability of distributed learning in byzantium. *arXiv preprint arXiv:1802.07927*.
- Mishchenko, K.; Islamov, R.; Gorbunov, E.; and Horváth, S. 2023. Partially personalized federated learning: Breaking the curse of data heterogeneity. *arXiv preprint arXiv:2305.18285*.
- Moulines, E.; and Bach, F. 2011. Non-Asymptotic Analysis of Stochastic Approximation Algorithms for Machine Learning. In Shawe-Taylor, J.; Zemel, R.; Bartlett, P.; Pereira, F.; and Weinberger, K., eds., *Advances in Neural Information Processing Systems*, volume 24. Curran Associates, Inc.
- Nguyen, L. M.; Liu, J.; Scheinberg, K.; and Takáč, M. 2017. SARAH: A novel method for machine learning problems using stochastic recursive gradient. In *International conference on machine learning*, 2613–2621. PMLR.
- Nguyen, T. D.; Rieger, P.; De Viti, R.; Chen, H.; Brandenburg, B. B.; Yalame, H.; Möllering, H.; Fereidooni, H.; Marchal, S.; Miettinen, M.; et al. 2022. {FLAME}: Taming backdoors in federated learning. In *31st USENIX Security Symposium (USENIX Security 22)*, 1415–1432.
- Noh, H.; and Yi, Y. 2022. FedMix: Approximation of MixUp for Federated Learning. In *International Conference on Machine Learning (ICML)*.
- Park, J.; Han, D.-J.; Choi, M.; and Moon, J. 2021. Sageflow: Robust federated learning against both stragglers and adversaries. *Advances in neural information processing systems*, 34: 840–851.
- Qin, T.; and Liu, T. 2013. Introducing LETOR 4.0 Datasets. *CoRR*, abs/1306.2597.
- Recht, B.; and Ré, C. 2013. Parallel stochastic gradient algorithms for large-scale matrix completion. *Mathematical Programming Computation*, 5(2): 201–226.
- Reddi, S.; Charles, Z.; Zaheer, M.; Garrett, Z.; Rush, K.; Konečný, J.; Kumar, S.; and McMahan, H. B. 2020. Adaptive federated optimization. *arXiv preprint arXiv:2003.00295*.
- Robbins, H.; and Monro, S. 1951. A stochastic approximation method. *The annals of mathematical statistics*, 400–407.
- Rodríguez-Barroso, N.; Martínez-Cámara, E.; Luzón, M. V.; and Herrera, F. 2022. Dynamic defense against byzantine poisoning attacks in federated learning. *Future Generation Computer Systems*, 133: 1–9.
- Sadiev, A.; Beznosikov, A.; Almansoori, A. J.; Kamzolov, D.; Tappenden, R.; and Takáč, M. 2024. Stochastic gradient

- methods with preconditioned updates. *Journal of Optimization Theory and Applications*, 1–19.
- Sadiev, A.; Borodich, E.; Beznosikov, A.; Dvinskikh, D.; Chezhegov, S.; Tappenden, R.; Takáč, M.; and Gasnikov, A. 2022. Decentralized personalized federated learning: Lower bounds and optimal algorithm for all personalization modes. *EURO Journal on Computational Optimization*, 10: 100041.
- Shalev-Shwartz, S.; and Ben-David, S. 2014. *Understanding machine learning: From theory to algorithms*. Cambridge university press.
- Shalev-Shwartz, S.; Shamir, O.; Srebro, N.; and Sridharan, K. 2009. Stochastic Convex Optimization. In *COLT*, volume 2, 5.
- Smith, V.; Chiang, C.-K.; Sanjabi, M.; and Talwalkar, A. S. 2017. Federated multi-task learning. *Advances in neural information processing systems*, 30.
- Stich, S. U. 2019. Unified optimal analysis of the (stochastic) gradient method. *arXiv preprint arXiv:1907.04232*.
- Tieleman, T.; and Hinton, G. 2012. Lecture 6.5-rmsprop, coursera: Neural networks for machine learning. *University of Toronto, Technical Report*, 6.
- Tupitsa, N.; Horváth, S.; Takáč, M.; and Gorbunov, E. 2024. Federated Learning Can Find Friends That Are Beneficial. *arXiv preprint arXiv:2402.05050*.
- Vaswani, A.; Shazeer, N.; Parmar, N.; Uszkoreit, J.; Jones, L.; Gomez, A. N.; Kaiser, Ł.; and Polosukhin, I. 2017. Attention is all you need. *Advances in neural information processing systems*, 30.
- Verbraeken, J.; Wolting, M.; Katzy, J.; Kloppenburg, J.; Verbelen, T.; and Rellermeyer, J. S. 2020. A survey on distributed machine learning. *Acm computing surveys (csur)*, 53(2): 1–33.
- Wagner, P.; Strodtzoff, N.; Bousseljot, R.-D.; Kreiseler, D.; Lunze, F. I.; Samek, W.; and Schaeffter, T. 2020. PTB-XL, a large publicly available electrocardiography dataset. *Scientific data*, 7(1): 1–15.
- Wang, H.; Yurochkin, M.; Sun, Y.; Papailiopoulos, D.; and Khazaeni, Y. 2020. Federated learning with matched averaging. *arXiv preprint arXiv:2002.06440*.
- Wang, S.; and Ji, M. 2022. A unified analysis of federated learning with arbitrary client participation. *Advances in Neural Information Processing Systems*, 35: 19124–19137.
- Wang, Y.; Sun, T.; Li, S.; Yuan, X.; Ni, W.; Hossain, E.; and Poor, H. V. 2023. Adversarial attacks and defenses in machine learning-empowered communication systems and networks: A contemporary survey. *IEEE Communications Surveys & Tutorials*.
- Woodworth, B. E.; Patel, K. K.; and Srebro, N. 2020. Mini-batch vs local sgd for heterogeneous distributed learning. *Advances in Neural Information Processing Systems*, 33: 6281–6292.
- Wu, Z.; Ling, Q.; Chen, T.; and Giannakis, G. B. 2020. Federated variance-reduced stochastic gradient descent with robustness to byzantine attacks. *IEEE Transactions on Signal Processing*, 68: 4583–4596.
- Xie, C.; Koyejo, O.; and Gupta, I. 2020. Fall of empires: Breaking byzantine-tolerant sgd by inner product manipulation. In *Uncertainty in Artificial Intelligence*, 261–270. PMLR.
- Xie, C.; Koyejo, S.; and Gupta, I. 2019. Zeno: Distributed stochastic gradient descent with suspicion-based fault-tolerance. In *International Conference on Machine Learning*, 6893–6901. PMLR.
- Xu, X.; and Lyu, L. 2020. A reputation mechanism is all you need: Collaborative fairness and adversarial robustness in federated learning. *arXiv preprint arXiv:2011.10464*.
- Yan, H.; Zhang, W.; Chen, Q.; Li, X.; Sun, W.; Li, H.; and Lin, X. 2024. Recess vaccine for federated learning: Proactive defense against model poisoning attacks. *Advances in Neural Information Processing Systems*, 36.
- Yang, H.; Fang, M.; and Liu, J. 2021. Achieving linear speedup with partial worker participation in non-iid federated learning. *arXiv preprint arXiv:2101.11203*.
- Yao, Z.; Gholami, A.; Shen, S.; Mustafa, M.; Keutzer, K.; and Mahoney, M. 2021. Adahessian: An adaptive second order optimizer for machine learning. In *proceedings of the AAAI conference on artificial intelligence*, volume 35, 10665–10673.
- Yin, D.; Chen, Y.; Kannan, R.; and Bartlett, P. 2018. Byzantine-robust distributed learning: Towards optimal statistical rates. In *International Conference on Machine Learning*, 5650–5659. Pmlr.
- Yurochkin, M.; Agarwal, M.; Ghosh, S.; Greenewald, K.; Hoang, N.; and Khazaeni, Y. 2019. Bayesian nonparametric federated learning of neural networks. In *International conference on machine learning*, 7252–7261. PMLR.
- Zhang, Z.; Cao, X.; Jia, J.; and Gong, N. Z. 2022. Fldetector: Defending federated learning against model poisoning attacks via detecting malicious clients. In *Proceedings of the 28th ACM SIGKDD Conference on Knowledge Discovery and Data Mining*, 2545–2555.

Appendix

A Additional Experiments

Overview. This section provides an extensive overview of additional experiments. We begin by outlining the key technical details relevant to our experimental setup, including a description of the computational resources and a complete list of hyperparameters for all compared methods. We then present a series of extended experiments across various settings.

In Section A.2, we compare the final test accuracies of all methods under different attack scenarios, accompanied by training loss curves over epochs. We also provide a comprehensive table reporting the runtime of all methods both in the absence of attacks and under the ALIE attack.

We then address another important factor: the number of samples used in the trial function. A key question in our methodology is how the size of the local dataset on the honest device influences convergence. We demonstrate that while such an effect exists, it remains minor, and even with a small number of samples, our methods maintain strong convergence properties.

Next, we analyze how the solution quality of the inner minimization problem in `AutoBant` affects the final performance. By varying the depth of the mirror descent procedure, we obtain different levels of accuracy in solving the inner problem and assess their influence on downstream metrics.

In Section A.3, we investigate the impact of scaling the number of clients and data heterogeneity. As claimed in the main part of the paper, our methods remain effective in these stressful conditions. For the first one, we split the CIFAR-10 training dataset between 100 clients. For the second, we simulate heterogeneity using a $\text{Dirichlet}(\alpha)$ distribution with varying values of α .

Section A.4 focuses on experiments in the ECG domain. We start by analyzing the sensitivity of the ZENO algorithm to its hyperparameters. Although ZENO performs well in the main part of the paper, we show that this is largely due to a correctly chosen estimate of the number of Byzantine clients. In scenarios where this proportion is unknown, the method fails to converge. We also provide extended results on the detection of various cardiac conditions, including AFIB, 1AVB, PVC, and CLBBB.

Finally, we present additional experiments for the Learning-to-Rank task in Section A.5. While the main part of the paper includes a comparison of our proposed methods with only the most robust baselines under strong attacks, this section offers a broader experimental validation to further support the superiority of our approach.

A.1 Technical details

Compute resources. Our implementation is developed in Python 3.10. We simulate a distributed system on a server. The server is equipped with an AMD EPYC 7513 32-Core Processor running at 2.6 GHz and 4×Nvidia A100 SXM4 40GB. This configuration is used for the experiments described in Section 6.

Table 2: General hyperparameter setup

Hyperparameters	CIFAR-10, LTR	ECG
Batch Size	32	64
Client lr	0.003	0.003
Loss	Cross-Entropy (CE)	Binary CE

Hyperparameters and strategies. To ensure a fair comparison, we maintain consistent hyperparameters across all methods. Table 2 summarizes them. The batch size is set to 32 for CIFAR-10 and 64 for the ECG dataset, with a local client learning rate of 0.003 and ADAM preconditioner. All clients perform local computations for 1 epoch. For CIFAR-10, cross-entropy was used as the local client loss function, while for ECG it was its binary version. To address the problem of imbalance of positive and negative examples in the ECG, the minority class was reweighted to the majority in the corresponding loss function. For the ECG classification task, we train the models on 10-second 12-lead ECG records, with all records resampled to a frequency of 500 Hz. Additionally, we train the models exclusively on patients older than 18 years of age.

We also select specific parameters for the implemented methods. Table 3 summarizes them. For the `SAFEGUARD` method, we use window sizes of 1 and 6 for two different accumulation settings, with the threshold chosen automatically, as described in the original paper. We adapt the `CC` method to a local computation case and set the clipping coefficient $\tau = 0.1$ and the SGD momentum $\beta = 0.9$ for CIFAR-10, as well as $\tau = 1$ and $\beta = 0.5$ for the ECG case. For both setups we fixed the number of clipping iterations to $l = 1$. For the `FIXING-BY-MIXING` technique, we set the number of Byzantine clients f to be less than half of all clients as suggested in the article: for the CIFAR-10 and LTR $f = 4$, while for the ECG $f = 2$. For the `BUCKETING` technique we apply *2-bucketing* strategy with global learning rate $\eta = 0.9$. For the `RECESS` method, we set the decrease score equal to 0.1. For the `Bant` method, we set the momentum parameter $\beta = 0.5$. The `AutoBant` method uses the number of optimization epochs equal to 5 and $\gamma = 1$. For `SimBant`, we set the softmax temperature parameter for the model logits to 0.05. Specifically, we want to highlight the choice of hyperparameters for the ZENO method. We set the regularization weight $\rho = 0.0005$ as a default value in the paper. As for the threshold for defining Byzantines – trim parameter – we set $b = 2$ for the ECG setup, $b = 3$ for CIFAR-10 and $b = 5$ for Learning-to-Rank. We address the choice of hyperparameter b in Table 7 in Appendix A.4, as it is critical in real-world scenarios.

Table 3: Specific hyperparameter setup

Method	Hyperparameters			
SAFEGUARD	<ul style="list-style-type: none"> • CIFAR-10, LTR: • ECG: 	Window Sizes (T_0, T_1)		
		$T_0 = 1, T_1 = 6$ $T_0 = 1, T_1 = 6$		
CENTRAL CLIP	<ul style="list-style-type: none"> • CIFAR-10: • ECG: 	Clip coefficient (τ)	Momentum (β)	Clip iterations (l)
		$\tau = 0.1$ $\tau = 1$	$\beta = 0.9$ $\beta = 0.5$	$l = 1$ $l = 1$
FIXING-BY-MIXING	<ul style="list-style-type: none"> • CIFAR-10, LTR: • ECG: 	Number of Byzantines (f)		
		$f = 4$ $f = 2$		
BUCKETING	<ul style="list-style-type: none"> • CIFAR-10: • ECG: 	Global Learning Rate (η)		
		$\eta = 0.9$ $\eta = 0.9$		
RECESS	<ul style="list-style-type: none"> • CIFAR-10, LTR: • ECG: 	Decrease Score (d)		
		$d = 0.1$ $d = 0.1$		
ZENO	<ul style="list-style-type: none"> • CIFAR-10, LTR: • ECG: 	Regularization weight (ρ)	Trim parameter (b)	
		$\rho = 0.005$ $\rho = 0.005$	$b = 3, 5$ $b = 2$	
Bant	<ul style="list-style-type: none"> • CIFAR-10, LTR: • ECG: 	Momentum (β)	Trial size (ts)	
		$\beta = 0.5$ $\beta = 0.5$	$ts = 500$ $ts = 100$	
AutoBant	<ul style="list-style-type: none"> • CIFAR-10, LTR: • ECG: 	Mirror epochs (e)	Mirror γ	Trial size (ts)
		$e = 5$ $e = 5$	$\gamma = 1$ $\gamma = 1$	$ts = 500$ $ts = 100$
SimBant	<ul style="list-style-type: none"> • CIFAR-10, LTR: • ECG: 	Softmax temperature (T)	Similarity function γ	Trial size (ts)
		$T = 0.05$ $T = 0.05$	see eq. (3) see eq. (2)	$ts = 500$ $ts = 100$

Additionally, we define distinct functions for `SimBant` based on the dataset, as ECG classification is binary, whereas CIFAR-10 is a multi-class classification problem. Specifically, for the ECG dataset, we use:

$$sim_{ECG}(x, y) = 1 - |x - y|, \quad (2)$$

where x is the output of the client model, and y is the output of the model fine-tuned on the server. For the CIFAR-10 dataset, we apply cosine similarity:

$$sim_{CIFAR}(x, y) = \frac{x \cdot y}{\|x\| \cdot \|y\|}, \quad (3)$$

where y is one-hot encode targets.

A.2 CIFAR-10 Experiments

Final accuracy. In this section, we present supplementary data regarding the experiments conducted. As mentioned in the main part of the paper, we utilized RESNET-18 models on the CIFAR-10 dataset. We begin with a comparative Table 4 of the methods applied to the CIFAR-10 dataset.

This table illustrates the performance of different algorithms under various attacks, highlighting their effectiveness. We've supplemented it with scenarios of Sign Flipping (40%) and IPM (50%) attacks compared to the main part to demonstrate the results of baselines in less stressful conditions. It is noteworthy that while existing methods provide some level of protection against certain attacks, none are effective when faced with a majority of malicious clients in gradient attacks, as well as in IPM (70%) and ALIE (40%), which simulates the majority. In contrast, all three of our methods demonstrate impressive performance in such attack scenarios. Furthermore, it is important to compare these results with those in the first column, which represents the metric in the absence of attacks. As we can see, our methods achieve only a slight reduction in the metric, yet they maintain relatively strong performance even under the most severe attacks. This resilience underscores the effectiveness of our approaches and their potential for real-world applications where robust defense mechanisms are crucial.

Table 4: RESNET18 on CIFAR-10. Accuracy under various attacks.

Algorithm	Without Attack	Label Flipping (50%)	Sign Flipping (60%)	Random Gradients (50%)	IPM (70%)	ALIE (40%)	Sign Flipping (40%)	IPM (50%)
ADAM	0.902	0.207	0.100	0.100	0.100	0.100	0.624	0.832
FLTRUST	0.767	0.694	0.100	0.100	0.100	0.100	0.254	0.519
RECESS	0.887	0.633	0.100	0.103	0.106	0.128	0.488	0.774
ZENO	0.910	0.156	0.410	0.100	0.100	0.100	0.838	0.100
CC	0.917	0.603	0.102	0.100	0.100	0.100	0.511	0.864
CC+FBM	0.915	0.887	0.098	0.100	0.101	0.100	0.823	0.923
CC+BUCKETING	0.845	0.818	0.089	0.101	0.100	0.101	0.815	0.100
SAFEGUARD	0.918	0.102	0.100	0.102	0.104	0.113	0.826	0.112
VR MARINA	0.100	0.100	0.100	0.100	0.100	0.100	0.100	0.100
Bant	0.864	0.861	0.846	0.846	0.725	0.856	0.856	0.751
AutoBant	0.906	0.884	0.783	0.898	0.666	0.882	0.839	0.847
SimBant	0.909	0.855	0.827	0.865	0.623	0.878	0.852	0.827

Decrease of loss functions. Now we examine the graphs depicting the reduction of loss over the course of training (Figure 4). The result is similar: as the number of attackers increases, the existing methods exhibit divergence, while our methods continue to decrease the loss effectively. As mentioned in the main part of the paper, AutoBant may behave inconsistently under Random Gradients and ALIE attacks. This instability can be attributed to the solution of an additional minimization problem and the absence of an indicator that prevents theoretical advancement in non-convex scenarios. Nevertheless, even under these circumstances, AutoBant demonstrates significantly better results compared to its counterparts.

Table 5: Time per communication round under ALIE attack (40%). RESNET18 on CIFAR-10 and RESNET1D18 on ECG (AFIB).

CIFAR-10 (ResNet18)		ECG (AFIB) (ResNet1d18)	
Algorithm	ALIE (40%)	Method	ALIE (40%)
ADAM	15.38 \pm 0.94	ADAM	32.14 \pm 2.83
FLTRUST	36.38 \pm 0.92	FLTRUST	48.57 \pm 8.17
RECESS	38.50 \pm 3.14	RECESS	49.55 \pm 2.24
ZENO	27.44 \pm 2.36	ZENO	34.23 \pm 4.22
CC	21.67 \pm 3.14	CC	43.36 \pm 3.47
CC+FBM	23.59 \pm 3.98	CC + FBM	45.84 \pm 4.41
CC+BUCKETING	21.73 \pm 3.10	CC + BUCKETING	47.13 \pm 3.56
SAFEGUARD	29.15 \pm 1.16	SAFEGUARD	35.67 \pm 2.34
VR MARINA	36.96 \pm 3.45	VR MARINA	45.13 \pm 6.41
Bant	27.94 \pm 3.14	Bant (ours)	36.10 \pm 2.63
AutoBant	33.63 \pm 1.74	AutoBant (ours)	41.34 \pm 1.03
SimBant	30.05 \pm 4.35	SimBant (ours)	36.24 \pm 3.82

Time measurement. Tables above report the average time per communication round, including standard deviation for various federated learning algorithms using RESNET18 on CIFAR-10 and RESNET1D18 on ECG (AFIB) in two settings: Without attack and ALIE. We see that RECESS took the longest time, since it requires double local calculations of the client in one round of communication. AutoBant requires a little more time compared to baselines, except for the RECESS and FLTRUST methods. We attribute this to the solution of the auxiliary task Algorithm 5.3, Line 10), which is slightly longer than in the ECG setup and has a greater impact on the execution time. However, it is not expected that the size of \hat{f} increases significantly as the system scales. Thus, this contribution is negligible in real-world scenarios, as demonstrated by the ECG experiment in Table 5. In addition, these computations are performed on the central node, which has more computational resources in the federated learning paradigm. All of this reflects the applicability of the proposed methods in real-world setups.

Sensitivity to Trial Set Size. The trial dataset plays a central role in all proposed methods, serving as a reference for evaluating client gradients via the surrogate loss \hat{f} . While our theoretical analysis suggests that the impact of finite sampling is mild (via $\zeta(N)$), it remains essential to validate this empirically – particularly for small N , which is desirable in privacy-sensitive or resource-constrained settings. A robust method should maintain performance even when the server has access to only a limited

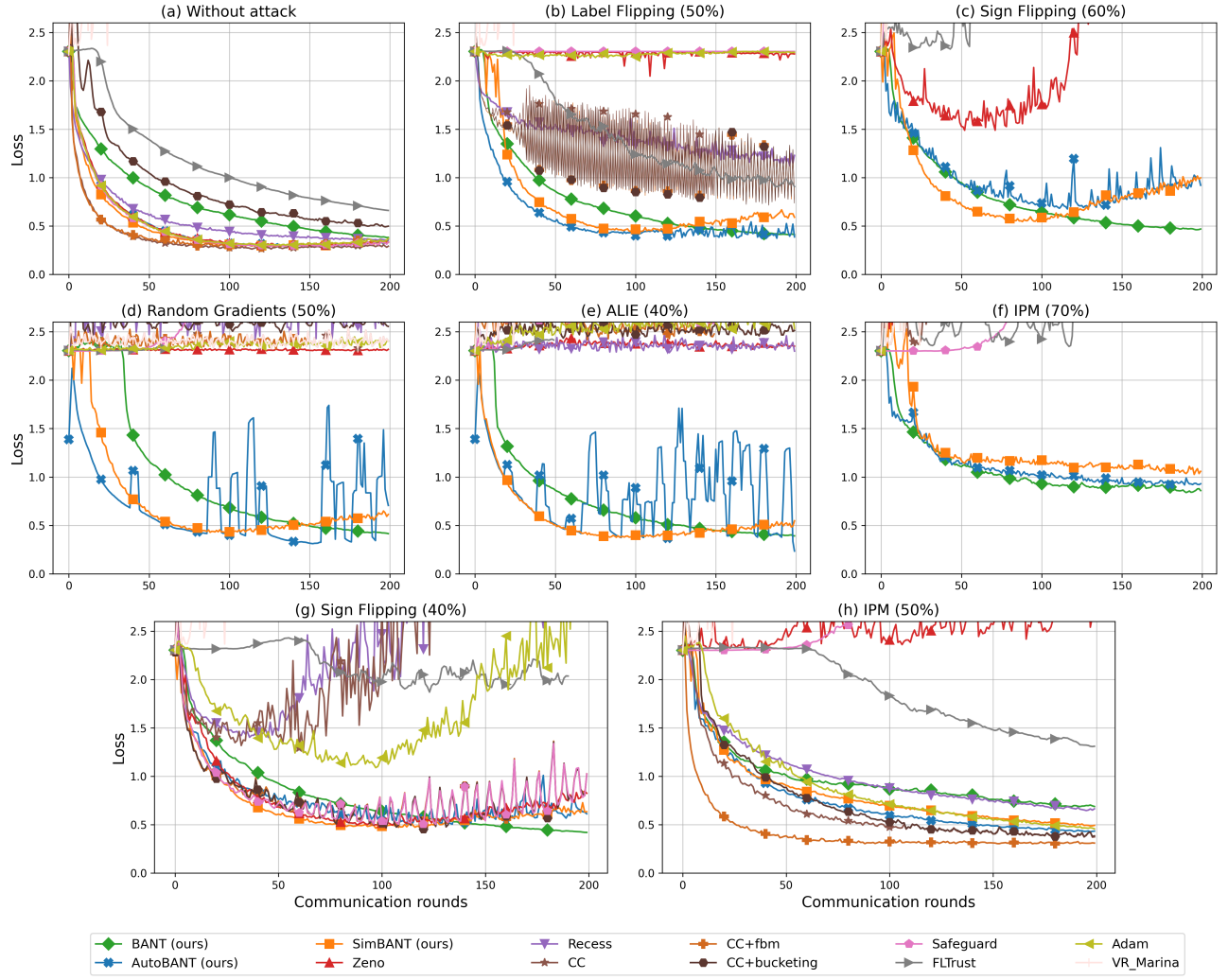


Figure 4: RESNET18 on CIFAR-10. Loss on test for Byzantine-tolerance techniques under various attacks.

trial set. To this end, we investigate the impact of the trial set size N on convergence and stability for Bant, SimBant, and AutoBant. In the main experiments, we use $N = 500$. Here, we vary $N \in \{100, 150, 200, 250, 500, 1000\}$. Bant and SimBant demonstrate stable convergence across all values of N , even as low as 100, confirming their robustness to trial set sampling. AutoBant, however, exhibits higher sensitivity. At $N = 100$, convergence breaks down entirely, and even for $N \leq 200$, we observe increased variance and less stable updates. Nonetheless, performance remains strong in the range $N = 250$ – 1000 , with fluctuations that do not degrade the overall results. This behavior aligns with the design of AutoBant, which solves an optimization problem over client weights using noisy evaluations of the surrogate objective \hat{f} . When N is too small, noise dominates, leading to unstable direction selection. In contrast, the trust-averaged updates in Bant and SimBant mitigate this effect and remain effective even under highly reduced supervision. Nevertheless, we address the issue related to unstable minimization problem solving in the AutoBant algorithm below.

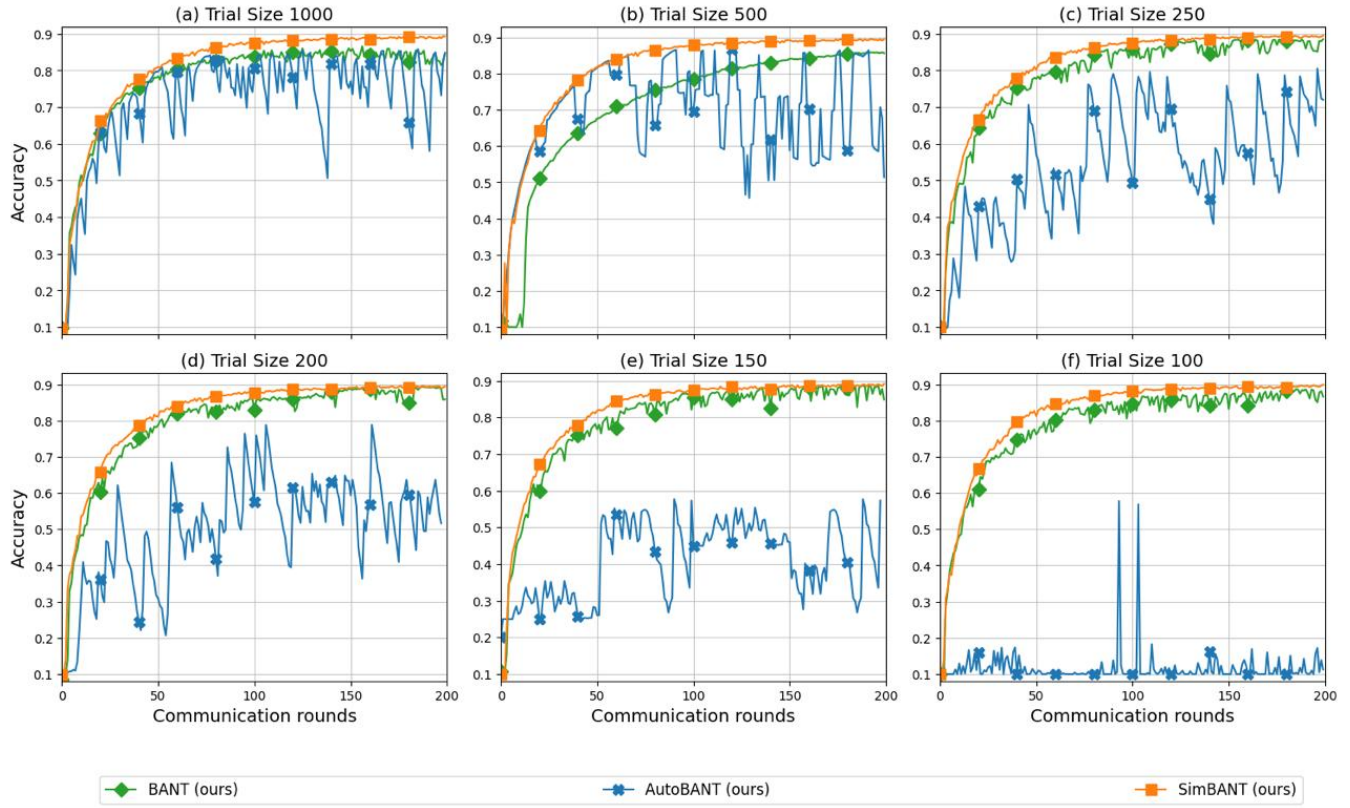


Figure 5: Test accuracy for RESNET18 on CIFAR-10 with different number of samples to obtain trial data.

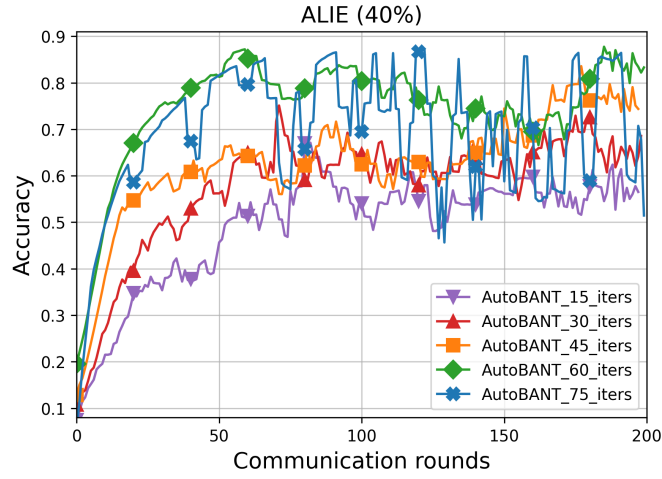


Figure 6: Number of Mirror Descent steps impact on global convergence

Study on precision of the auxiliary minimization task in AutoBant. AutoBant introduces an adaptive weighting mechanism via an optimization step over the client weight simplex. The quality of this step is controlled by the number of iterations in the mirror descent routine, corresponding to a target precision δ . From a practical perspective, this parameter governs a trade-off between computational cost and stability. On the one hand, too coarse a solution may lead to noisy updates. On the other hand, the method may overfit transient fluctuations in the trial loss. Therefore, it is important to assess how sensitive the method is to this optimization accuracy and whether reliable convergence is retained under realistic constraints. In our main experiments, we set the number of mirror descent steps to $T = 75$. Here, we vary $T \in \{15, 30, 45, 60, 75\}$.

Table 6: Accuracy and training time from the Number of Mirror Descent steps.

T	Accuracy	Mirror Time
15	0.565	18.35 \pm 4.19
30	0.686	27.62 \pm 5.11
45	0.744	37.58 \pm 3.16
60	0.833	50.43 \pm 4.25
75	0.715	67.27 \pm 3.49

We mention that due to the inherent stochasticity arisen from solving a convex minimization problem over the client weight simplex, the method is potentially unstable. To mitigate this, we adopt a natural stabilization strategy in our experimental setup. Thus, we leverage the history of client weights over the last round via momentum mechanism, thereby smoothing abrupt shifts that may result from sample-level variability. This prevents the algorithm from over-committing to transiently favorable clients and promotes consistent progress.

We observe that:

- At $T = 15$ and $T = 30$, a low deterioration in convergence occurs.
- At $T = 45$ and $T = 60$, convergence improves significantly, yielding smooth and high-quality updates.
- At $T = 75$, performance becomes less stable due to overfitting to a single dominant client, a known issue when mirror descent pushes weights too aggressively toward one vertex of the simplex.

Despite this instability, convergence is preserved, and the method still outperforms baselines. Moreover, according to our convergence analysis (see Theorem 4.3), the error introduced by inexact minimization—quantified by the optimization precision parameter δ —only enters as a second-order additive term and does not fundamentally affect the convergence rate. As evident from Table 6, reducing the number of mirror descent iterations directly corresponds to a lower computational overhead, with $T = 45$ requiring approximately 45% less computation time than $T = 75$ while still maintaining reasonable accuracy. This trade-off is particularly valuable for resource-constrained server node where computation time can bottleneck synchronization, affecting overall system efficiency. These findings highlight that AutoBant benefits from moderate optimization depth and additional smoothing over rounds, confirming that its performance can be controlled through simple and intuitive mechanisms without excessive parameter tuning.

A.3 Stress Testing conditions

To further test the proposed methods, we examine the stress conditions of the experiments. For this purpose, the strongest Byzantine attacks (Random Gradients, ALIE, IPM) were considered, in which only Bant-like methods show resistance. The first experiment splits CIFAR-10 homogeneously among 100 clients, while the second splits heterogeneously among 10 clients using the Dirichlet distribution.

CIFAR-10 on 100 clients. To test the robustness of the methods in a scalable setup, we split CIFAR-10 homogeneously among 100 clients. In this case, each client has less local data and its results are less representative compared to the Byzantine, which affects our methods when measuring \hat{f} . Due to computational challenges, we test only the ALIE (40%) attack. Figure 7 illustrates the convergence results on the test part of the dataset.

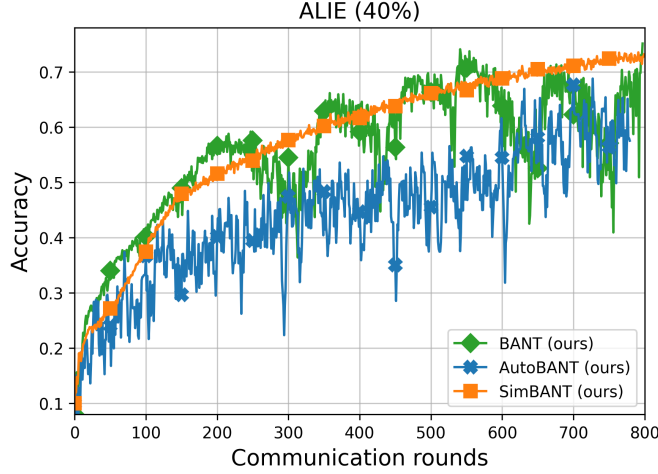


Figure 7: Test Accuracy for RESNET18 on CIFAR-10 with 100 clients.

Comparing with the corresponding plot in Figure 1, we observe visible changes for the `Bant` and `AutoBant` methods. However, the effects described below are due to the complication of an already extreme setup. All methods demonstrate fundamental robustness, which was the goal of this experiment. More noisy results for `AutoBant` are related to solving an additional subproblem on a higher-dimensional simplex. As we mentioned in the main part of the paper, the method produces small non-zero trust scores for Byzantine clients, which is further highlighted when the number of clients increases. The `Bant` method directly compares the Byzantines to the global state of the model, so we observe periodic dips during federated training. All methods are trained over 800 rounds and exhibit slower convergence.

Dirichlet Scenario. To examine the robustness of the proposed methods under a heterogeneous setup, we perform Byzantine attacks on CIFAR-10 with Dirichlet distribution of client data (Yurochkin et al. 2019; Wang et al. 2020; Noh and Yi 2022). We partition each global dataset among n clients according to Dirichlet distribution with concentration parameter α . As α decreases, the distributions on different clients become more skewed, which empirically increases both the inter-client gradient variance and the bias of each client’s expected gradient from the true global gradient. Concretely, under a $\text{Dirichlet}(\alpha)$ partition, one observes that δ_1 and δ_2 grow monotonically as $\alpha \rightarrow 0$ (stronger non-IID) and shrink as $\alpha \rightarrow \infty$ (nearly IID).

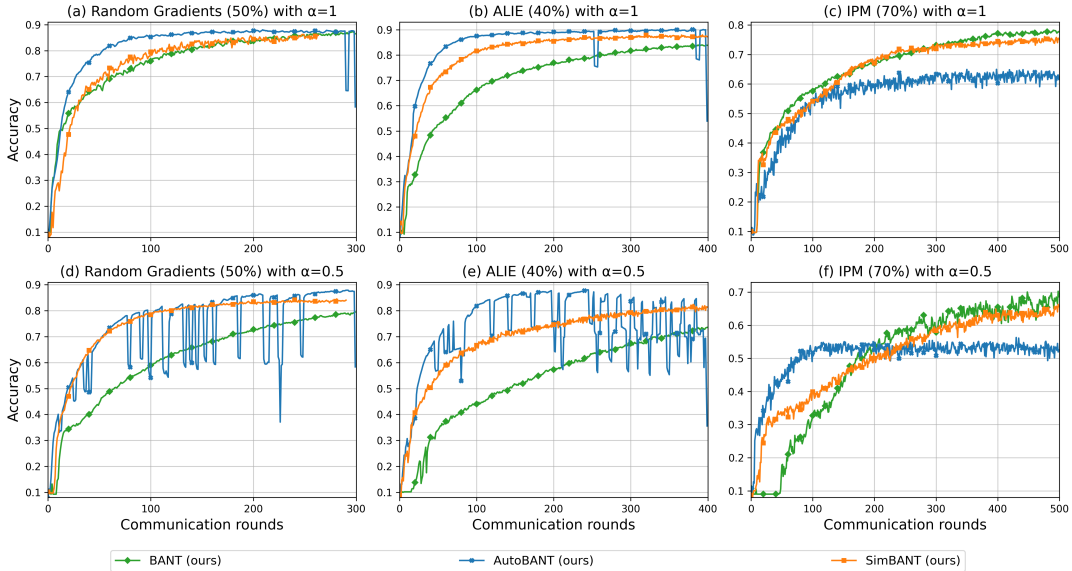


Figure 8: Test accuracy for RESNET18 on CIFAR-10 with Dirichlet heterogeneity.

We note that $\mathbf{p}_k \sim \text{Dir}(\alpha \cdot \mathbf{1}_n)$ represents distribution of samples with label $k = \overline{1, K}$ over n clients, i.e. $\mathbf{p}_k \in S_n(1)$ where $S_n(1)$ is the standard n unit simplex. We address two heterogeneity regimes: medium with $\alpha = 1$ and strong with $\alpha = 0.5$. Since the goal of the experiment is to test the robustness of the proposed methods, we consider the 3 strongest attacks in our setup:

Table 7: RESNET1D18 on ECG (AFIB). G-mean and f1-score for Zeno under various attacks. The value in parentheses indicates the assumed number of Byzantines.

Algorithm	Without Attack		Label Flipping (60%)		Random Gradients (60%)		IPM (80 %)		ALIE (40 %)	
	G-mean	f1-score	G-mean	f1-score	G-mean	f1-score	G-mean	f1-score	G-mean	f1-score
ZENO (80%)	0.860±0.016	0.707±0.015	0.735±0.023	0.619±0.010	0.824±0.018	0.696±0.014	0.930±0.011	0.715±0.023	0.930±0.017	0.705±0.013
ZENO (60%)	0.953±0.018	0.806±0.017	0.950±0.020	0.753±0.019	0.954±0.020	0.770±0.017	0.945±0.017	0.730±0.020	0.946±0.015	0.717±0.016
ZENO	0.921±0.012	0.787±0.014	0.014±0.017	0.110±0.015	0.163±0.010	0.089±0.014	0.102±0.012	0.066±0.018	0.010±0.009	0.091±0.011

Random Gradient (50%), ALIE (40%), and IPM (70%). Figure 8, 9 illustrates the performance of the Bant-based methods. In the presence of Dirichlet-induced heterogeneity and high-fraction Byzantine attacks, the proposed automated defenses exhibit fast convergence and generalization compared to the original Bant protocol. As shown in Figures 8 (a - c) and 9 (a - c), under mild skew ($\alpha = 1$) and Random Gradient, ALIE, or IPM attacks, AutoBant drives test accuracy above 80% and reduces test loss below 0.7 in roughly 100 communication rounds, approximately half the rounds required by Bant, while SimBant achieve intermediate performance.

As illustrated in Figures 8 (d - f) and 9 (d - f), when the heterogeneity is intensified ($\alpha = 0.5$), Bant’s accuracy curves develop large oscillations and its loss decay slows substantially, whereas both AutoBant and SimBant maintain smooth, rapid descent to peak accuracies of 85–88% and asymptotic losses in the 0.5–0.9 range.

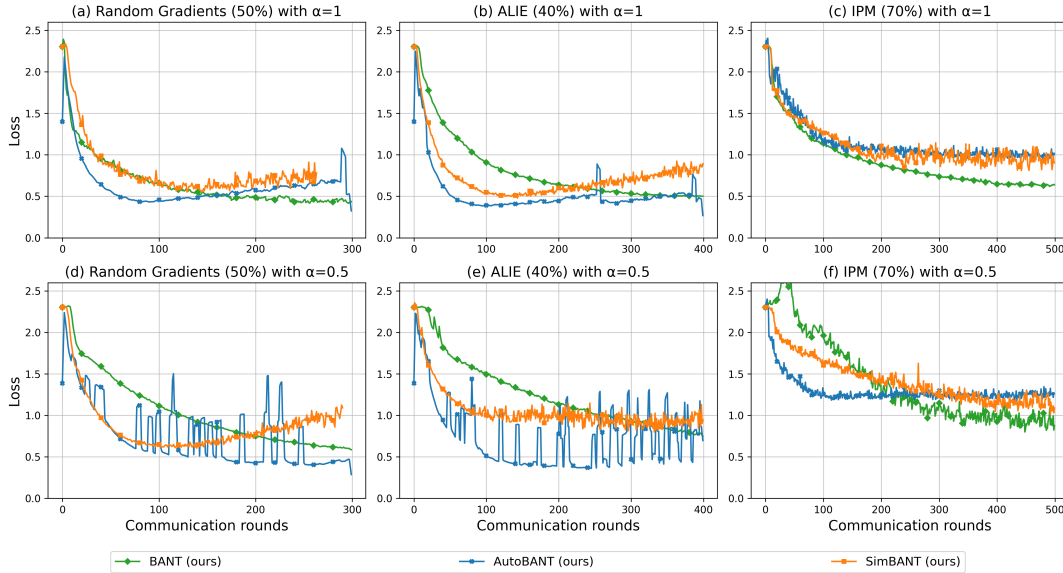


Figure 9: Test loss for RESNET18 on CIFAR-10 with Dirichlet heterogeneity.

A.4 ECG Experiments

On ZENO’s sensitivity to hyperparameters. Now, let us move on to the choice of the trim hyperparameter b in the ZENO method. This parameter cuts off the number of clients that will not be used in the aggregation of the global model in the training round. The ranking of clients is based on $Score_{\gamma, \rho}$, which exploits the trial function approach. In the paper, it is assumed that $b \geq q$, where q is the number of Byzantines participating in the training. Thus, the method provides protection against an arbitrary number of malicious participants and can be stable in critical attack setups. However, in real-world scenarios, we do not have a priori information about the number of Byzantines. As a result, ZENO does not show comparable quality metrics in the ECG setup for $b = 2$ compared to the Bant-like methods, which is reflected in Table 1. We address the issue of choosing this hyperparameter in the ECG setup in Table 7. As can be seen from the results, a suitably selected trim coefficient value of $b = 3$, which cuts off 60% of Byzantine clients, shows comparable results with the Bant-like methods in all considered attack scenarios. Cutting 80% of Byzantines leads to a slightly lower quality, which also highlights the hyperparameter sensitivity.

Metrics for all abnormalities. Here, we present all the obtained metric results for the four heart abnormalities we investigated: Atrial FIBrillation (AFIB), First-degree AV block (1AVB), Premature Ventricular Complex (PVC), and Complete Left Bundle Branch Block (CLBBB). In Table 8, we show results for AFIB pathology under 2 additional attacks scenarios: Sign Flipping (60%) and IPM (60%). In addition, we compare all methods for the attacks described in 6 section in Tables 9 - 12. To obtain confidence intervals in Tables 1, 7, 8, each run was repeated 5 times. We do not report the variance of metrics for the 1AVB,

PVC and CLBBB pathologies in Tables 10-12 due to overabundance and computational factor.

Table 8: RESNET1D18 on ECG (AFIB). G-mean and f1-score for Byzantine-tolerance techniques under 2 attacks.

Algorithm	Sign Flipping (60 %)		IPM (60%)	
	G-mean	f1-score	G-mean	f1-score
ADAM	0.304±0.015	0.116±0.018	0.952±0.014	0.738±0.011
FLTRUST	0.586±0.018	0.179±0.015	0.011±0.014	0.123±0.013
RECESS	0.359±0.018	0.115±0.014	0.933±0.017	0.611±0.018
ZENO	0.017±0.016	0.130±0.018	0.010±0.018	0.140±0.020
CC	0.479±0.020	0.124±0.017	0.945±0.020	0.710±0.016
CC+FBM	0.155±0.016	0.124±0.017	0.948±0.018	0.695±0.020
CC+BUCKETING	0.137±0.017	0.119±0.010	0.944±0.016	0.689±0.013
SAFEGUARD	0.084±0.016	0.014±0.018	0.109±0.010	0.123±0.016
VR MARINA	0.096±0.017	0.078±0.019	0.098±0.011	0.110±0.014
Bant	0.943±0.019	0.792±0.019	0.949±0.020	0.704±0.017
AutoBant	0.737±0.020	0.243±0.019	0.948±0.018	0.695±0.015
SimBant	0.951±0.020	0.760±0.020	0.965±0.017	0.753±0.020

Table 9: RESNET1D18 on ECG (AFIB).

	Algorithm	Sensitivity	Specificity	G-mean	f1-score
Without Attack	ADAM	0.940	0.974	0.956	0.811
	FLTRUST	0.932	0.972	0.952	0.800
	RECESS	0.929	0.969	0.949	0.783
	ZENO	0.890	0.952	0.921	0.787
	CC	0.932	0.966	0.949	0.772
	CC+FBM	0.930	0.978	0.954	0.808
	CC+BUCKETING	0.910	0.985	0.947	0.790
	SAFEGUARD	0.940	0.976	0.957	0.821
	VR MARINA	0.150	0.001	0.010	0.120
	Bant	0.929	0.978	0.953	0.830
	AutoBant	0.940	0.967	0.953	0.781
	SimBant	0.943	0.969	0.956	0.790
Label Flip (60%)	ADAM	0.089	0.774	0.262	0.041
	FLTRUST	0.943	0.961	0.952	0.753
	RECESS	0.146	0.920	0.366	0.128
	ZENO	0.160	0.001	0.014	0.110
	CC	0.840	0.097	0.285	0.114
	CC+FBM	0.880	0.801	0.840	0.716
	CC+BUCKETING	0.870	0.789	0.829	0.708
	SAFEGUARD	0.018	0.063	0.107	0.123
	VR MARINA	0.210	0.003	0.027	0.123
	Bant	0.947	0.966	0.956	0.777
	AutoBant	0.964	0.647	0.790	0.276
	SimBant	0.932	0.967	0.949	0.774
Sign Flip (60%)	ADAM	0.096	0.961	0.304	0.116
	FLTRUST	0.466	0.738	0.586	0.179
	RECESS	0.142	0.906	0.359	0.115
	ZENO	0.230	0.001	0.017	0.130
	CC	0.328	0.701	0.479	0.124
	CC+FBM	0.270	0.089	0.155	0.124
	CC+BUCKETING	0.250	0.075	0.137	0.119
	SAFEGUARD	0.007	0.998	0.084	0.014
	VR MARINA	0.150	0.061	0.096	0.078
	Bant	0.915	0.972	0.943	0.792
	AutoBant	0.854	0.636	0.737	0.243
	SimBant	0.940	0.963	0.951	0.760
Random Gradients (60%)	ADAM	0.136	0.893	0.348	0.126
	FLTRUST	0.623	0.611	0.617	0.174
	RECESS	0.562	0.626	0.593	0.163
	ZENO	0.300	0.088	0.163	0.089
	CC	0.459	0.733	0.580	0.155
	CC+FBM	0.500	0.632	0.562	0.252
	CC+BUCKETING	0.420	0.774	0.570	0.164
	SAFEGUARD	0.929	0.071	0.258	0.124
	VR MARINA	0.320	0.096	0.176	0.103
	Bant	0.922	0.975	0.948	0.809
	AutoBant	0.932	0.961	0.946	0.748
	SimBant	0.951	0.940	0.945	0.712
IPM (60 %)	ADAM	0.947	0.957	0.952	0.738
	FLTRUST	0.210	0.001	0.011	0.123
	RECESS	0.947	0.919	0.933	0.611
	ZENO	0.200	0.001	0.010	0.140
	CC	0.940	0.950	0.945	0.710
	CC+FBM	0.950	0.946	0.948	0.695
	CC+BUCKETING	0.940	0.948	0.944	0.689
	SAFEGUARD	0.190	0.062	0.109	0.123
	VR MARINA	0.170	0.056	0.098	0.110
	Bant	0.950	0.947	0.949	0.704
	AutoBant	0.950	0.945	0.948	0.695
	SimBant	0.974	0.955	0.965	0.753
IPM (80 %)	ADAM	0.043	0.904	0.197	0.036
	FLTRUST	0.220	0.016	0.061	0.124
	RECESS	0.456	0.533	0.493	0.112
	ZENO	0.131	0.080	0.102	0.066
	CC	0.007	0.997	0.084	0.014
	CC+FBM	0.210	0.003	0.027	0.123
	CC+BUCKETING	0.220	0.005	0.035	0.118
	SAFEGUARD	0.200	0.060	0.110	0.082
	VR MARINA	0.240	0.067	0.127	0.079
	Bant	0.954	0.939	0.946	0.676
	AutoBant	0.940	0.945	0.942	0.690
	SimBant	0.950	0.960	0.955	0.783
ALIE (40%)	ADAM	0.265	0.058	0.125	0.123
	FLTRUST	0.220	0.001	0.017	0.123
	RECESS	0.249	0.811	0.450	0.127
	ZENO	0.180	0.001	0.010	0.091
	CC	0.370	0.758	0.530	0.154
	CC+FBM	0.870	0.882	0.876	0.594
	CC+BUCKETING	0.890	0.850	0.870	0.587
	SAFEGUARD	0.150	0.000	0.010	0.123
	VR MARINA	0.200	0.001	0.012	0.108
	Bant	0.929	0.966	0.947	0.770
	AutoBant	0.861	0.924	0.892	0.585
	SimBant	0.943	0.949	0.946	0.705

Table 10: RESNET1D18 on ECG (1AVB).

	Algorithm	Sensitivity	Specificity	G-mean	f1-score
Without Attack	ADAM	0.896	0.871	0.884	0.335
	FLTRUST	0.857	0.883	0.870	0.344
	RECESS	0.909	0.870	0.889	0.337
	ZENO	0.890	0.883	0.886	0.353
	CC	0.864	0.896	0.880	0.371
	CC+FBM	0.888	0.868	0.877	0.353
	CC+BUCKETING	0.869	0.887	0.877	0.351
	SAFEGUARD	0.877	0.883	0.880	0.350
	VR MARINA	0.825	0.922	0.872	0.420
	Bant	0.831	0.916	0.873	0.408
	AutoBant	0.825	0.922	0.872	0.420
	FINETUNED	0.851	0.894	0.872	0.362
Label Flip (60%)	ADAM	0.210	0.002	0.022	0.069
	FLTRUST	0.870	0.903	0.886	0.388
	RECESS	0.210	0.001	0.017	0.113
	ZENO	0.400	0.039	0.125	0.309
	CC	0.290	0.120	0.187	0.112
	CC+FBM	0.725	0.866	0.792	0.265
	CC+BUCKETING	0.740	0.818	0.778	0.305
	SAFEGUARD	0.100	0.001	0.010	0.069
	VR MARINA	0.220	0.002	0.023	0.125
	Bant	0.812	0.934	0.871	0.455
	AutoBant	0.877	0.895	0.886	0.373
	FINETUNED	0.890	0.857	0.873	0.311
Sign Flip (60%)	ADAM	0.597	0.685	0.640	0.119
	FLTRUST	0.007	0.980	0.080	0.008
	RECESS	0.058	0.874	0.226	0.026
	ZENO	0.190	0.079	0.123	0.015
	CC	1.000	0.002	0.041	0.070
	CC+FBM	0.260	0.080	0.145	0.122
	CC+BUCKETING	0.250	0.076	0.138	0.117
	SAFEGUARD	0.981	0.030	0.170	0.070
	VR MARINA	0.130	0.058	0.087	0.065
	Bant	0.669	0.951	0.797	0.447
	AutoBant	0.916	0.845	0.879	0.301
	FINETUNED	0.617	0.616	0.616	0.103
Random Gradients (60%)	ADAM	0.220	0.005	0.036	0.074
	FLTRUST	1.000	0.001	0.027	0.069
	RECESS	0.468	0.757	0.595	0.117
	ZENO	0.220	0.061	0.116	0.098
	CC	0.909	0.227	0.455	0.080
	CC+FBM	0.610	0.390	0.487	0.362
	CC+BUCKETING	0.650	0.416	0.520	0.340
	SAFEGUARD	1.000	0.020	0.140	0.071
	VR MARINA	0.230	0.057	0.115	0.103
	Bant	0.805	0.919	0.860	0.405
	AutoBant	0.896	0.864	0.880	0.324
	FINETUNED	0.857	0.890	0.873	0.357
IPM (60 %)	ADAM	0.933	0.622	0.762	0.154
	FLTRUST	0.013	0.964	0.112	0.013
	RECESS	0.922	0.852	0.886	0.313
	ZENO	0.260	0.169	0.210	0.098
	CC	0.571	0.649	0.609	0.104
	CC+FBM	0.700	0.480	0.580	0.130
	CC+BUCKETING	0.610	0.374	0.478	0.142
	SAFEGUARD	0.050	0.001	0.008	0.078
	VR MARINA	0.200	0.036	0.085	0.115
	Bant	0.721	0.945	0.825	0.449
	AutoBant	0.890	0.865	0.877	0.323
	FINETUNED	0.857	0.893	0.875	0.363
IPM (80 %)	ADAM	0.312	0.580	0.425	0.050
	FLTRUST	0.201	0.751	0.389	0.051
	RECESS	0.558	0.508	0.533	0.076
	ZENO	0.240	0.065	0.125	0.110
	CC	0.857	0.310	0.515	0.084
	CC+FBM	0.220	0.220	0.038	0.113
	CC+BUCKETING	0.230	0.008	0.045	0.107
	SAFEGUARD	0.481	0.499	0.490	0.064
	VR MARINA	0.260	0.063	0.128	0.083
	Bant	0.857	0.884	0.870	0.345
	AutoBant	0.851	0.900	0.875	0.375
	FINETUNED	0.903	0.876	0.889	0.344
ALIE (40%)	ADAM	1.000	0.001	0.031	0.069
	FLTRUST	0.220	0.032	0.085	0.150
	RECESS	0.220	0.055	0.110	0.065
	ZENO	0.220	0.025	0.075	0.124
	CC	0.520	0.443	0.480	0.115
	CC+FBM	0.690	0.626	0.657	0.350
	CC+BUCKETING	0.700	0.585	0.640	0.380
	SAFEGUARD	1.000	0.000	0.000	0.069
	VR MARINA	0.200	0.001	0.010	0.103
	Bant	0.935	0.850	0.892	0.314
	AutoBant	0.818	0.888	0.852	0.339
	SimBant	0.968	0.818	0.890	0.282

Table 11: RESNET1D18 on ECG (PVC).

	Algorithm	Sensitivity	Specificity	G-mean	f1-score
Without Attack	ADAM	0.977	0.974	0.975	0.790
	FLTRUST	0.972	0.971	0.972	0.772
	RECESS	0.972	0.961	0.967	0.720
	ZENO	0.977	0.975	0.976	0.801
	CC	0.972	0.959	0.965	0.707
	CC+FBM	0.960	0.980	0.970	0.755
	CC+BUCKETING	0.950	0.986	0.968	0.740
	SAFEGUARD	0.977	0.965	0.971	0.743
	VR MARINA	0.240	0.060	0.120	0.098
	Bant	0.931	0.981	0.955	0.810
	AutoBant	0.972	0.970	0.971	0.765
	FINETUNED	0.963	0.971	0.967	0.770
Label Flip (60%)	ADAM	0.639	0.710	0.673	0.180
	FLTRUST	0.220	0.059	0.114	0.096
	RECESS	0.931	0.937	0.934	0.596
	ZENO	0.310	0.037	0.108	0.210
	CC	0.005	0.999	0.068	0.009
	CC+FBM	0.930	0.920	0.925	0.760
	CC+BUCKETING	0.910	0.910	0.910	0.735
	SAFEGUARD	0.981	0.971	0.976	0.782
	VR MARINA	0.200	0.036	0.085	0.115
	Bant	0.870	0.979	0.923	0.767
	AutoBant	0.972	0.976	0.974	0.805
	FINETUNED	0.944	0.957	0.951	0.686
Sign Flip (60%)	ADAM	0.639	0.710	0.673	0.180
	FLTRUST	0.220	0.032	0.085	0.118
	RECESS	0.931	0.937	0.934	0.596
	ZENO	0.190	0.069	0.115	0.010
	CC	0.005	0.999	0.068	0.009
	CC+FBM	0.250	0.072	0.135	0.117
	CC+BUCKETING	0.230	0.055	0.113	0.096
	SAFEGUARD	0.981	0.971	0.976	0.782
	VR MARINA	0.120	0.035	0.065	0.010
	Bant	0.870	0.979	0.923	0.767
	AutoBant	0.972	0.976	0.974	0.805
	FINETUNED	0.944	0.957	0.951	0.686
Random Gradients (60%)	ADAM	0.220	0.005	0.035	0.120
	FLTRUST	0.220	0.063	0.118	0.110
	RECESS	0.255	0.845	0.464	0.122
	ZENO	0.180	0.053	0.098	0.010
	CC	0.250	0.048	0.110	0.130
	CC+FBM	0.270	0.083	0.150	0.117
	CC+BUCKETING	0.220	0.043	0.098	0.123
	SAFEGUARD	0.009	0.997	0.096	0.017
	VR MARINA	0.120	0.037	0.067	0.010
	Bant	0.944	0.969	0.957	0.747
	AutoBant	0.963	0.978	0.970	0.809
	FINETUNED	0.963	0.945	0.954	0.644
IPM (60 %)	ADAM	0.796	0.976	0.882	0.708
	FLTRUST	0.240	0.046	0.106	0.114
	RECESS	0.944	0.938	0.941	0.608
	ZENO	0.220	0.025	0.075	0.124
	CC	0.944	0.933	0.939	0.590
	CC+FBM	0.930	0.960	0.945	0.625
	CC+BUCKETING	0.930	0.950	0.940	0.610
	SAFEGUARD	0.782	0.217	0.412	0.095
	VR MARINA	0.190	0.037	0.084	0.115
	Bant	0.931	0.977	0.954	0.790
	AutoBant	0.949	0.971	0.960	0.762
	FINETUNED	0.954	0.965	0.959	0.729
IPM (80 %)	ADAM	0.958	0.005	0.069	0.093
	FLTRUST	0.005	0.991	0.068	0.008
	RECESS	0.426	0.502	0.462	0.079
	ZENO	0.300	0.225	0.260	0.108
	CC	0.463	0.265	0.350	0.061
	CC+FBM	0.220	0.010	0.047	0.114
	CC+BUCKETING	0.200	0.006	0.035	0.105
	SAFEGUARD	0.065	0.831	0.232	0.031
	VR MARINA	0.210	0.063	0.115	0.086
	Bant	0.931	0.980	0.955	0.807
	AutoBant	0.970	0.965	0.968	0.820
	FINETUNED	0.963	0.937	0.950	0.611
ALIE (40%)	ADAM	0.200	0.021	0.065	0.120
	FLTRUST	0.398	0.581	0.481	0.086
	RECESS	0.200	0.028	0.075	0.135
	ZENO	0.190	0.063	0.110	0.078
	CC	0.913	0.116	0.325	0.084
	CC+FBM	0.880	0.821	0.850	0.580
	CC+BUCKETING	0.890	0.870	0.880	0.610
	SAFEGUARD	0.218	0.881	0.438	0.126
	VR MARINA	0.240	0.064	0.124	0.105
	Bant	0.954	0.955	0.954	0.680
	AutoBant	0.954	0.981	0.967	0.826
	FINETUNED	0.917	0.954	0.935	0.658

Table 12: RESNET1D18 on ECG (CLBBB).

	Algorithm	Sensitivity	Specificity	G-mean	f1-score
Without Attack	ADAM	0.979	0.957	0.968	0.508
	FLTRUST	0.990	0.947	0.968	0.462
	RECESS	0.969	0.963	0.966	0.538
	ZENO	0.990	0.957	0.973	0.509
	CC	0.979	0.945	0.962	0.445
	CC+FBM	0.970	0.970	0.970	0.480
	CC+BUCKETING	0.950	0.950	0.950	0.465
	SAFEGUARD	0.990	0.961	0.975	0.537
	VR MARINA	0.220	0.021	0.068	0.117
	Bant	0.990	0.947	0.968	0.460
	AutoBant	0.989	0.936	0.962	0.415
	FINETUNED	0.990	0.953	0.971	0.491
Label Flip (60%)	ADAM	0.220	0.065	0.120	0.115
	FLTRUST	0.198	0.630	0.353	0.023
	RECESS	0.021	0.873	0.135	0.006
	ZENO	0.190	0.084	0.127	0.005
	CC	0.764	0.854	0.808	0.199
	CC+FBM	0.860	0.800	0.830	0.210
	CC+BUCKETING	0.790	0.830	0.810	0.214
	SAFEGUARD	0.989	0.958	0.974	0.517
	VR MARINA	0.260	0.042	0.105	0.125
	Bant	0.990	0.923	0.956	0.370
	AutoBant	0.990	0.955	0.972	0.502
	FINETUNED	0.990	0.952	0.971	0.487
Sign Flip (60%)	ADAM	1.000	0.001	0.027	0.044
	FLTRUST	0.865	0.747	0.804	0.134
	RECESS	0.220	0.102	0.150	0.044
	ZENO	0.250	0.193	0.220	0.054
	CC	0.260	0.177	0.215	0.117
	CC+FBM	0.320	0.204	0.256	0.117
	CC+BUCKETING	0.300	0.052	0.125	0.240
	SAFEGUARD	0.698	0.617	0.656	0.076
	VR MARINA	0.210	0.029	0.078	0.112
	Bant	0.979	0.944	0.962	0.444
	AutoBant	0.969	0.934	0.951	0.401
	FINETUNED	0.969	0.958	0.964	0.512
Random Gradients (60%)	ADAM	1.000	0.007	0.085	0.044
	FLTRUST	1.000	0.003	0.054	0.044
	RECESS	0.427	0.963	0.641	0.282
	ZENO	0.310	0.054	0.130	0.210
	CC	0.130	0.120	0.125	0.044
	CC+FBM	0.310	0.201	0.250	0.130
	CC+BUCKETING	0.190	0.170	0.180	0.054
	SAFEGUARD	0.052	0.987	0.227	0.064
	VR MARINA	0.210	0.030	0.080	0.112
	Bant	0.990	0.948	0.969	0.465
	AutoBant	0.990	0.931	0.960	0.396
	FINETUNED	0.990	0.971	0.980	0.607
IPM (60 %)	ADAM	0.979	0.957	0.968	0.511
	FLTRUST	0.979	0.296	0.538	0.060
	RECESS	0.958	0.945	0.951	0.438
	ZENO	0.330	0.027	0.095	0.215
	CC	0.958	0.950	0.954	0.465
	CC+FBM	0.950	0.940	0.945	0.440
	CC+BUCKETING	0.940	0.936	0.938	0.460
	SAFEGUARD	0.979	0.539	0.727	0.089
	VR MARINA	0.230	0.041	0.098	0.115
	Bant	0.813	0.982	0.893	0.629
	AutoBant	0.979	0.941	0.960	0.429
	FINETUNED	0.938	0.930	0.934	0.376
IPM (80 %)	ADAM	0.073	0.506	0.192	0.006
	FLTRUST	0.330	0.017	0.075	0.210
	RECESS	0.042	0.952	0.199	0.026
	ZENO	0.230	0.141	0.180	0.048
	CC	0.073	0.884	0.254	0.024
	CC+FBM	0.190	0.075	0.120	0.065
	CC+BUCKETING	0.220	0.200	0.210	0.020
	SAFEGUARD	1.000	0.002	0.046	0.044
	VR MARINA	0.220	0.005	0.035	0.118
	Bant	0.990	0.951	0.970	0.481
	AutoBant	0.979	0.947	0.963	0.459
	FINETUNED	0.990	0.943	0.966	0.441
ALIE (40%)	ADAM	0.250	0.176	0.210	0.123
	FLTRUST	0.220	0.089	0.140	0.065
	RECESS	1.000	0.005	0.071	0.044
	ZENO	0.220	0.032	0.085	0.114
	CC	0.460	0.599	0.525	0.160
	CC+FBM	0.490	0.470	0.480	0.210
	CC+BUCKETING	0.540	0.463	0.500	0.120
	SAFEGUARD	0.220	0.060	0.115	0.087
	VR MARINA	0.200	0.078	0.125	0.072
	Bant	0.979	0.968	0.973	0.578
	AutoBant	1.000	0.814	0.902	0.198
	FINETUNED	0.958	0.957	0.958	0.501

A.5 Learning-to-rank Experiments

In the main body, we introduced our approach and presented a subset of results for the Learning-to-Rank (LTR) task under Byzantine settings. Here, we expand on the experimental setup, covering all baseline models and proposed methods across the full spectrum of adversarial scenarios considered.

Problem Formulation. The LTR task is defined over a set of queries \mathcal{Q} , where each query $q \in \mathcal{Q}$ is associated with a set of documents D_q . For each document $d_i \in D_q$, a feature vector x_i and a relevance label $y_i \in \{0, \dots, r-1\}$ are provided. The objective is to learn a scoring function $f(x; \theta)$ such that, for any query q , the induced ordering of scores $s_i = f(x_i; \theta)$ approximates the ideal relevance ordering.

We use the Normalized Discounted Cumulative Gain at cutoff k (NDCG@ k) to assess ranking quality. First, we define the Discounted Cumulative Gain (DCG@ k) for a ranking π (a permutation of documents based on predicted scores) as:

$$\text{DCG}@k = \sum_{i=1}^k \frac{2^{y_{\pi(i)}} - 1}{\log_2(i + 1)},$$

where $y_{\pi(i)}$ is the relevance label of the document ranked at position i . This formulation assigns higher weight to highly relevant documents that appear earlier in the ranking, with a logarithmic discount applied to lower positions.

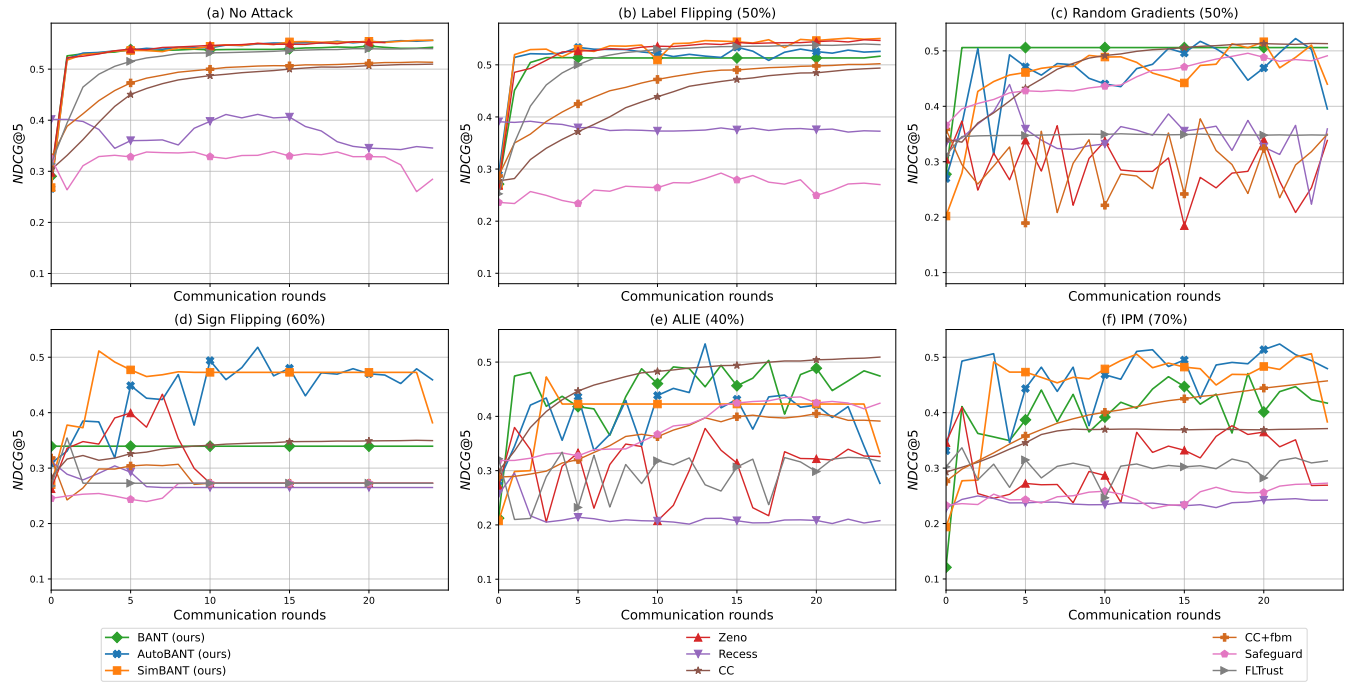


Figure 10: Test NDCG@5 for TRANSFORMER on the Learning-to-Rank task.

The Ideal DCG (IDCG@ k) is the maximum possible DCG@ k obtained by sorting documents in descending order of their true relevance labels.

The final evaluation metric, Normalized DCG (NDCG@ k), is computed as:

$$\text{NDCG}@k = \frac{\text{DCG}@k}{\text{IDCG}@k}.$$

This normalization bounds the metric between 0 and 1, where 1 indicates a perfect ranking.

Experimental Scope. We evaluate models on the WEB30K dataset (Qin and Liu 2013), a standard benchmark for LTR consisting of 30,000 queries with graded relevance labels. While the main section highlights our method’s applicability to LTR, here we provide complete validation across:

- Baseline defenses, including ZENO, RECESS, CENTERED CLIP, SAFEGUARD and FLTRUST.
- Our proposed methods: Bant, AutoBant, and SimBant.
- All adversarial scenarios introduced in the main paper: Label Flipping, Sign Flipping, Random Gradients, IPM, and ALIE.

For consistency with ZENO’s assumptions, we set the threshold for Byzantine tolerance to $|\mathcal{B}| = 0.5n$, where n is the number of clients as it is unknown a priori. While ZENO might perform well when the fraction of adversarial clients is close to 50%, it suffers significant degradation (or divergence) when this assumption is violated. This sensitivity underscores the need for defenses that do not rely on tight prior knowledge of Byzantine ratios.

B Notation

The following sections will be dedicated to the theoretical proof of all aspects discussed in the main body of the paper. In order to facilitate the understanding of the proofs presented in the appendix, as well as to simplify the interaction with all the formulas throughout this paper, we provide a comprehensive list of notation used in this study in the form of the following table.

Table 13: Notation Reference.

N	Number of samples in the trial function	γ	Learning rate (stepsize) in optimization	\hat{f}	Trial loss function on the server	$\mathbb{I}_{[a>0]}$	Indicator function taking value 1 if $a > 0$, otherwise 0
d	Dimensionality of the parameter space \mathbb{R}^d	L	Smoothness constant (3.1)	f	Objective function $f(x)$ in distributed learning	\tilde{P}^t	Adaptive preconditioner matrix at iteration t
$n = n(t)$	Number of workers in the distributed system	μ	Strong convexity constant (3.2(a))	f_i	Local objective function on i -th worker	$\langle a, b \rangle_{\hat{P}}$	Weighted inner product with \hat{P}
$\mathcal{G}(t)$	Set of honest workers	β	Momentum parameter for weights ω_i^t	f_1	Local objective function on the server	α	Lower bound on the preconditioner (F.1)
$G(t) = \mathcal{G}(t) $	Number of honest workers	δ	Approximation error in arg min finding (2)	g_i	Stochastic gradient of worker i	Γ	Upper bound on the preconditioner (F.1)
$\mathcal{B}(t)$	Set of Byzantine workers	δ_1	(δ_1, δ_2) —heterogeneity parameter (3.4)	g_i^t	Gradient from worker i at iteration t	$\ \cdot\ _\infty$	$\max_{1 \leq i \leq d} \cdot _i$
$B(t) = \mathcal{B}(t) $	Number of Byzantine workers	δ_2	(δ_1, δ_2) —heterogeneity parameter (3.4)	x^*	Optimal solution of the objective function	Δ_d^1	d -dimensional simplex constraint on weights
t	Current iteration number	σ^2	Variance of stochastic gradients (3.3)	\bar{x}^t	$\frac{1}{G} \sum_{i \in \mathcal{G}} x_i^t$	ω_i^t	Weight assigned to worker i at iteration t
T	Total number of iterations in training	l	Local round length	$\mathcal{KL}(p q)$	Kullback-Leibler divergence between distributions p and q	$[\cdot]_0$	Non-negative projection: $\max\{0, \cdot\}$
\mathcal{X}	Domain: $x \in \mathcal{X}$	\mathcal{F}	function class $\mathcal{F} : \xi \mapsto \nabla f(x; \xi), x \in \mathcal{X}$	V^t	$\frac{1}{G} \sum_{i \in \mathcal{G}} \ x_i^t - \bar{x}^t\ ^2$	ε	Radius of balls in the covering net in Lemma C.1
$\mathcal{W} = \mathcal{W}(t)$	Number of workers	G	$\min_{t \leq T} G(t)$	S	Bound on \mathcal{X} in Lemma C.1	$\ \cdot\ $	If not specified other, $\ \cdot\ _2 = \sqrt{\langle \cdot, \cdot \rangle}$

C General Inequalities and Lemmas

First, mention important inequalities that are used in further proofs. Consider a function f satisfying Assumption 3.1, g satisfying Assumptions 3.2(a) and φ complying with Assumption 3.2(b). Then for any i in the real numbers and for all vectors x, y, x_i in \mathbb{R}^n with a positive scalar p , the following inequalities hold.

$$|\langle x, y \rangle| \leq \frac{\|x\|^2}{2p} + \frac{p\|y\|^2}{2} \quad (\text{Young})$$

$$\begin{aligned} -\langle x, y \rangle &= -\frac{\|x\|^2}{2} - \frac{\|y\|^2}{2} + \frac{\|x - y\|^2}{2} \\ \|x + y\|^2 &= \|x\|^2 + \|y\|^2 + 2\langle x, y \rangle \end{aligned} \quad (\text{Norm})$$

$$g(y) \geq g(x) - \langle \nabla g(y), x - y \rangle - \frac{1}{2\mu} \|\nabla g(x) - \nabla g(y)\|^2 \quad (\mu\text{-Conv})$$

$$\begin{aligned} \varphi(y) &\geq \varphi(x) + \langle \nabla \varphi(x), y - x \rangle \\ 0 &\geq \langle \nabla \varphi(x) - \nabla \varphi(y), y - x \rangle \end{aligned} \quad (\text{Conv})$$

$$\begin{aligned} \|\nabla f(x) - \nabla f(y)\|^2 &\leq L^2 \|x - y\|^2 \\ f(x) &\leq f(y) + \langle \nabla f(y), x - y \rangle + \frac{L}{2} \|x - y\|^2 \\ f(x) &\leq f(y) - \langle \nabla f(x), y - x \rangle - \frac{1}{2L} \|\nabla f(x) - \nabla f(y)\|^2 \end{aligned} \quad (\text{Lip})$$

$$\begin{aligned} \left\| \sum_{i=1}^n x_i \right\|^2 &\leq n \sum_{i=1}^n \|x_i\|^2 \\ \|x + y\|^2 &\leq (1 + p)\|x\|^2 + \left(1 + \frac{1}{p}\right)\|y\|^2 \end{aligned} \quad (\text{CS})$$

$$\varphi\left(\frac{\sum_{i=1}^n w_i x_i}{\sum_{i=1}^n w_i}\right) \leq \frac{\sum_{i=1}^n w_i \varphi(x_i)}{\sum_{i=1}^n w_i} \quad (\text{Jen})$$

This section delineates a series of lemmas that form the cornerstone of our subsequent proofs. These lemmas encapsulate critical properties and bounds that are instrumental in establishing the theorems elaborated later in this paper.

The following lemma addresses a critical issue concerning the evaluation of the trial function and its deviation from ∇f_1 . As highlighted in the main part of our work, existing literature frequently overlooks the additional term in convergence that arises when employing a trial function. In this study, we rectify this oversight, thereby providing a more comprehensive understanding of the convergence behavior associated with trial functions.

Lemma C.1. *Suppose Assumption 3.1 holds. Then for all $x \in \mathcal{X} \subset \mathbb{R}^d$ with probability of at least $1 - \tilde{\delta}$ over a sample of size N , the following estimate, linking the trial function with the objective function on the server, is valid:*

$$\|\nabla f_1(x) - \nabla \hat{f}(x)\|_2^2 \leq \zeta(N) = \tilde{\mathcal{O}}\left(\frac{1}{N}\right),$$

Proof. Given the norm inequality $\|\cdot\|_2 \leq \sqrt{d} \cdot \|\cdot\|_\infty$, we can recast the scalar product in the following manner:

$$\|\nabla f_1(x) - \nabla \hat{f}(x)\|_2^2 \leq d \cdot \|\nabla f_1(x) - \nabla \hat{f}(x)\|_\infty^2. \quad (4)$$

To establish the uniform convergence of $\|\nabla f_1(x) - \nabla \hat{f}(x)\|_\infty^2$, we employ Theorem 5 from (Shalev-Shwartz et al. 2009). This theorem provides a bound on the ℓ_∞ -covering number of the function class $\mathcal{F} = \{\xi \mapsto \nabla f_1(x; \xi) \mid x \in \mathcal{X}\}$. Given that \mathcal{X} resides within an ℓ_2 -sphere, let us define it bound by S , the covering number for \mathcal{X} using the Euclidean metric $d_2(x_i, x_j) = \|x_i - x_j\|_2$ is constrained as follows for $d > 3$:

$$N(\varepsilon, \mathcal{X}, d_2) = \mathcal{O}\left(d^2 \left(\frac{S}{\varepsilon}\right)^d\right).$$

In evaluating the covering numbers for \mathcal{F} under the ℓ_∞ metric, where $\|\nabla f_1(x_i; \cdot) - \nabla f_1(x_j; \cdot)\|_\infty = \sup_\xi |\nabla f_1(x_i; \xi) - \nabla f_1(x_j; \xi)|$, the L -smoothness property facilitates the following assertion:

$$\forall x_i, x_j \in \mathcal{X} \hookrightarrow \|\nabla f_1(x_i; \cdot) - \nabla f_1(x_j; \cdot)\|_\infty \leq \|\nabla f_1(x_i; \cdot) - \nabla f_1(x_j; \cdot)\|_2 \leq L\|x_i - x_j\|.$$

This indicates that an ε -net for \mathcal{X} in d_2 space concurrently serves as an $L\varepsilon$ -net for \mathcal{F} in d_∞ space:

$$N(\varepsilon, \mathcal{F}, d_\infty) \leq N(\varepsilon/L, \mathcal{X}, d_2) = \mathcal{O}\left(d^2 \left(\frac{LS}{\varepsilon}\right)^d\right).$$

Following this analysis, we derive an estimation consistent with the findings in (Shalev-Shwartz et al. 2009):

$$\|\nabla f_1(x) - \nabla \hat{f}(x)\|_\infty^2 = \tilde{\mathcal{O}}\left(\frac{1}{N}\right).$$

Defining the notation

$$\zeta(N) \stackrel{\text{def}}{=} \tilde{\mathcal{O}}\left(\frac{1}{N}\right),$$

and substituting this into (4) concludes the proof of the lemma. □

This lemma is technical in nature, and we significantly benefit from the assertion established in the previous lemma. Ultimately, we derive an important estimate for the scalar product, which appears in many subsequent proofs throughout this work.

Lemma C.2. *Suppose Assumption 3.1 holds. Then for all $x \in \mathbb{R}^d$ and $g_i = g_i(x, \xi_i)$, the following estimate is valid:*

$$-\gamma \left\langle \nabla \hat{f}(x), \frac{1}{G} \sum_{i \in \mathcal{G}} \nabla f_i(x) \right\rangle \leq -\frac{\gamma}{2} \|\nabla f(x)\|^2 + \gamma \cdot \zeta(N) + \frac{3\gamma}{2} (\delta_1 + \delta_2 \|\nabla f(x^t)\|^2).$$

Proof. We commence by examining the difference $\nabla f(x) - \nabla \hat{f}(x)$:

$$\begin{aligned} -\gamma \left\langle \nabla \hat{f}(x), \frac{1}{G} \sum_{i \in \mathcal{G}} \nabla f_i(x) \right\rangle &= \gamma \left\langle \nabla f(x) - \nabla \hat{f}(x), \frac{1}{G} \sum_{i \in \mathcal{G}} \nabla f_i(x) \right\rangle \\ &\quad - \gamma \left\langle \nabla f(x), \frac{1}{G} \sum_{i \in \mathcal{G}} \nabla f_i(x) \right\rangle. \end{aligned}$$

Next, we continue with further manipulations on the first term:

$$\gamma \left\langle \nabla f(x) - \nabla \hat{f}(x), \frac{1}{G} \sum_{i \in \mathcal{G}} \nabla f_i(x) \right\rangle$$

$$\begin{aligned}
& \stackrel{\text{(Young)}}{\leq} \frac{\gamma}{2} \left\| \nabla f(x) - \nabla \hat{f}(x) \right\|^2 + \frac{\gamma}{2} \left\| \frac{1}{G} \sum_{i \in \mathcal{G}} \nabla f_i(x) \right\|^2 \\
& \stackrel{\text{(Young)}}{\leq} \frac{\gamma}{2} \left(\left\| \nabla f(x) - \nabla f_1(x) \right\|^2 + \left\| \nabla f_1(x) - \nabla \hat{f}(x) \right\|^2 \right) + \frac{\gamma}{2} \left\| \frac{1}{G} \sum_{i \in \mathcal{G}} \nabla f_i(x) \right\|^2 \\
& \stackrel{\text{(Lemma C.1)}}{\leq} \gamma \left(\zeta(N) + \delta_1 + \delta_2 \left\| \nabla f(x) \right\|^2 \right) + \frac{\gamma}{2} \left\| \frac{1}{G} \sum_{i \in \mathcal{G}} \nabla f_i(x) \right\|^2,
\end{aligned}$$

and with the second term,

$$\begin{aligned}
-\gamma \left\langle \nabla f(x), \frac{1}{G} \sum_{i \in \mathcal{G}} \nabla f_i(x) \right\rangle & \stackrel{\text{(Norm)}}{=} -\frac{\gamma}{2} \left\| \nabla f(x) \right\|^2 - \frac{\gamma}{2} \left\| \frac{1}{G} \sum_{i \in \mathcal{G}} \nabla f_i(x) \right\|^2 \\
& \quad + \frac{\gamma}{2} \left\| \frac{1}{G} \sum_{i \in \mathcal{G}} (\nabla f_i(x) - \nabla f(x)) \right\|^2 \\
& \stackrel{\text{(CS)}}{\leq} -\frac{\gamma}{2} \left\| \nabla f(x) \right\|^2 - \frac{\gamma}{2} \left\| \frac{1}{G} \sum_{i \in \mathcal{G}} \nabla f_i(x) \right\|^2 \\
& \quad + \frac{\gamma}{2G} \sum_{i \in \mathcal{G}} \left\| \nabla f_i(x) - \nabla f(x) \right\|^2 \\
& \stackrel{\text{(Ass. 3.4)}}{\leq} -\frac{\gamma}{2} \left\| \nabla f(x) \right\|^2 - \frac{\gamma}{2} \left\| \frac{1}{G} \sum_{i \in \mathcal{G}} \nabla f_i(x) \right\|^2 \\
& \quad + \frac{\gamma}{2} \left(\delta_1 + \delta_2 \left\| \nabla f(x) \right\|^2 \right).
\end{aligned}$$

In summary, this supports the claim of the lemma. \square

With this, we conclude the discussion of general statements. They are frequently used in our proofs in the upcoming sections of the Appendix. Next, we begin the examination of each method obtained individually.

D Proofs of Bant

In this section, we explore the theoretical underpinnings of the first proposed method, Bant . As outlined in Algorithm 1, this step diverges from the standard SGD approach primarily due to the distinct weight distribution that we subsequently allocate to the devices. Consequently, it is essential to conduct an analysis that takes this particular characteristic into account. To achieve final convergence rate, we demonstrate a supporting lemma that reinforces our findings.

Lemma D.1. *Under Assumptions 3.1, 3.2(b), 3.5, the following holds for the iteration of Algorithm 1:*

$$\hat{f}(x^{t+1}) \leq \hat{f}(x^t) - \frac{\gamma\beta}{n} \left\langle \nabla \hat{f}(x^t), \sum_{i \in \mathcal{G}} g_i^t \right\rangle + \frac{L\gamma^2\beta}{2n} \sum_{i \in \mathcal{G}} \|g_i^t\|^2.$$

Proof. Actually, the update step of the algorithm 1 is given by:

$$x^{t+1} = x^t - \gamma \sum_{i=1}^n \mathbb{I}_{[\theta_i^t > 0]} \omega_i^t g_i^t,$$

where $g_i^t = g_i(x^t, \xi_i^t)$ and $\sum_{i=1}^n \omega_i^t = 1$. Applying Jensen's inequality for the convex function \hat{f} (Assumption 3.2(b)) and denoting $\bar{\omega}_i^t = \frac{[\theta_i^t]_0}{\sum_{j=1}^n [\theta_j^t]_0}$:

$$\begin{aligned} \hat{f}(x^{t+1}) &= \hat{f}\left(\sum_{i=1}^n \omega_i^t \left[x^t - \gamma \mathbb{I}_{[\theta_i^t > 0]} g_i^t\right]\right) \\ &\leq \sum_{i=1}^n \omega_i^t \hat{f}\left(x^t - \gamma \mathbb{I}_{[\theta_i^t > 0]} g_i^t\right) \\ &= \sum_{i \in \mathcal{B}} \omega_i^t \hat{f}\left(x^t - \gamma \mathbb{I}_{[\theta_i^t > 0]} g_i^t\right) + \sum_{i \in \mathcal{G}} \omega_i^t \hat{f}\left(x^t - \gamma \mathbb{I}_{[\theta_i^t > 0]} g_i^t\right) \\ &\leq \sum_{i \in \mathcal{B}} (1 - \beta) \omega_i^{t-1} \hat{f}(x^t) + \sum_{i \in \mathcal{B}} \beta \bar{\omega}_i^t \hat{f}\left(x^t - \gamma \mathbb{I}_{[\theta_i^t > 0]} g_i^t\right) \\ &\quad + \sum_{i \in \mathcal{G}} (1 - \beta) \omega_i^{t-1} \hat{f}(x^t) + \sum_{i \in \mathcal{G}} \beta \bar{\omega}_i^t \hat{f}\left(x^t - \gamma \mathbb{I}_{[\theta_i^t > 0]} g_i^t\right) \\ &= (1 - \beta) \hat{f}(x^t) + \sum_{i \in \mathcal{B}} \beta \bar{\omega}_i^t \hat{f}\left(x^t - \gamma \mathbb{I}_{[\theta_i^t > 0]} g_i^t\right) + \sum_{i \in \mathcal{G}} \beta \bar{\omega}_i^t \hat{f}\left(x^t - \gamma \mathbb{I}_{[\theta_i^t > 0]} g_i^t\right). \end{aligned}$$

In the inequality above, we make an estimation $\hat{f}\left(x^t - \gamma \mathbb{I}_{[\theta_i^t > 0]} g_i^t\right) \leq \hat{f}(x^t)$, since the indicator guarantees us that we do not increase the trial function \hat{f} by performing a step. By eliminating the weights ω_i^{t-1} accumulated from past iterations, we can rearrange the coefficients between Byzantine and honest workers in such a way that honest workers have higher weights. To achieve this, we sort the honest workers by increasing values of \hat{f} and assign them coefficients ω_i in decreasing order. This permutation ensures that honest workers have higher weights and Byzantine workers have lower weights. This operation is valid because if $\bar{\omega}$ for some Byzantine worker is higher than for a honest worker, then this Byzantine has a greater influence on \hat{f} , and changing the weights would worsen the overall influence of these two workers. Therefore, with new weights $\{\bar{\omega}_i^t\}_{i=1}^n$:

$$\begin{aligned} \hat{f}(x^{t+1}) &\leq (1 - \beta) \hat{f}(x^t) + \sum_{i \in \mathcal{B}} \beta \bar{\omega}_i^t \hat{f}\left(x^t - \gamma \mathbb{I}_{[\theta_i^t > 0]} g_i^t\right) \\ &\quad + \sum_{i \in \mathcal{G}} \beta \bar{\omega}_i^t \hat{f}\left(x^t - \gamma \mathbb{I}_{[\theta_i^t > 0]} g_i^t\right) \\ &\leq (1 - \beta) \hat{f}(x^t) + \sum_{i \in \mathcal{B}} \beta \bar{\omega}_i^t \hat{f}(x^t) + \sum_{i \in \mathcal{G}} \beta \bar{\omega}_i^t \hat{f}\left(x^t - \gamma \mathbb{I}_{[\theta_i^t > 0]} g_i^t\right) \\ &= \hat{f}(x^t) + (1 - \beta) \left[\hat{f}(x^t) - \hat{f}(x^t)\right] + \sum_{i \in \mathcal{B}} \beta \bar{\omega}_i^t \left[\hat{f}(x^t) - \hat{f}(x^t)\right] \\ &\quad + \sum_{i \in \mathcal{G}} \beta \bar{\omega}_i^t \left[\hat{f}\left(x^t - \gamma \mathbb{I}_{[\theta_i^t > 0]} g_i^t\right) - \hat{f}(x^t)\right]. \end{aligned}$$

Let us assign the coefficient $1/n$ to all honest workers. This procedure is also valid. We sorted the weights and honest workers now have the greatest weights, thus, the sum of the coefficients of honest workers is at least G/n . Moreover, the honest workers

with the stronger influence have the greater weights which allows to equalize the total weight G/n between all G workers. Thus, we get

$$\hat{f}(x^{t+1}) \leq \hat{f}(x^t) + \frac{\beta}{n} \sum_{i \in \mathcal{G}} \left[\hat{f}(x^t - \gamma \mathbb{I}_{[\theta_i^t > 0]} g_i^t) - \hat{f}(x^t) \right].$$

Now we can remove the indicator function because if g_i^t minimizes the trial function, the indicator equals 1. If g_i^t maximizes the trial function, the indicator excludes this gradient. However, we still account for it and maximize the trial function, thus:

$$\begin{aligned} \hat{f}(x^{t+1}) &\leq \hat{f}(x^t) + \frac{\beta}{n} \sum_{i \in \mathcal{G}} \left[\hat{f}(x^t - \gamma g_i^t) - \hat{f}(x^t) \right] \\ &\stackrel{(\text{Lip})}{\leq} \hat{f}(x^t) + \frac{\beta}{n} \sum_{i \in \mathcal{G}} \left[\hat{f}(x^t) - \gamma \langle \nabla \hat{f}(x^t), g_i^t \rangle + \frac{L\gamma^2}{2} \|g_i^t\|^2 - \hat{f}(x^t) \right] \\ &= \hat{f}(x^t) - \frac{\gamma\beta}{n} \left\langle \nabla \hat{f}(x^t), \sum_{i \in \mathcal{G}} g_i^t \right\rangle + \frac{L\gamma^2\beta}{2n} \sum_{i \in \mathcal{G}} \|g_i^t\|^2. \end{aligned}$$

□

We are now prepared to present the final result for the convex case. This theorem was introduced in the main part of our work, however, we will reiterate its formulation once more.

Theorem 4.1. *Under Assumptions 3.1, 3.2(b), 3.3, 3.4 with $\delta_2 \leq \frac{1}{12}$, 3.5, for solving the problem described in the equation (1) after T iterations of Algorithm 1 with $\gamma \leq \frac{1}{13L}$, the following holds:*

$$\frac{1}{T} \sum_{t=0}^{T-1} \mathbb{E} \|\nabla f(x^t)\|^2 \leq \frac{\mathbb{E} [\hat{f}(x^0) - \hat{f}(\hat{x}^*)]}{\gamma T} \cdot \frac{4n}{\beta G} + 3\delta_1 + 6L\gamma\sigma^2 + 4\zeta(N).$$

Proof. According to the lemma (D.1):

$$\hat{f}(x^{t+1}) \leq \hat{f}(x^t) - \gamma\beta \left\langle \nabla \hat{f}(x^t), \frac{1}{n} \sum_{i \in \mathcal{G}} \nabla g_i^t \right\rangle + \frac{L\gamma^2\beta}{2n} \sum_{i \in \mathcal{G}} \|g_i^t\|^2.$$

Taking the expectation of both sides of the inequality:

$$\begin{aligned} \mathbb{E} \hat{f}(x^{t+1}) &\leq \mathbb{E} \hat{f}(x^t) - \gamma\beta \cdot \frac{G}{n} \left\langle \nabla \hat{f}(x^t), \frac{1}{G} \sum_{i \in \mathcal{G}} \nabla f_i(x^t) \right\rangle + \frac{L\gamma^2\beta}{2n} \sum_{i \in \mathcal{G}} \mathbb{E} \|g_i^t\|^2 \\ &\stackrel{(\text{Lemma C.2})}{\leq} \mathbb{E} \hat{f}(x^t) + \frac{\gamma\beta G}{n} \zeta(N) - \frac{\gamma\beta G}{2n} \|\nabla f(x^t)\|^2 \\ &\quad + \frac{3\gamma\beta G}{2n} (\delta_1 + \delta_2 \|\nabla f(x^t)\|^2) + \frac{L\gamma^2\beta}{2n} \sum_{i \in \mathcal{G}} \mathbb{E} \|g_i^t\|^2 \\ &\stackrel{(\text{CS})}{\leq} \mathbb{E} \hat{f}(x^t) + \frac{\gamma\beta G}{n} \zeta(N) - \frac{\gamma\beta G}{2n} \|\nabla f(x^t)\|^2 \\ &\quad + \frac{3\gamma\beta G}{2n} (\delta_1 + \delta_2 \|\nabla f(x^t)\|^2) \\ &\quad + \frac{3L\gamma^2\beta}{2n} \left(\sum_{i \in \mathcal{G}} \mathbb{E} \|\nabla f(x^t) - f_i(x^t)\|^2 + \sum_{i \in \mathcal{G}} \mathbb{E} \|\nabla f_i(x^t) - g_i^t\|^2 \right) \\ &\quad + \frac{3L\gamma^2\beta G}{2n} \|\nabla f(x^t)\|^2 \\ &\stackrel{(\text{Ass. 3.3, 3.4})}{\leq} \mathbb{E} \hat{f}(x^t) + \frac{\gamma\beta G}{n} \zeta(N) - \frac{\gamma\beta G}{2n} \|\nabla f(x^t)\|^2 + \frac{3\gamma\beta G}{2n} (\delta_1 + \delta_2 \|\nabla f(x^t)\|^2) \\ &\quad + \frac{3L\gamma^2\beta G}{2n} (\delta_1 + \delta_2 \|\nabla f(x^t)\|^2 + \sigma^2) + \frac{3L\gamma^2\beta G}{2n} \|\nabla f(x^t)\|^2 \\ &\stackrel{(\text{Ass. 3.3})}{\leq} \mathbb{E} [\hat{f}(x^t)] - \frac{\gamma\beta G}{2n} [1 - 3L\gamma - (3 + 3L\gamma)\delta_2] \|\nabla f(x^t)\|^2 \end{aligned}$$

$$+ \frac{\gamma\beta G}{2n}(3 + 3L\gamma)\delta_1 + \frac{3\gamma^2\beta LG}{2n}\sigma^2 + \frac{\gamma\beta G}{n}\zeta(N).$$

We first fix $\delta_2 \leq \frac{1}{12}$. Then by choosing $\gamma \leq \frac{1}{13L} \leq \frac{1}{12L(1+\delta_2)}$ and summing over the iterations, we get the bound:

$$\frac{1}{T} \sum_{t=0}^{T-1} \mathbb{E} \|\nabla f(x^t)\|^2 \leq \frac{\mathbb{E} [\hat{f}(x^0) - \hat{f}(\hat{x}^*)]}{\gamma T} \cdot \frac{4n}{\beta G} + 3\delta_1 + 6L\gamma\sigma^2 + 4\zeta(N).$$

□

We have obtained the final statement of the theorem. From this, we can derive the convergence rate:

Corollary 4.2 *Under the assumptions of Theorem 4.1, for solving the problem (1), after T iterations with $\gamma \leq \min \left\{ \frac{1}{13L}, \frac{\sqrt{2\mathbb{E}[\hat{f}(x^0) - \hat{f}(\hat{x}^*)]n}}{\sigma\sqrt{3LG\beta T}} \right\}$, the following holds:*

$$\frac{1}{T} \sum_{i=1}^{T-1} \mathbb{E} \|\nabla f(x^t)\|^2 = \mathcal{O} \left(\frac{\mathbb{E} [\hat{f}(x^0) - \hat{f}(\hat{x}^*)] Ln}{\beta GT} + \frac{\sigma \sqrt{\mathbb{E} [\hat{f}(x^0) - \hat{f}(\hat{x}^*)] Ln}}{\sqrt{\beta GT}} + \delta_1 + \zeta(N) \right).$$

Proof of Corollary 4.2. We proceed estimation, analogous to Lemma 4 from (Stich 2019). Using the result of Theorem 4.1, we choose the appropriate $\gamma \leq \min \left\{ \frac{1}{13L}, \frac{\sqrt{2\mathbb{E}[\hat{f}(x^0) - \hat{f}(\hat{x}^*)]n}}{\sigma\sqrt{3LG\beta T}} \right\}$. In that way, we obtain

$$\frac{1}{T} \sum_{i=1}^{T-1} \mathbb{E} \|\nabla f(x^t)\|^2 \leq \frac{\mathbb{E} [\hat{f}(x^0) - \hat{f}(\hat{x}^*)] 52Ln}{\beta GT} + \frac{2\sigma \sqrt{6\mathbb{E} [\hat{f}(x^0) - \hat{f}(\hat{x}^*)] Ln}}{\sqrt{\beta GT}} + 3\delta_1 + 2\zeta(N),$$

that ends the proof. □

We have obtained the result for the convex case. However, we wish to extend the theory to other cases. Using the obtained result, let us proceed to the μ -strongly convex case and derive an estimate for it.

Theorem D.2. *Under Assumptions 3.1, 3.2(a), 3.3, 3.4 with $\delta_2 \leq \frac{1}{12}$, 3.5, for solving the problem described in the equation (1) after T iterations of Algorithm 1 with $\gamma \leq \frac{1}{13L}$, the following holds:*

$$\mathbb{E} [\hat{f}(x^t) - \hat{f}(\hat{x}^*)] \leq \left(1 - \frac{\gamma\beta G\mu}{4n} \right)^t \mathbb{E} [\hat{f}(x^0) - \hat{f}(\hat{x}^*)] + \frac{3}{\mu}\delta_1 + \frac{6L\gamma}{\mu}\sigma^2 + \frac{2}{\mu}\zeta(N).$$

Proof. From Theorem 4.1, we have

$$\mathbb{E} \|\nabla f(x^t)\|^2 \leq \frac{4n}{\gamma\beta G} \mathbb{E} [\hat{f}(x^t) - \hat{f}(\hat{x}^{t+1})] + 3\delta_1 + 6L\gamma\sigma^2 + 4\zeta(N).$$

Let us examine the left-hand side of the inequality in more detail:

$$\begin{aligned} \mathbb{E} \|\nabla f(x^t)\|^2 &= \mathbb{E} \|\nabla f(x^t)\|^2 + \mathbb{E} \|\nabla \hat{f}(x^t) - \nabla f(x^t)\|^2 - \mathbb{E} \|\nabla \hat{f}(x^t) - \nabla f(x^t)\|^2 \\ &\stackrel{(CS)}{\geq} \frac{1}{2} \mathbb{E} \|\nabla f(x^t) + \nabla \hat{f}(x^t) - \nabla f(x^t)\|^2 - \mathbb{E} \|\nabla \hat{f}(x^t) - \nabla f(x^t)\|^2 \\ &\stackrel{(Lemma C.1)}{\geq} \frac{1}{2} \mathbb{E} \|\nabla \hat{f}(x^t)\|^2 - 2\zeta(N) - 2\delta_1 - 2\delta_2 \|\nabla f(x^t)\|^2. \end{aligned}$$

Returning to the initial inequality,

$$\left(\frac{1}{2} - 2\delta_2 \right) \mathbb{E} \|\nabla \hat{f}(x^t) - \nabla \hat{f}(\hat{x}^*)\|^2 \leq \frac{4n}{\gamma\beta G} \mathbb{E} [\hat{f}(x^0) - \hat{f}(\hat{x}^*)] + 5\delta_1 + 6L\gamma\sigma^2 + 6\zeta(N)$$

Taking into account that $\delta_2 \leq \frac{1}{12}$ and due to $(\mu\text{-Conv})$, we get:

$$\underbrace{\frac{1}{2} \mathbb{E} \|\nabla \hat{f}(x^t) - \nabla \hat{f}(\hat{x}^*)\|^2}_{\geq \mu [\hat{f}(x^t) - \hat{f}(\hat{x}^*)]} \leq \frac{6n}{\gamma\beta G} \mathbb{E} [\hat{f}(x^0) - \hat{f}(\hat{x}^*)] + 8\delta_1 + 9L\gamma\sigma^2 + 9\zeta(N)$$

$$\frac{6n}{\gamma\beta G}\mathbb{E}\hat{f}(x^{t+1}) - \mu\mathbb{E}\hat{f}(\hat{x}^*) \leq \left(\frac{6n}{\gamma\beta G} - \mu\right)\mathbb{E}\hat{f}(x^t) + 8\delta_1 + 9L\gamma\sigma^2 + 9\zeta(N).$$

Defining $\gamma' = \frac{\gamma\beta G}{6n}$,

$$\mathbb{E}\hat{f}(x^{t+1}) - \gamma'\mu\mathbb{E}\hat{f}(\hat{x}^*) \leq (1 - \gamma'\mu)\mathbb{E}\hat{f}(x^t) + 8\gamma'\delta_1 + 9\gamma' L\gamma\sigma^2 + 9\gamma'\zeta(N).$$

We add to both sides of inequality the term $(-1 + \gamma'\mu)\mathbb{E}\hat{f}(\hat{x}^*)$:

$$\left[\mathbb{E}\hat{f}(x^{t+1}) - \mathbb{E}\hat{f}(\hat{x}^*)\right] \leq (1 - \gamma'\mu)\left[\mathbb{E}\hat{f}(x^t) - \mathbb{E}\hat{f}(\hat{x}^*)\right] + 8\gamma'\delta_1 + \frac{9L\gamma\gamma'}{G}\sigma^2 + 9\gamma'\zeta(N).$$

Applying this inequality to the first term on the right side t times, we obtain:

$$\begin{aligned} \mathbb{E}\left[\hat{f}(x^t) - \hat{f}(\hat{x}^*)\right] &\leq (1 - \gamma'\mu)^t \mathbb{E}\left[\hat{f}(x^0) - \hat{f}(\hat{x}^*)\right] \\ &\quad + \underbrace{\sum_{i=0}^{t-1} (1 - \gamma'\mu)^i \left[8\gamma'\delta_1 + 9L\gamma\gamma'\sigma^2 + 9\gamma'\zeta(N)\right]}_{\leq \frac{1}{\gamma'\mu}}, \\ \mathbb{E}\left[\hat{f}(x^t) - \hat{f}(\hat{x}^*)\right] &\leq (1 - \gamma'\mu)^t \mathbb{E}\left[\hat{f}(x^0) - \hat{f}(\hat{x}^*)\right] + \frac{8}{\mu}\delta_1 + \frac{9L\gamma}{\mu}\sigma^2 + \frac{9}{\mu}\zeta(N). \end{aligned}$$

□

Similarly, from this estimate, we derive the final convergence rate for the μ -strongly convex setting.

Corollary D.3. *Under the assumptions of Theorem D.2, for solving the problem (1), after T iterations with special tunings of γ :*

$$\mathbb{E}\left[\hat{f}(x^T) - \hat{f}(\hat{x}^*)\right] = \tilde{\mathcal{O}}\left(\mathbb{E}\left[\hat{f}(x^0) - \hat{f}(\hat{x}^*)\right] \exp\left[-\frac{\mu\beta GT}{4Ln}\right] + \frac{Ln}{\mu^2\beta GT}\sigma^2 + \frac{1}{\mu}\delta_1 + \frac{1}{\mu}\zeta(N)\right).$$

Proof. In Theorem D.2, we obtain classical result for SGD. We use Lemma 2 from (Stich 2019) and appropriate special tunings of γ :

$$\gamma \leq \min\left\{\frac{1}{13L}, \frac{4n \log\left(\max\left\{2, \frac{\mu^2\beta G\mathbb{E}[\hat{f}(x^0) - \hat{f}(\hat{x}^*)]}{36Ln\sigma_*^2}\right\}\right)}{\mu\beta GT}\right\}.$$

We obtain the final convergence. □

With this, we conclude this section. In summary, we examine the proof for both the convex and strongly convex cases and obtain the final convergence estimates.

E Proofs of AutoBant

Now, let us turn our attention to the second of our methods. As previously mentioned, `Bant` has certain moments to be discussed. It is important to note the adverse impact of the parameter β . The introduction of this momentum term aimed to protect honest clients from rapidly decreasing their trust scores due to unfavorable stochastic gradients, but it inadvertently enables Byzantine agents to maintain their weights despite their attacks. To address this issue, we add an indicator to the algorithm for detecting Byzantine devices, although this limits its theoretical part in common non-convex scenarios.

Our goal is to learn how to circumvent this limitation. To achieve this, we tackle an additional subproblem related to weight assignment. This step represents a key distinction in our theoretical analysis. We assert that we can solve this weight distribution minimization subproblem to any predefined accuracy. Next, we present the theorem discussed in the main part of the paper, along with its complete proof.

Theorem 4.3. *Under Assumptions 3.1, 3.2(c), 3.3, 3.4 with $\delta_2 \leq \frac{1}{12}$, 3.5, for solving the problem described in the equation (1) after T iterations of Algorithm 2 with $\gamma \leq \frac{1}{13L}$, the following holds:*

$$\frac{1}{T} \sum_{t=0}^{T-1} \mathbb{E} \|\nabla f(x^t)\|^2 \leq \frac{4\mathbb{E} [\hat{f}(x^0) - \hat{f}(\hat{x}^*)]}{\gamma T} + 3\delta_1 + \frac{6L\gamma}{G} \sigma^2 + 4\zeta(N).$$

Proof. The iterative update formula for x^{t+1} is given by

$$x^{t+1} = x^t - \gamma \sum_{i=1}^n \left(\arg \min_{\omega \in \Delta_1^n} \hat{f} \left[x^t - \gamma \sum_{i=1}^n \omega_i g_i^t \right] \right) g_i^t,$$

which leads to an upper bound on $\hat{f}(x^{t+1})$:

$$\begin{aligned} \hat{f}(x^{t+1}) &= \min_{\omega \in \Delta_1^n} \hat{f} \left[x^t - \gamma \sum_{i=1}^n \omega_i g_i^t \right] \\ &\leq \hat{f} \left[x^t - \frac{\gamma}{G} \sum_{i \in \mathcal{G}} g_i^t \right] \\ &\stackrel{(\text{Lip})}{\leq} \hat{f}(x^t) - \left\langle \nabla \hat{f}(x^t), \frac{\gamma}{G} \sum_{i \in \mathcal{G}} g_i^t \right\rangle + \frac{L\gamma^2}{2} \left\| \frac{1}{G} \sum_{i \in \mathcal{G}} g_i^t \right\|^2 \end{aligned}$$

Taking the expectation,

$$\begin{aligned} \mathbb{E} \hat{f}(x^{t+1}) &\leq \mathbb{E} \hat{f}(x^t) - \left\langle \nabla \hat{f}(x^t), \frac{\gamma}{G} \sum_{i \in \mathcal{G}} \nabla f_i(x^t) \right\rangle + \frac{L\gamma^2}{2} \mathbb{E} \left\| \frac{1}{G} \sum_{i \in \mathcal{G}} g_i^t \right\|^2 \\ &\stackrel{(\text{Lemma C.2})}{\leq} \mathbb{E} \hat{f}(x^t) + \gamma \zeta(N) - \frac{\gamma}{2} \|\nabla f(x^t)\|^2 \\ &\quad + \frac{3\gamma}{2} (\delta_1 + \delta_2 \|\nabla f(x^t)\|^2) + \frac{L\gamma^2}{2} \mathbb{E} \left\| \frac{1}{G} \sum_{i \in \mathcal{G}} g_i^t \right\|^2 \\ &\stackrel{(\text{CS})}{\leq} \mathbb{E} \hat{f}(x^t) + \gamma \zeta(N) - \frac{\gamma}{2} \|\nabla f(x^t)\|^2 + \frac{3\gamma}{2} (\delta_1 + \delta_2 \|\nabla f(x^t)\|^2) \\ &\quad + \frac{3L\gamma^2}{2} \left\| \frac{1}{G} \sum_{i \in \mathcal{G}} (\nabla f(x^t) - \nabla f_i(x^t)) \right\|^2 \\ &\quad + \frac{3L\gamma^2}{2} \mathbb{E} \left\| \frac{1}{G} \sum_{i \in \mathcal{G}} (\nabla f_i(x^t) - g_i^t) \right\|^2 + \frac{3L\gamma^2}{2} \left\| \frac{1}{G} \sum_{i \in \mathcal{G}} \nabla f(x^t) \right\|^2. \end{aligned}$$

Due to the fact that $\mathbb{E} g_i^t = \nabla f_i(x^t)$ and $\mathbb{E} \langle \nabla f_i(x^t) - g_i^t, \nabla f_j(x^t) - g_j^t \rangle = 0$,

$$\begin{aligned} \mathbb{E} \hat{f}(x^{t+1}) &\stackrel{(\text{CS})}{\leq} \mathbb{E} \hat{f}(x^t) + \gamma \zeta(N) - \frac{\gamma}{2} \|\nabla f(x^t)\|^2 + \frac{3\gamma}{2} (\delta_1 + \delta_2 \|\nabla f(x^t)\|^2) \\ &\quad + \frac{3L\gamma^2}{2} \left(\frac{1}{G} \sum_{i \in \mathcal{G}} \|\nabla f(x^t) - \nabla f_i(x^t)\|^2 + \frac{1}{G^2} \sum_{i \in \mathcal{G}} \mathbb{E} \|\nabla f_i(x^t) - g_i^t\|^2 \right) \end{aligned}$$

$$\begin{aligned}
& + \frac{3L\gamma^2}{2} \|\nabla f(x^t)\|^2 \\
& \stackrel{(\text{Ass. 3.3, 3.4})}{\leq} \mathbb{E} \hat{f}(x^t) + \gamma \zeta(N) - \frac{\gamma}{2} \|\nabla f(x^t)\|^2 + \frac{3\gamma}{2} (\delta_1 + \delta_2 \|\nabla f(x^t)\|^2) \\
& \quad + \frac{3L\gamma^2}{2} \left(\delta_1 + \delta_2 \|\nabla f(x^t)\|^2 + \frac{\sigma^2}{G} \right) + \frac{3L\gamma^2}{2} \|\nabla f(x^t)\|^2 \\
& = \mathbb{E}[\hat{f}(x^t)] - \frac{\gamma}{2} [1 - 3L\gamma - (3 + 3L\gamma)\delta_2] \|\nabla f(x^t)\|^2 \\
& \quad + \frac{2\gamma}{2} (1 + 3L\gamma)\delta_1 + \frac{3L\gamma^2}{2G} \sigma^2 + \gamma \zeta(N).
\end{aligned}$$

We first fix $\delta_2 \leq \frac{1}{12}$. By choosing $\gamma \leq \frac{1}{13L} \leq \frac{1}{12L(1+\delta_2)}$, and summing over the iterations, we get

$$\frac{1}{T} \sum_{t=0}^{T-1} \mathbb{E} \|\nabla f(x^t)\|^2 \leq \frac{4\mathbb{E} [\hat{f}(x^0) - \hat{f}(\hat{x}^*)]}{\gamma T} + 3\delta_1 + \frac{6L\gamma}{G} \sigma^2 + 4\zeta(N).$$

□

We have successfully proven the obtained result. Let us also recall that we formulated the final estimate in Corollary 4.4. We will omit the proof of Corollary 4.4 since it entirely replicates the proof of Corollary 4.2.

With this, we conclude our proof of the foundational versions of the algorithms. We establish all the formulated statements and derive convergence estimates for the strongly convex, convex, and non-convex cases. The subsequent sections of the Appendix are dedicated to exploring extensions that hold significant importance in our study.

F Scaled methods

In this section, we provide a detailed analysis of our Byzantine-robust methods extended to adaptive methods, as mentioned in the main part. Specifically, we consider the application of our techniques to methods like ADAM and RMSPROP. We describe the formal description of SCALED BANT and SCALED AUTOBANT methods, which utilize a diagonal preconditioner $(\hat{P}^t)^{-1}$, which scales a gradient to $(\hat{P}^t)^{-1}g_i^t$, and the step is performed using this scaled gradient. From iteration to iteration, the matrix P^t changes, e.g. the following rule can be used.

$$(P^t)^2 = \beta_t(P^{t-1})^2 + (1 - \beta_t)(H^t)^2. \quad (5)$$

This update scheme is satisfied by ADAM-based methods with $(H^t)^2 = \text{diag}(g^t \odot g^t)$ and by ADAHESSIAN (Yao et al. 2021) with $(H^t)^2 = \text{diag}(z^t \odot \nabla^2 f(x^t))^2$, where \odot denotes the component-wise product between two vectors, and z^t are from Rademacher distribution, i.e. all components from vector are independent and equal to ± 1 with probability $1/2$.

We want the preconditioner being a positive define matrix, thus, it is typical to modify P^t a bit:

$$(\hat{P}^t)_{ii} = \max\{e, |P^t|_{ii}\}, \quad (6)$$

where e is a (small) positive parameter. There are also other possible update rules, one of which is

$$P^t = \beta_t(P^{t-1}) + (1 - \beta_t)H^t.$$

For example, such a rule is extended in OASIS (Jahani et al. 2022) with $\beta_t \equiv \beta$ and $H^t = \text{diag}(z^t \odot \nabla^2 f(x^t))$. We also note additional details in the construction of a positively defined preconditioner. We can also alternatively define \hat{P}^t as $(\hat{P}^t)_{ii} = |P|_{ii} + e$. Most importantly, both of these approaches construct diagonal matrices with positive elements. We introduce the crucial for our analysis assumption.

Assumption F.1. For any $t \geq 1$, we have $\alpha I \preceq \hat{P}^t \preceq \Gamma I$.

The correct proof of this statement, as well as a more detailed description of the diagonal preconditioner, is provided in (Sadiev et al. 2024). We mention that for ADAHESSIAN and OASIS preconditioners, $\Gamma = \sqrt{d}L$, and for ADAM and RMSPROP, under the condition $\|\nabla f(x)\| \leq M$, $\Gamma = M$. Thus, having constructed a diagonal preconditioner, we can proceed to the analysis of scaled methods.

F.1 Scaled Bant

Before presenting the results for SCALED BANT (Algorithm 5), we need to provide the preliminary analysis. To derive the final estimation, let us prove auxiliary lemmas.

Lemma F.2. If the diagonal preconditioner \hat{P} is such that $\alpha I \preceq \hat{P} \preceq \Gamma I$, the following estimates are valid:

$$(a) \quad \frac{1}{\Gamma} \|g\|^2 \leq \|g\|_{\hat{P}^{-1}}^2 \leq \frac{1}{\alpha} \|g\|^2,$$

$$(b) \quad \frac{1}{\Gamma^2} \|g\|^2 \leq \|\hat{P}^{-1}g\|^2 \leq \frac{1}{\alpha^2} \|g\|^2,$$

where $\langle h, g \rangle_{\hat{P}^{-1}} \stackrel{\text{def}}{=} \langle h, \hat{P}^{-1}g \rangle$, $h, g \in \mathbb{R}^d$

Proof.

$$\begin{aligned} I \preceq \frac{1}{\alpha} \hat{P} &\Rightarrow \|\hat{P}^{-1}g\|^2 = \langle I\hat{P}^{-1}g, \hat{P}^{-1}g \rangle \leq \frac{1}{\alpha} \langle g, \hat{P}^{-1}g \rangle \stackrel{\text{def}}{=} \frac{1}{\alpha} \langle g, g \rangle_{\hat{P}^{-1}} = \frac{1}{\alpha} \|g\|_{\hat{P}^{-1}}^2. \\ &\quad \langle g, \hat{P}^{-1}g \rangle \leq \frac{1}{\alpha} \langle g, g \rangle = \frac{1}{\alpha} \|g\|^2. \\ \hat{P} \preceq \Gamma I &\Rightarrow \|\hat{P}^{-1}g\|^2 = \langle I\hat{P}^{-1}g, \hat{P}^{-1}g \rangle \geq \frac{1}{\Gamma} \langle g, \hat{P}^{-1}g \rangle \stackrel{\text{def}}{=} \frac{1}{\Gamma} \langle g, g \rangle_{\hat{P}^{-1}} = \frac{1}{\Gamma} \|g\|_{\hat{P}^{-1}}^2. \\ &\quad \langle g, \hat{P}^{-1}g \rangle \geq \frac{1}{\Gamma} \langle g, g \rangle = \frac{1}{\Gamma} \|g\|^2. \end{aligned}$$

□

Lemma F.3 (Scaled version of Lemma D.1). *Under Assumptions 3.1, 3.2(b), 3.5, F.1, the following holds for the iteration of Algorithm 5:*

$$\hat{f}(x^{t+1}) \leq \hat{f}(x^t) - \gamma\beta \frac{1}{n} \sum_{i \in \mathcal{G}} \langle \nabla \hat{f}(x^t), (\hat{P}^t)^{-1}g_i^t \rangle + \frac{L\gamma^2\beta}{2n} \sum_{i \in \mathcal{G}} \|(\hat{P}^t)^{-1}g_i^t\|^2$$

Algorithm 5 Scaled Bant

```
1: Input: Starting point  $x^0 \in \mathbb{R}^d$ 
2: Parameters: Stepsize  $\gamma > 0$ , momentum parameter  $\beta \in [0, 1]$ 
3: for  $t = 0, 1, 2, \dots, T - 1$  do
4:   Server sends  $x^t$  to each worker
5:   for all workers  $i = 0, 1, 2, \dots, n$  in parallel do
6:     Generate  $\xi_i^t$  independently
7:     Compute stochastic gradient  $g_i(x^t, \xi_i)$ 
8:     Send  $g_i^t = g_i(x^t, \xi_i)$  to server
9:   end for
10:   $\omega^t = (1 - \beta)\omega_i^{t-1} + \beta \frac{[\hat{f}(x^t) - \hat{f}(x^t - \gamma(\hat{P}^t)^{-1}g_i^t)]_0}{\sum_{j=1}^n [\hat{f}(x^t) - \hat{f}(x^t - \gamma(\hat{P}^t)^{-1}g_j^t)]_0}$ 
11:  if each  $\left[ \hat{f}(x^t) - \hat{f}(x^t - \gamma(\hat{P}^t)^{-1}g_i^t) \right]_0 = 0$  then
12:     $\omega_i^t = (1 - \beta)\omega_i^{t-1} + \beta \frac{1}{n}$ 
13:  end if
14:   $x^{t+1} = x^t - \gamma(\hat{P}^t)^{-1} \sum_{i=1}^n \mathbb{I}_{[\hat{f}(x^t) - \hat{f}(x^t - \gamma(\hat{P}^t)^{-1}g_i^t) > 0]} \omega_i^t g_i^t$ 
15:   $\hat{P}^t$  is the function of  $\hat{P}^{t-1}$  and  $H^t$ , e.g., as (5) + (6)
16: end for
17: Output:  $\frac{1}{T} \sum_{t=0}^{T-1} x^t$ 
```

Proof. Our analysis implies the same as was done in Lemma D.1. Since the only thing that has changed is that we additionally scale the gradient at each step, the analysis is similar and we obtain the final estimate. \square

Lemma F.4 (Scaled version of Lemma C.2). *Suppose Assumption 3.1 holds. Then for all $x \in \mathbb{R}^d$ and $g_i = g_i(x, \xi_i)$, the following estimate is valid:*

$$-\gamma \left\langle \nabla \hat{f}(x), \frac{1}{G} \sum_{i \in \mathcal{G}} \nabla f_i(x) \right\rangle^2 \leq -\frac{\gamma}{2\Gamma} \|\nabla f(x)\|^2 + \frac{\gamma}{2\alpha} \zeta(N) + \frac{\gamma}{2\alpha} (\delta_1 + \delta_2 \|\nabla f(x^t)\|^2).$$

Proof. We commence by examining the difference $\nabla f(x) - \nabla \hat{f}(x)$:

$$\begin{aligned} -\gamma \left\langle \nabla \hat{f}(x), \frac{1}{G} \sum_{i \in \mathcal{G}} \nabla f_i(x) \right\rangle_{\hat{P}^{-1}} &= \gamma \left\langle \nabla f(x) - \nabla \hat{f}(x), \frac{1}{G} \sum_{i \in \mathcal{G}} \nabla f_i(x) \right\rangle_{\hat{P}^{-1}} \\ &\quad - \gamma \left\langle \nabla f(x), \frac{1}{G} \sum_{i \in \mathcal{G}} \nabla f_i(x) \right\rangle_{\hat{P}^{-1}}. \end{aligned}$$

Next, we continue with further manipulations on the first term:

$$\begin{aligned} &\gamma \left\langle \nabla f(x) - \nabla \hat{f}(x), \frac{1}{G} \sum_{i \in \mathcal{G}} \nabla f_i(x) \right\rangle_{\hat{P}^{-1}} \\ &\stackrel{\text{(Young)}}{\leq} \frac{\gamma}{2} \left\| \nabla f(x) - \nabla \hat{f}(x) \right\|_{\hat{P}^{-1}}^2 + \frac{\gamma}{2} \left\| \frac{1}{G} \sum_{i \in \mathcal{G}} \nabla f_i(x) \right\|_{\hat{P}^{-1}}^2 \\ &\stackrel{\text{(Lemma F.2(a))}}{\leq} \frac{\gamma}{2\alpha^2} \left\| \nabla f(x) - \nabla \hat{f}(x) \right\|^2 + \frac{\gamma}{2} \left\| \frac{1}{G} \sum_{i \in \mathcal{G}} \nabla f_i(x) \right\|_{\hat{P}^{-1}}^2 \\ &\stackrel{\text{(Lemma C.1)}}{\leq} \frac{\gamma}{2\alpha} \zeta(N) + \frac{\gamma}{2} \left\| \frac{1}{G} \sum_{i \in \mathcal{G}} \nabla f_i(x) \right\|_{\hat{P}^{-1}}^2, \end{aligned}$$

and with the second term,

$$\begin{aligned}
-\gamma \left\langle \nabla f(x), \frac{1}{G} \sum_{i \in \mathcal{G}} \nabla f_i(x) \right\rangle_{\hat{P}^{-1}} &\stackrel{(\text{Norm})}{=} -\frac{\gamma}{2} \|\nabla f(x)\|_{\hat{P}^{-1}}^2 - \frac{\gamma}{2} \left\| \frac{1}{G} \sum_{i \in \mathcal{G}} \nabla f_i(x) \right\|_{\hat{P}^{-1}}^2 \\
&\quad + \frac{\gamma}{2} \left\| \frac{1}{G} \sum_{i \in \mathcal{G}} (\nabla f_i(x) - \nabla f(x)) \right\|_{\hat{P}^{-1}}^2 \\
&\stackrel{(\text{CS})}{\leq} -\frac{\gamma}{2} \|\nabla f(x)\|_{\hat{P}^{-1}}^2 - \frac{\gamma}{2} \left\| \frac{1}{G} \sum_{i \in \mathcal{G}} \nabla f_i(x) \right\|_{\hat{P}^{-1}}^2 \\
&\quad + \frac{\gamma}{2G} \sum_{i \in \mathcal{G}} \|(\nabla f_i(x) - \nabla f(x))\|_{\hat{P}^{-1}}^2 \\
&\stackrel{(\text{Lemma F.2})}{\leq} -\frac{\gamma}{2\Gamma} \|\nabla f(x)\|^2 - \frac{\gamma}{2} \left\| \frac{1}{G} \sum_{i \in \mathcal{G}} \nabla f_i(x) \right\|_{\hat{P}^{-1}}^2 \\
&\quad + \frac{\gamma}{2\alpha G} \sum_{i \in \mathcal{G}} \|(\nabla f_i(x) - \nabla f(x))\|^2 \\
&\stackrel{(\text{Ass. 3.4})}{\leq} -\frac{\gamma}{2\Gamma} \|\nabla f(x)\|^2 - \frac{\gamma}{2} \left\| \frac{1}{G} \sum_{i \in \mathcal{G}} \nabla f_i(x) \right\|_{\hat{P}^{-1}}^2 \\
&\quad + \frac{\gamma}{2\alpha} (\delta_1 + \delta_2 \|\nabla f(x)\|^2).
\end{aligned}$$

Summing up substantiates the claim of the lemma. \square

We are now ready to write out the main results for the scaled methods.

Theorem F.5. *Under Assumptions 3.1, 3.2(b), 3.3, 3.4 with $\delta_2 \leq \frac{2\Gamma - \alpha}{\alpha + \frac{4\Gamma^2}{\alpha^2}}$, 3.5, F.1, for solving the problem (1), after T iteration of Algorithm 5 with $\gamma \leq \frac{\alpha}{12L}$, it holds that*

$$\frac{1}{T} \sum_{t=0}^{T-1} \mathbb{E} \|\nabla f(x^t)\|^2 \leq \frac{4\mathbb{E} [\hat{f}(x^0) - \hat{f}(\hat{x}^*)]}{\gamma T} \cdot \frac{n\Gamma}{\beta G} + \frac{3\Gamma}{\alpha} \delta_1 + \frac{6L\gamma\Gamma}{\alpha^2} \sigma^2 + \frac{2\Gamma}{\alpha} \zeta(N).$$

Proof of Theorem F.5. Similar to the aforementioned Lemma D.1 (with the preconditioner added):

$$\begin{aligned}
\hat{f}(x^{t+1}) &\leq \hat{f}(x^t) - \gamma\beta \frac{1}{n} \sum_{i \in \mathcal{G}} \left\langle \nabla \hat{f}(x^t), (\hat{P}^t)^{-1} g_i^t \right\rangle + \frac{L\gamma^2\beta}{2n} \sum_{i \in \mathcal{G}} \|(\hat{P}^t)^{-1} g_i^t\|^2 \\
&\stackrel{(\text{Lemma F.2})}{\leq} \hat{f}(x^t) - \gamma\beta \frac{1}{n} \sum_{i \in \mathcal{G}} \left\langle \nabla \hat{f}(x^t), g_i^t \right\rangle_{(\hat{P}^t)^{-1}} + \frac{L\gamma^2\beta}{2n\alpha^2} \sum_{i \in \mathcal{G}} \|g_i^t\|^2.
\end{aligned}$$

Taking the expectation of both sides of the inequality:

$$\begin{aligned}
\mathbb{E} \hat{f}(x^{t+1}) &\leq \mathbb{E} \hat{f}(x^t) - \gamma\beta \cdot \frac{G}{n} \left\langle \nabla \hat{f}(x^t), \frac{1}{G} \sum_{i \in \mathcal{G}} \nabla f_i(x^t) \right\rangle_{(\hat{P}^t)^{-1}} \\
&\quad + \frac{L\gamma^2\beta}{2n\alpha^2} \sum_{i \in \mathcal{G}} \mathbb{E} \|g_i^t\|^2 \\
&\stackrel{(\text{Lemma F.4})}{\leq} \mathbb{E} \hat{f}(x^t) + \frac{\gamma\beta G}{2n\alpha} \zeta(N) - \frac{\gamma\beta G}{2n\Gamma} \|\nabla f(x^t)\|^2 \\
&\quad + \frac{\gamma\beta G}{2n\alpha} (\delta_1 + \delta_2 \|\nabla f(x^t)\|^2) + \frac{L\gamma^2\beta}{2n\alpha^2} \sum_{i \in \mathcal{G}} \mathbb{E} \|g_i^t\|^2 \\
&\stackrel{(\text{CS})}{\leq} \mathbb{E} \hat{f}(x^t) + \frac{\gamma\beta G}{2n\alpha} \zeta(N) - \frac{\gamma\beta G}{2n\Gamma} \|\nabla f(x^t)\|^2 + \frac{\gamma\beta G}{2n\alpha} (\delta_1 + \delta_2 \|\nabla f(x^t)\|^2)
\end{aligned}$$

$$\begin{aligned}
& + \frac{3L\gamma^2\beta}{2n\alpha^2} \left(\sum_{i \in \mathcal{G}} \mathbb{E} \|\nabla f(x^t) - f_i(x^t)\|^2 + \sum_{i \in \mathcal{G}} \mathbb{E} \|\nabla f_i(x^t) - g_i^t\|^2 \right) \\
& + \frac{3L\gamma^2\beta G}{2n\alpha^2} \|\nabla f(x^t)\|^2 \\
& \stackrel{(\text{Ass. 3.3, 3.4})}{\leq} \mathbb{E} \hat{f}(x^t) + \frac{\gamma\beta G}{2n\alpha} \zeta(N) - \frac{\gamma\beta G}{2n\Gamma} \|\nabla f(x^t)\|^2 + \frac{\gamma\beta G}{2n\alpha} (\delta_1 + \delta_2 \|\nabla f(x^t)\|^2) \\
& + \frac{3L\gamma^2\beta G}{2n\alpha^2} (\delta_1 + \delta_2 \|\nabla f(x^t)\|^2 + \sigma^2) + \frac{3L\gamma^2\beta G}{2n\alpha^2} \|\nabla f(x^t)\|^2 \\
& \stackrel{(\text{Ass. 3.3})}{\leq} \mathbb{E}[\hat{f}(x^t)] - \frac{\gamma\beta G}{2n\Gamma} \left[1 - 3L\gamma \frac{\Gamma}{\alpha^2} - (1 + 3L\gamma) \frac{\Gamma}{\alpha^2} \delta_2 \right] \|\nabla f(x^t)\|^2 \\
& + \frac{\gamma\beta G}{2n\alpha} (1 + \frac{3L\gamma}{\alpha}) \delta_1 + \frac{3\gamma^2\beta LG}{2n\alpha^2} \sigma^2 + \frac{\gamma\beta G}{2n\alpha} \zeta(N).
\end{aligned}$$

Now we have to choose γ . We want $[1 - 3L\gamma \frac{\Gamma}{\alpha^2} - (1 + 3L\gamma) \frac{\Gamma}{\alpha^2} \delta_2] \geq \frac{1}{2}$. Then

$$\gamma \leq \frac{1 - \frac{2\Gamma}{\alpha^2} \delta_2}{6L \frac{\Gamma}{\alpha^2} (1 + \delta_2)}.$$

Let us choose $\delta_2 \leq \frac{2\Gamma - \alpha}{\alpha + \frac{4\Gamma^2}{\alpha^2}}$, then we have $\frac{1}{2} \leq \frac{1 - \frac{2\Gamma}{\alpha^2} \delta_2}{\frac{\Gamma}{\alpha} (1 + \delta_2)}$. Thus,

$$\gamma \leq \frac{\alpha}{12L} \leq \frac{1 - \frac{2\Gamma}{\alpha^2} \delta_2}{6L \frac{\Gamma}{\alpha^2} (1 + \delta_2)}.$$

Using $\gamma \leq \frac{\alpha}{12L}$ and summing over the iterations, we get the bound:

$$\frac{1}{T} \sum_{t=0}^{T-1} \mathbb{E} \|\nabla f(x^t)\|^2 \leq \frac{\mathbb{E} [\hat{f}(x^0) - \hat{f}(\hat{x}^*)]}{\gamma T} \cdot \frac{4n\Gamma}{\beta G} + \frac{3\Gamma}{\alpha} \delta_1 + \frac{6L\gamma\Gamma}{\alpha^2} \sigma^2 + \frac{2\Gamma}{\alpha} \zeta(N).$$

□

Now we provide the final convergence rate.

Corollary F.6. *Under assumptions of Theorem F.5 for solving the problem (1), after T iterations of Algorithm F.1 with special tunings of γ , the following holds:*

$$\frac{1}{T} \sum_{i=1}^{T-1} \|\nabla f(x^t)\|^2 = \mathcal{O} \left(\frac{\mathbb{E} [\hat{f}(x^0) - \hat{f}(\hat{x}^*)] Ln}{\beta GT} \cdot \frac{\Gamma}{\alpha} + \frac{\sigma \sqrt{\mathbb{E} [\hat{f}(x^0) - \hat{f}(\hat{x}^*)] Ln}}{\sqrt{\beta GT}} \cdot \frac{\Gamma}{\alpha} + (\delta_1 + \zeta(N)) \cdot \frac{\Gamma}{\alpha} \right).$$

The proof of Corollary F.6 completely mirrors the proof of Corollary 4.2.

Remark F.7. We get a result similar to Corollary 4.2, but with the deterioration that each term is multiplied by an additional constant $\Gamma/\alpha > 1$. This result suits us, since in (Sadiev et al. 2024) the result for the SCALED SARAH method corresponds similarly to the result for the classical SARAH (Nguyen et al. 2017) method.

F.2 Scaled AutoBant

Now, let us consider the second algorithm for scaled methods - SCALED AUTOBANT (Algorithm 6). This section presents an algorithm which is an adaptive version of Algorithm 2 taking into account the diagonal preconditioner. Now we provide an estimate for the convergence of the SCALED AUTOBANT method.

Theorem F.8. *Under Assumptions 3.1, 3.2(c) 3.3, 3.4 with $\delta_2 \leq 0.25$, 3.5, F.1, for solving the problem (1), after T iterations of Algorithm 6 with $\gamma \leq \frac{\alpha}{12L}$, the following holds:*

$$\frac{1}{T} \sum_{t=0}^{T-1} \mathbb{E} \|\nabla f(x^t)\|^2 \leq \frac{\mathbb{E} [\hat{f}(x^0) - \hat{f}(\hat{x}^*)] \cdot 4\Gamma}{\gamma T} + \frac{3\Gamma}{\alpha} \delta_1 + \frac{6L\gamma\Gamma}{\alpha^2 G} \sigma^2 + \frac{2\Gamma}{\alpha} \zeta(N).$$

Algorithm 6 Scaled AutoBant

```
1: Input: Starting point  $x^0 \in \mathbb{R}^d$ 
2: Parameters: Stepsize  $\gamma > 0$ , error accuracy  $\delta$ 
3: for  $t = 0, 1, 2, \dots, T - 1$  do
4:   Server sends  $x^t$  to each worker
5:   for all workers  $i = 0, 1, 2, \dots, n$  in parallel do
6:     Generate  $\xi_i^t$  independently
7:     Compute stochastic gradient  $g_i(x^t, \xi_i)$ 
8:     Send  $g_i^t = g_i(x^t, \xi_i)$  to server
9:   end for
10:   $\omega^t \approx \arg \min_{\omega \in \Delta_1^n} \hat{f} \left( x^t - \gamma (\hat{P}^t)^{-1} \sum_{i=1}^n \omega_i g_i^t \right)$ 
11:   $x^{t+1} = x^t - \gamma (\hat{P}^t)^{-1} \sum_{i=1}^n \omega_i^t g_i^t$ 
12:   $\hat{P}^t$  is the function of  $\hat{P}^{t-1}$  and  $H^t$ , e.g., as (5) + (6)
13: end for
14: Output:  $\frac{1}{T} \sum_{t=0}^{T-1} x^t$ 
```

Proof of Theorem F.8. Note we estimate the trial function value:

$$\begin{aligned} \hat{f}(x^{t+1}) &= \min_{\omega \in \Delta_1^n} \hat{f} \left(x^t - \gamma (\hat{P}^t)^{-1} \sum_{i=1}^n \omega_i g_i^t \right) \\ &\leq \hat{f} \left(x^t - \gamma (\hat{P}^t)^{-1} \frac{1}{G} \sum_{i \in \mathcal{G}} g_i^t \right) \\ &\stackrel{(\text{Lip})}{\leq} \hat{f}(x^t) - \gamma \left\langle \nabla \hat{f}(x^t), (\hat{P}^t)^{-1} \frac{1}{G} \sum_{i \in \mathcal{G}} g_i^t \right\rangle \\ &\quad + \frac{L\gamma^2}{2} \left\| (\hat{P}^t)^{-1} \frac{1}{G} \sum_{i \in \mathcal{G}} g_i^t \right\|^2 \\ &\stackrel{(\text{Lemma F.2})}{\leq} \hat{f}(x^t) - \gamma \left\langle \nabla \hat{f}(x^t), \frac{1}{G} \sum_{i \in \mathcal{G}} g_i^t \right\rangle_{(\hat{P}^t)^{-1}} + \frac{L\gamma^2}{2\alpha^2} \left\| \frac{1}{G} \sum_{i \in \mathcal{G}} g_i^t \right\|^2. \end{aligned}$$

Taking the expectation of both sides of the inequality:

$$\begin{aligned} \mathbb{E} \hat{f}(x^{t+1}) &\leq \mathbb{E} \hat{f}(x^t) - \gamma \left\langle \nabla \hat{f}(x^t), \frac{1}{G} \sum_{i \in \mathcal{G}} \nabla f_i(x^t) \right\rangle_{(\hat{P}^t)^{-1}} \\ &\quad + \frac{L\gamma^2}{2\alpha^2} \mathbb{E} \left\| \frac{1}{G} \sum_{i \in \mathcal{G}} g_i^t \right\|^2 \\ &\stackrel{(\text{Lemma F.4})}{\leq} \mathbb{E} \hat{f}(x^t) + \frac{\gamma}{2\alpha} \zeta(N) - \frac{\gamma}{2\Gamma} \|\nabla f(x^t)\|^2 \\ &\quad + \frac{\gamma}{2\alpha} (\delta_1 + \delta_2 \|\nabla f(x^t)\|^2) + \frac{L\gamma^2}{2\alpha^2} \mathbb{E} \left\| \frac{1}{G} \sum_{i \in \mathcal{G}} g_i^t \right\|^2 \\ &\stackrel{(\text{CS})}{\leq} \mathbb{E} \hat{f}(x^t) + \frac{\gamma}{2\alpha} \zeta(N) - \frac{\gamma}{2\Gamma} \|\nabla f(x^t)\|^2 + \frac{\gamma}{2\alpha} (\delta_1 + \delta_2 \|\nabla f(x^t)\|^2) \\ &\quad + \frac{3L\gamma^2}{2\alpha^2} \left(\mathbb{E} \left\| \frac{1}{G} \sum_{i \in \mathcal{G}} (\nabla f(x^t) - f_i(x^t)) \right\|^2 \right) \end{aligned}$$

$$+ \mathbb{E} \left\| \frac{1}{G} \sum_{i \in \mathcal{G}} \nabla(f_i(x^t) - g_i^t) \right\|^2 \right) + \frac{3L\gamma^2}{2\alpha^2} \|\nabla f(x^t)\|^2.$$

Due to the fact that $\mathbb{E}g_i^t = \nabla f_i(x^t)$ and $\mathbb{E}\langle \nabla f_i(x^t) - g_i^t, \nabla f_j(x^t) - g_j^t \rangle = 0$,

$$\begin{aligned} \mathbb{E}\hat{f}(x^{t+1}) &\leq \mathbb{E}\hat{f}(x^t) + \frac{\gamma}{2\alpha}\zeta(N) - \frac{\gamma}{2\Gamma} \|\nabla f(x^t)\|^2 + \frac{\gamma}{2\alpha} (\delta_1 + \delta_2 \|\nabla f(x^t)\|^2) \\ &\quad + \frac{3L\gamma^2}{2G\alpha^2} \sum_{i \in \mathcal{G}} \mathbb{E} \|\nabla f(x^t) - f_i(x^t)\|^2 \\ &\quad + \frac{3L\gamma^2}{2G^2\alpha^2} \sum_{i \in \mathcal{G}} \mathbb{E} \|\nabla(f_i(x^t) - g_i^t)\|^2 + \frac{3L\gamma^2}{2\alpha^2} \|\nabla f(x^t)\|^2 \\ &\stackrel{(\text{Ass. 3.3,3.4})}{\leq} \mathbb{E}\hat{f}(x^t) + \frac{\gamma}{2\alpha}\zeta(N) - \frac{\gamma}{2\Gamma} \|\nabla f(x^t)\|^2 + \frac{\gamma}{2\alpha} (\delta_1 + \delta_2 \|\nabla f(x^t)\|^2) \\ &\quad + \frac{3L\gamma^2}{2\alpha^2} \left(\delta_1 + \delta_2 \|\nabla f(x^t)\|^2 + \frac{1}{G}\sigma^2 \right) + \frac{3L\gamma^2}{2\alpha^2} \|\nabla f(x^t)\|^2 \\ &\stackrel{(\text{Ass.3.3})}{\leq} \mathbb{E}[\hat{f}(x^t)] - \frac{\gamma}{2\Gamma} \left[1 - 3L\gamma\frac{\Gamma}{\alpha^2} - (1 + 3L\gamma)\frac{\Gamma}{\alpha^2}\delta_2 \right] \|\nabla f(x^t)\|^2 \\ &\quad + \frac{\gamma}{2\alpha} \left(1 + \frac{3L\gamma}{\alpha} \right) \delta_1 + \frac{3L\gamma^2}{2\alpha^2 G} \sigma^2 + \frac{\gamma}{2\alpha} \zeta(N). \end{aligned}$$

Now we have to choose γ : We want $\left[1 - 3L\gamma\frac{\Gamma}{\alpha^2} - (1 + 3L\gamma)\frac{\Gamma}{\alpha^2}\delta_2 \right] \geq \frac{1}{2}$. Then

$$\gamma \leq \frac{1 - \frac{2\Gamma}{\alpha^2}\delta_2}{6L\frac{\Gamma}{\alpha^2}(1 + \delta_2)}.$$

Let us choose $\delta_2 \leq \frac{2\Gamma - \alpha}{\alpha + \frac{4\Gamma^2}{\alpha^2}}$, then we have $\frac{1}{2} \leq \frac{1 - \frac{2\Gamma}{\alpha^2}\delta_2}{\frac{\Gamma}{\alpha}(1 + \delta_2)}$. Thus,

$$\gamma \leq \frac{\alpha}{12L} \leq \frac{1 - \frac{2\Gamma}{\alpha^2}\delta_2}{6L\frac{\Gamma}{\alpha^2}(1 + \delta_2)}.$$

Using $\gamma \leq \frac{\alpha}{12L}$, summing over the iterations and taking the expected value at the initial point and at the optimum point, we get the bound:

$$\frac{1}{T} \sum_{t=0}^{T-1} \mathbb{E} \|\nabla f(x^t)\|^2 \leq \frac{\mathbb{E} [\hat{f}(x^0) - \hat{f}(\hat{x}^*)] \cdot 4\Gamma}{\gamma T} + \frac{3\Gamma}{\alpha} \delta_1 + \frac{6L\gamma\Gamma}{\alpha^2 G} \sigma^2 + \frac{2\Gamma}{\alpha} \zeta(N).$$

□

Now, let us present the final convergence rate for this algorithm.

Corollary F.9. *Under assumptions of Theorem F.8, for solving the problem (1), after T iterations of Algorithm (6) with special tunings of γ , the following holds:*

$$\frac{1}{T} \sum_{i=1}^{T-1} \|\nabla f(x^t)\|^2 = \mathcal{O} \left(\frac{\mathbb{E} [\hat{f}(x^0) - \hat{f}(\hat{x}^*)] LG}{T} \cdot \frac{\Gamma}{\alpha} + \frac{\sigma \sqrt{\mathbb{E} [\hat{f}(x^0) - \hat{f}(\hat{x}^*)] LG}}{\sqrt{T}} \cdot \frac{\Gamma}{\alpha} + (\delta_1 + \zeta(N)) \cdot \frac{\Gamma}{\alpha} \right)$$

Remark F.10. The boundary is the same as for `AutoBant`, with the only aggravation that several summands are multiplied by $\frac{\Gamma}{\alpha} > 1$. This result suits us for the same reason as the result of the `SCALED BANT` method.

The proof of Corollary F.9 completely mirrors the proof of Corollary 4.4.

G Local methods

As highlighted in the main section, the significant expense associated with communication remains a critical concern in various fields. The communication bottleneck can act as a substantial barrier, limiting efficiency and hindering progress. To address this challenge, many researches are turning to local approaches, which focus on minimizing the need for exchanging the information (Woodworth, Patel, and Srebro 2020; Koloskova et al. 2020; Khaled, Mishchenko, and Richtárik 2020; Gorbunov, Hanzely, and Richtárik 2021). The idea is that each device performs a predefined number of local steps without utilizing information from other devices, and at the end of such a round, the server performs a mutual update. In this section we adapt our AutoBant algorithm to this scenario. Below we present the formal description of the LOCAL AUTOBANT method (Algorithm 7).

Algorithm 7 Local AutoBant

```

1: Input: Starting point  $x^0 \in \mathbb{R}^d$ , local round length  $l$ 
2: Parameters: Stepsize  $\gamma > 0$ , error accuracy  $\delta$ 
3: for  $t = 0, 1, 2, \dots, T - 1$  do
4:   if  $t = 0$  then
5:     Server sends  $x^0$  to each worker
6:   end if
7:   for all workers  $i = 0, 1, 2, \dots, n$  in parallel do
8:     Generate  $\xi_i^t$  independently
9:     Compute stochastic gradient  $g_i^t = g_i(x^t, \xi_i)$ 
10:    if  $t \neq t_{k,l}$  (for some  $k = \overline{0, \lfloor T/l \rfloor}$ )  $\wedge t \neq T - 1$  then
11:       $x_i^{t+1} = x_i^t - \gamma g_i^t$ 
12:    else
13:      Send  $x_i^t - \gamma g_i^t$  to server
14:    end if
15:  end for
16:  if  $t = t_{k,l}$  (for some  $k = \overline{0, \lfloor T/l \rfloor}$ )  $\vee t = T - 1$  then
17:     $\omega^t \approx \arg \min_{\omega \in \Delta_1^n} \hat{f} \left( \sum_{i=1}^n \omega_i (x_i^t - \gamma g_i^t) \right)$ 
18:     $x^{t+1} = \sum_{i=1}^n \omega_i^t (x_i^t - \gamma g_i^t)$ 
19:    Server sends  $x^{t+1}$  to each worker
20:  end if
21: end for
22: Output:  $\frac{1}{T} \sum_{t=0}^{T-1} x^t$ 

```

In the convergence analysis of Algorithm 7, we assume that at each local round, at least one device (including the server) acts as an honest worker. This implies that this device computes an honest stochastic gradient at each iteration of the round. This requirement is a natural extension of the assumption made in the analysis of the basic version of our methods, where we required at least one honest device (including the server) at each iteration (or in a local round of length 1).

The analysis has some specific details. The key component is estimating how far devices can "move apart" from each other during a local round. We begin with this estimation and present the following lemma.

Lemma G.1. *Under Assumptions 3.1, 3.2(b), 3.3, 3.4, 3.5, at each iteration t of Algorithm 7 with $\gamma \leq \frac{1}{4(l-1)L}$, the following estimate is valid:*

$$\mathbb{E} V^t \leq \frac{9\delta_2\gamma}{2L} \sum_{j=t_{k,l}}^{t-1} \mathbb{E} \|\nabla f(\bar{x}^j)\|^2 + \frac{9\delta_1\gamma}{2L} (l-1) + 3\gamma^2\sigma^2(l-1),$$

where $t_{k,l}$ for some $k = \overline{0, \lfloor T/l \rfloor}$ is the past to t -th iteration aggregation round, $V^t = \frac{1}{G} \sum_{i \in \mathcal{G}} \|x_i^t - \bar{x}^t\|^2$ and $\bar{x}^t = \frac{1}{G} \sum_{i \in \mathcal{G}} x_i^t$.

Proof. Utilizing notation $V^t = \frac{1}{G} \sum_{i \in \mathcal{G}} \|x_i^t - \bar{x}^t\|^2$ and $\bar{x}^t = \frac{1}{G} \sum_{i \in \mathcal{G}} x_i^t$ we mention, that for all iterations $t + 1$, such that

$t + 1 = t_{k,l}$ we have $V^{t+1} = \frac{1}{G} \sum_{i \in \mathcal{G}} \left\| x_i^{t+1} - \frac{1}{G} \sum_{i \in \mathcal{G}} x_i^{t+1} \right\|^2 = \frac{1}{G} \sum_{i \in \mathcal{G}} \left\| x_i^{t+1} - \frac{1}{G} \sum_{i \in \mathcal{G}} x_i^{t+1} \right\|^2 = 0$. For the rest iterations we

write the step of the local update and use (Norm):

$$\begin{aligned}
\mathbb{E} \|x_i^{t+1} - \bar{x}^{t+1}\|^2 &= \mathbb{E} \|x_i^t - \bar{x}^t\|^2 + \gamma^2 \mathbb{E} \left\| g_i^t - \frac{1}{G} \sum_{i \in \mathcal{G}} g_i^t \right\|^2 \\
&\quad - 2\gamma \mathbb{E} \left\langle x_i^t - \bar{x}^t, g_i^t - \frac{1}{G} \sum_{i \in \mathcal{G}} g_i^t \right\rangle \\
&= \mathbb{E} \|x_i^t - \bar{x}^t\|^2 + \gamma^2 \mathbb{E} \left\| g_i^t - \frac{1}{G} \sum_{i \in \mathcal{G}} g_i^t \right\|^2 \\
&\quad - 2\gamma \mathbb{E} \left\langle x_i^t - \bar{x}^t, \nabla f_i(x_i^t) - \frac{1}{G} \sum_{i \in \mathcal{G}} \nabla f_i(x_i^t) \right\rangle.
\end{aligned}$$

Taking average over $i \in \mathcal{G}$,

$$\begin{aligned}
\mathbb{E} V^{t+1} &= \mathbb{E} V^t + \frac{\gamma^2}{G} \sum_{i \in \mathcal{G}} \mathbb{E} \left\| g_i^t - \frac{1}{G} \sum_{i \in \mathcal{G}} g_i^t \right\|^2 - \frac{2\gamma}{G} \sum_{i \in \mathcal{G}} \langle x_i^t - \bar{x}^t, \nabla f_i(x_i^t) \rangle \\
&\quad + 2\gamma \left\langle \bar{x}^t - \bar{x}^t, \frac{1}{G} \sum_{i \in \mathcal{G}} \nabla f_i(x_i^t) \right\rangle \\
&= \mathbb{E} V^t + \frac{\gamma^2}{G} \sum_{i \in \mathcal{G}} \mathbb{E} \left\| g_i^t - \frac{1}{G} \sum_{i \in \mathcal{G}} g_i^t \right\|^2 - \frac{2\gamma}{G} \sum_{i \in \mathcal{G}} \langle x_i^t - \bar{x}^t, \nabla f_i(x_i^t) \rangle. \tag{7}
\end{aligned}$$

Now we need to estimate the second term. We start with (Norm):

$$\begin{aligned}
\mathbb{E} \left\| g_i^t - \frac{1}{G} \sum_{i \in \mathcal{G}} g_i^t \right\|^2 &= \mathbb{E} \left\| g_i^t - \frac{1}{G} \sum_{i \in \mathcal{G}} \nabla f_i(x_i^t) \right\|^2 + \mathbb{E} \left\| \frac{1}{G} \sum_{i \in \mathcal{G}} \nabla f_i(x_i^t) - \frac{1}{G} \sum_{i \in \mathcal{G}} g_i^t \right\|^2 \\
&\quad + 2\mathbb{E} \left\langle g_i^t - \frac{1}{G} \sum_{i \in \mathcal{G}} \nabla f_i(x_i^t), \frac{1}{G} \sum_{i \in \mathcal{G}} \nabla f_i(x_i^t) - \frac{1}{G} \sum_{i \in \mathcal{G}} g_i^t \right\rangle \\
&\stackrel{(i)}{=} \mathbb{E} \|g_i^t - \nabla f_i(x_i^t)\|^2 + \mathbb{E} \left\| \nabla f_i(x_i^t) - \frac{1}{G} \sum_{i \in \mathcal{G}} \nabla f_i(x_i^t) \right\|^2 \\
&\quad + 2\mathbb{E} \left\langle g_i^t - \nabla f_i(x_i^t), \nabla f_i(x_i^t) - \frac{1}{G} \sum_{i \in \mathcal{G}} \nabla f_i(x_i^t) \right\rangle \\
&\quad + \mathbb{E} \left\| \frac{1}{G} \sum_{i \in \mathcal{G}} \nabla f_i(x_i^t) - \frac{1}{G} \sum_{i \in \mathcal{G}} g_i^t \right\|^2 \\
&\quad + 2\mathbb{E} \left\langle g_i^t - \frac{1}{G} \sum_{i \in \mathcal{G}} \nabla f_i(x_i^t), \frac{1}{G} \sum_{i \in \mathcal{G}} \nabla f_i(x_i^t) - \frac{1}{G} \sum_{i \in \mathcal{G}} g_i^t \right\rangle \\
&\stackrel{(ii)}{=} \mathbb{E} \|g_i^t - \nabla f_i(x_i^t)\|^2 + \left\| \nabla f_i(x_i^t) - \frac{1}{G} \sum_{i \in \mathcal{G}} \nabla f_i(x_i^t) \right\|^2 \\
&\quad + \mathbb{E} \left\| \frac{1}{G} \sum_{i \in \mathcal{G}} \nabla f_i(x_i^t) - \frac{1}{G} \sum_{i \in \mathcal{G}} g_i^t \right\|^2 \\
&\quad + 2\mathbb{E} \left\langle g_i^t - \frac{1}{G} \sum_{i \in \mathcal{G}} \nabla f_i(x_i^t), \frac{1}{G} \sum_{i \in \mathcal{G}} \nabla f_i(x_i^t) - \frac{1}{G} \sum_{i \in \mathcal{G}} g_i^t \right\rangle,
\end{aligned}$$

where (i) was made (Norm), applied to the first norm and (ii) by taking expectation of the first scalar product and obtaining it

equal to zero. Next, averaging over $i \in \mathcal{G}$ and transforming the scalar product,

$$\begin{aligned}
& \frac{1}{G} \sum_{i \in \mathcal{G}} \mathbb{E} \left\| g_i^t - \frac{1}{G} \sum_{i \in \mathcal{G}} g_i^t \right\|^2 \\
&= \frac{1}{G} \sum_{i \in \mathcal{G}} \mathbb{E} \|g_i^t - \nabla f_i(x_i^t)\|^2 + \frac{1}{G} \sum_{i \in \mathcal{G}} \left\| \nabla f_i(x_i^t) - \frac{1}{G} \sum_{i \in \mathcal{G}} \nabla f_i(x_i^t) \right\|^2 \\
&\quad + \mathbb{E} \left\| \frac{1}{G} \sum_{i \in \mathcal{G}} \nabla f_i(x_i^t) - \frac{1}{G} \sum_{i \in \mathcal{G}} g_i^t \right\|^2 - 2 \mathbb{E} \left\| \frac{1}{G} \sum_{i \in \mathcal{G}} \nabla f_i(x_i^t) - \frac{1}{G} \sum_{i \in \mathcal{G}} g_i^t \right\|^2 \\
&\leq \frac{1}{G} \sum_{i \in \mathcal{G}} \mathbb{E} \|g_i^t - \nabla f_i(x_i^t)\|^2 + \frac{1}{G} \sum_{i \in \mathcal{G}} \left\| \nabla f_i(x_i^t) - \frac{1}{G} \sum_{i \in \mathcal{G}} \nabla f_i(x_i^t) \right\|^2 \\
&\stackrel{(i)}{\leq} \frac{1}{G} \sum_{i \in \mathcal{G}} \left\| \nabla f_i(x_i^t) - \frac{1}{G} \sum_{i \in \mathcal{G}} \nabla f_i(x_i^t) \right\|^2 + \sigma^2, \tag{8}
\end{aligned}$$

where (i) was made according to Assumption 3.3. To estimate the norm, we again use (Norm):

$$\begin{aligned}
& \frac{1}{G} \sum_{i \in \mathcal{G}} \left\| \nabla f_i(x_i^t) - \frac{1}{G} \sum_{i \in \mathcal{G}} \nabla f_i(x_i^t) \right\|^2 \\
&= \frac{1}{G} \sum_{i \in \mathcal{G}} \left\| \nabla f_i(x_i^t) - \nabla f(\bar{x}^t) \right\|^2 + \frac{1}{G} \sum_{i \in \mathcal{G}} \left\| \nabla f(\bar{x}^t) - \frac{1}{G} \sum_{i \in \mathcal{G}} \nabla f_i(x_i^t) \right\|^2 \\
&\quad + \frac{2}{G} \sum_{i \in \mathcal{G}} \left\langle \nabla f_i(x_i^t) - \nabla f(\bar{x}^t), \nabla f(\bar{x}^t) - \frac{1}{G} \sum_{i \in \mathcal{G}} \nabla f_i(x_i^t) \right\rangle \\
&= \frac{1}{G} \sum_{i \in \mathcal{G}} \left\| \nabla f_i(x_i^t) - \nabla f(\bar{x}^t) \right\|^2 + \frac{1}{G} \sum_{i \in \mathcal{G}} \left\| \nabla f(\bar{x}^t) - \frac{1}{G} \sum_{i \in \mathcal{G}} \nabla f_i(x_i^t) \right\|^2 \\
&\quad - \frac{2}{G} \sum_{i \in \mathcal{G}} \left\| \nabla f(\bar{x}^t) - \frac{1}{G} \sum_{i \in \mathcal{G}} \nabla f_i(x_i^t) \right\|^2 \\
&\leq \frac{1}{G} \sum_{i \in \mathcal{G}} \left\| \nabla f_i(x_i^t) - \nabla f(\bar{x}^t) \right\|^2 \\
&\stackrel{\text{(CS)}}{\leq} \frac{2}{G} \sum_{i \in \mathcal{G}} \left\| \nabla f_i(x_i^t) - \nabla f_i(\bar{x}^t) \right\|^2 + \frac{2}{G} \sum_{i \in \mathcal{G}} \left\| \nabla f_i(\bar{x}^t) - \nabla f(\bar{x}^t) \right\|^2 \\
&\stackrel{(i)}{\leq} \frac{2}{G} \sum_{i \in \mathcal{G}} \left\| \nabla f_i(x_i^t) - \nabla f_i(\bar{x}^t) \right\|^2 + 2(\delta_1 + \delta_2 \|\nabla f(\bar{x}^t)\|^2) \\
&\stackrel{\text{(Lip)}}{\leq} \frac{2}{G} \sum_{i \in \mathcal{G}} (2L (f_i(\bar{x}^t) - f_i(x_i^t)) - \langle \nabla f_i(x_i^t), \bar{x}^t - x_i^t \rangle) \\
&\quad + 2(\delta_1 + \delta_2 \|\nabla f(\bar{x}^t)\|^2),
\end{aligned}$$

where (i) was made according to Assumption 3.4. Combining it with (7) and (8),

$$\begin{aligned}
\mathbb{E} V^{t+1} &\leq \mathbb{E} V^t - \frac{2\gamma}{G} \sum_{i \in \mathcal{G}} \langle x_i^t - \bar{x}^t, \nabla f_i(x_i^t) \rangle + \frac{4L\gamma^2}{G} \sum_{i \in \mathcal{G}} \langle x_i^t - \bar{x}^t, \nabla f_i(x_i^t) \rangle \\
&\quad + \frac{4L\gamma^2}{G} \sum_{i \in \mathcal{G}} (f_i(\bar{x}^t) - f_i(x_i^t)) + 2\gamma^2(\delta_1 + \delta_2 \|\nabla f(\bar{x}^t)\|^2) + \gamma^2 \sigma^2 \\
&= \mathbb{E} V^t - \frac{2\gamma(1 - 2L\gamma)}{G} \sum_{i \in \mathcal{G}} \langle x_i^t - \bar{x}^t, \nabla f_i(x_i^t) \rangle + \frac{4L\gamma^2}{G} \sum_{i \in \mathcal{G}} (f_i(\bar{x}^t) - f_i(x_i^t))
\end{aligned}$$

$$+2\gamma^2(\delta_1 + \delta_2 \|\nabla f(\bar{x}^t)\|^2) + \gamma^2 \sigma^2.$$

Taking $\gamma \leq \frac{1}{4L}$ and applying (Conv) to scalar product,

$$\begin{aligned}
\mathbb{E}V^{t+1} &\leq \mathbb{E}V^t + \frac{\gamma}{G} \sum_{i \in \mathcal{G}} (f_i(\bar{x}^t) - f_i(x_i^t)) + \frac{4L\gamma^2}{G} \sum_{i \in \mathcal{G}} (f_i(\bar{x}^t) - f_i(x_i^t)) \\
&\quad + 2\gamma^2(\delta_1 + \delta_2 \|\nabla f(\bar{x}^t)\|^2) + \gamma^2 \sigma^2 \\
&= \mathbb{E}V^t + \frac{\gamma(1+4L\gamma)}{G} \sum_{i \in \mathcal{G}} (f_i(\bar{x}^t) - f_i(x_i^t)) + 2\gamma^2(\delta_1 + \delta_2 \|\nabla f(\bar{x}^t)\|^2) + \gamma^2 \sigma^2 \\
&\stackrel{(\text{Lip})}{\leq} \mathbb{E}V^t + \frac{\gamma(1+4L\gamma)}{G} \sum_{i \in \mathcal{G}} \left(\langle \nabla f_i(x_i^t), \bar{x}^t - x_i^t \rangle + \frac{L}{2} \|\bar{x}^t - x_i^t\|^2 \right) \\
&\quad + 2\gamma^2(\delta_1 + \delta_2 \|\nabla f(\bar{x}^t)\|^2) + \gamma^2 \sigma^2 \\
&= \mathbb{E}V^t + \frac{\gamma(1+4L\gamma)}{G} \sum_{i \in \mathcal{G}} \left(\underbrace{\langle \nabla f_i(x_i^t) - \nabla f_i(\bar{x}^t), \bar{x}^t - x_i^t \rangle}_{\leq 0 \text{ (Conv)}} + \langle \nabla f_i(\bar{x}^t), \bar{x}^t - x_i^t \rangle \right. \\
&\quad \left. + \frac{L}{2} \|\bar{x}^t - x_i^t\|^2 \right) + 2\gamma^2(\delta_1 + \delta_2 \|\nabla f(\bar{x}^t)\|^2) + \gamma^2 \sigma^2 \\
&\leq \mathbb{E}V^t + \frac{\gamma(1+4L\gamma)}{G} \sum_{i \in \mathcal{G}} (\langle \nabla f_i(\bar{x}^t) - \nabla f(\bar{x}^t), \bar{x}^t - x_i^t \rangle + \langle \nabla f(\bar{x}^t), \bar{x}^t - x_i^t \rangle \\
&\quad + \frac{L}{2} \|\bar{x}^t - x_i^t\|^2) + 2\gamma^2(\delta_1 + \delta_2 \|\nabla f(\bar{x}^t)\|^2) + \gamma^2 \sigma^2 \\
&\stackrel{(i)}{\leq} \mathbb{E}V^t + \frac{\gamma(1+4L\gamma)}{G} \sum_{i \in \mathcal{G}} \left(\frac{1}{2L} \|\nabla f_i(\bar{x}^t) - \nabla f(\bar{x}^t)\|^2 + L \|\bar{x}^t - x_i^t\|^2 \right. \\
&\quad \left. + \frac{L}{2} \|\bar{x}^t - x_i^t\|^2 + f(\bar{x}^t) - f(x_i^t) \right) + 2\gamma^2(\delta_1 + \delta_2 \|\nabla f(\bar{x}^t)\|^2) + \gamma^2 \sigma^2, \tag{9}
\end{aligned}$$

where (i) was made with applying (Young) to the first scalar product and applying (Lip) to second one. Using (Jen) we derive $\frac{1}{G} \sum_{i \in \mathcal{G}} (f(\bar{x}^t) - f(x_i^t)) = \frac{1}{G} \sum_{i \in \mathcal{G}} \left(f\left(\frac{1}{G} \sum_{i \in \mathcal{G}} x_i^t\right) - f(x_i^t) \right) \leq \frac{1}{G} \sum_{i \in \mathcal{G}} \left(\frac{1}{G} \sum_{i \in \mathcal{G}} f(x_i^t) - f(x_i^t) \right) = 0$. In that way, we proceed (9) using this fact and taking expectation together with applying Assumption 3.4:

$$\begin{aligned}
\mathbb{E}V^{t+1} &\leq \mathbb{E}V^t + \frac{3L\gamma(1+4L\gamma)}{2} \mathbb{E}V^t + \frac{\gamma(1+4L\gamma)}{2L} \delta_2 \mathbb{E} \|\nabla f(\bar{x}^t)\|^2 + \frac{\gamma(1+4L\gamma)}{2L} \delta_1 \\
&\quad + 2\gamma^2 \left(\delta_1 + \delta_2 \mathbb{E} \|\nabla f(\bar{x}^t)\|^2 \right) + \gamma^2 \sigma^2
\end{aligned}$$

Going into recursion up to the past aggregation round, which was on the iteration $t_{k,l}$ for some $k = \overline{0, \lceil T/l \rceil}$, together with using $\gamma \leq \frac{1}{4L}$ choice, we obtain

$$\begin{aligned}
\mathbb{E}V^t &\leq (1+3L\gamma) \mathbb{E}V^{t-1} + \delta_2 \gamma \left(2\gamma + \frac{1}{L} \right) \mathbb{E} \|\nabla f(\bar{x}^{t-1})\|^2 + \delta_1 \gamma \left(2\gamma + \frac{1}{L} \right) + \gamma^2 \sigma^2 \\
&\leq (1+3L\gamma)^{t-t_{k,l}} \mathbb{E}V^{t_{k,l}} + \delta_2 \gamma \left(2\gamma + \frac{1}{L} \right) \sum_{j=t_{k,l}}^{t-1} (1+3L\gamma)^{j-t_{k,l}} \mathbb{E} \|\nabla f(\bar{x}^j)\|^2 \\
&\quad + \left(\delta_1 \gamma \left(2\gamma + \frac{1}{L} \right) + \gamma^2 \sigma^2 \right) \sum_{j=t_{k,l}}^{t-1} (1+3L\gamma)^{j-t_{k,l}} \\
&\leq \delta_2 \gamma \left(2\gamma + \frac{1}{L} \right) (1+3L\gamma)^{l-1} \sum_{j=t_{k,l}}^{t-1} \mathbb{E} \|\nabla f(\bar{x}^j)\|^2 \\
&\quad + \left(\delta_1 \gamma \left(2\gamma + \frac{1}{L} \right) + \gamma^2 \sigma^2 \right) (l-1)(1+3L\gamma)^{l-1}.
\end{aligned}$$

Now we tune $\gamma \leq \frac{1}{4(l-1)L}$. Note it is smallest of all previous γ , since $l \geq 2$ and consequently all previous transitions hold true. In that way, using $(1 + 3L\gamma)^{l-1} \leq \left(1 + \frac{3}{4(l-1)}\right)^{l-1} \leq \left(1 + \frac{1}{l-1}\right)^{l-1} \leq 3$,

$$\begin{aligned} \mathbb{E}V^t &\leq 3\delta_2\gamma \left(\frac{1}{2(l-1)L} + \frac{1}{L}\right) \sum_{j=t_{k,l}}^{t-1} \mathbb{E} \|\nabla f(\bar{x}^j)\|^2 \\ &\quad + 3 \left(\delta_1\gamma \left(\frac{1}{2(l-1)L} + \frac{1}{L}\right) + \gamma^2\sigma^2\right) (l-1) \\ &\leq \frac{9\delta_2\gamma}{2L} \sum_{j=t_{k,l}}^{t-1} \mathbb{E} \|\nabla f(\bar{x}^j)\|^2 + \frac{9\delta_1\gamma}{2L} (l-1) + 3\gamma^2\sigma^2(l-1). \end{aligned}$$

This proves the second statement and ends the proof of the lemma. \square

Now we move to descent lemma in the local setup.

Lemma G.2. *Under Assumptions 3.1, 3.2(c), 3.3, 3.4, 3.5, at each iteration t of Algorithm 7, the following estimation is valid:*

$$\begin{aligned} \mathbb{E}\hat{f}(\bar{x}^{t+1}) &\leq \mathbb{E}\hat{f}(\bar{x}^t) - \frac{\gamma}{2} ((1 - 4\delta_2) - 3L\gamma(1 + 2\delta_2)) \mathbb{E} \|\nabla f(\bar{x}^t)\|^2 \\ &\quad + L^2\gamma(1 + 3L\gamma) \frac{1}{G} \sum_{i \in \mathcal{G}} \mathbb{E} \|x_i^t - \bar{x}^t\|^2 + \frac{3L\gamma^2}{2G} \sigma^2 + \gamma(2 + 3L\gamma)\delta_1 + \gamma\zeta(N). \end{aligned}$$

Proof. To begin with, we consider iterations, when Algorithm 7 performs aggregations, i.e. $t = t_{k,l}$ for some $k = \overline{0, \lceil T/l \rceil}$. The update formula for such iterations is given by

$$x^{t+1} = x_i^{t+1} = \sum_{i=1}^n \left(\arg \min_{\omega \in \Delta_1^n} \hat{f} \left[\sum_{i=1}^n \omega_i (x_i^t - \gamma g_i^t) \right] \right) (x_i^t - \gamma g_i^t),$$

which leads to an upper bound on $\hat{f}(x^{t+1})$:

$$\hat{f}(x^{t+1}) \leq \min_{\omega \in \Delta_1^n} \hat{f} \left[\sum_{i=1}^n \omega_i (x_i^t - \gamma g_i^t) \right].$$

Using this estimate and additional notation $\bar{x}^t = \frac{1}{G} \sum_{i \in \mathcal{G}} x_i^t$ we proceed to the average per honest devices during this local round point estimate:

$$\begin{aligned} \hat{f}(\bar{x}^{t+1}) &= \hat{f}(x^{t+1}) \leq \min_{\omega \in \Delta_1^n} \hat{f} \left[\sum_{i=1}^n \omega_i (x_i^t - \gamma g_i^t) \right] \\ &\leq \hat{f} \left[\frac{1}{G} \sum_{i \in \mathcal{G}} x_i^t - \frac{\gamma}{G} \sum_{i \in \mathcal{G}} g_i^t \right] \\ &\stackrel{(\text{Lip})}{\leq} \hat{f}(\bar{x}^t) - \left\langle \nabla \hat{f}(\bar{x}^t), \frac{\gamma}{G} \sum_{i \in \mathcal{G}} g_i^t \right\rangle + \frac{L\gamma^2}{2} \left\| \frac{1}{G} \sum_{i \in \mathcal{G}} g_i^t \right\|^2. \end{aligned} \tag{10}$$

Taking expectation, we obtain

$$\begin{aligned} \mathbb{E}\hat{f}(\bar{x}^{t+1}) &\leq \mathbb{E}\hat{f}(\bar{x}^t) - \left\langle \nabla \hat{f}(\bar{x}^t), \frac{\gamma}{G} \sum_{i \in \mathcal{G}} \nabla f_i(x_i^t) \right\rangle + \frac{L\gamma^2}{2} \mathbb{E} \left\| \frac{1}{G} \sum_{i \in \mathcal{G}} g_i^t \right\|^2 \\ &= \mathbb{E}\hat{f}(\bar{x}^t) - \left\langle \nabla \hat{f}(\bar{x}^t), \frac{\gamma}{G} \sum_{i \in \mathcal{G}} \nabla f_i(x_i^t) \right\rangle \\ &\quad - \left\langle \nabla f(\bar{x}^t) - \nabla \hat{f}(\bar{x}^t), \frac{\gamma}{G} \sum_{i \in \mathcal{G}} \nabla f_i(x_i^t) \right\rangle + \frac{L\gamma^2}{2} \mathbb{E} \left\| \frac{1}{G} \sum_{i \in \mathcal{G}} g_i^t \right\|^2 \end{aligned}$$

$$\begin{aligned}
& \stackrel{(\text{Norm}), (\text{Young})}{\leq} \mathbb{E} \hat{f}(\bar{x}^t) - \frac{\gamma}{2} \|\nabla f(\bar{x}^t)\|^2 - \frac{\gamma}{2} \left\| \frac{1}{G} \sum_{i \in \mathcal{G}} \nabla f_i(x_i^t) \right\|^2 \\
& \quad + \frac{\gamma}{2} \left\| \nabla f(\bar{x}^t) - \frac{1}{G} \sum_{i \in \mathcal{G}} \nabla f_i(x_i^t) \right\|^2 + \frac{\gamma}{2} \left\| \frac{1}{G} \sum_{i \in \mathcal{G}} \nabla f_i(x_i^t) \right\|^2 \\
& \quad + \frac{\gamma}{2} \left\| \nabla \hat{f}(\bar{x}^t) - \nabla f(\bar{x}^t) \right\|^2 + \frac{L\gamma^2}{2} \mathbb{E} \left\| \frac{1}{G} \sum_{i \in \mathcal{G}} g_i^t \right\|^2 \\
& \stackrel{(\text{CS})}{\leq} \mathbb{E} \hat{f}(\bar{x}^t) - \frac{\gamma}{2} \|\nabla f(\bar{x}^t)\|^2 + \frac{\gamma}{2} \left\| \nabla f(\bar{x}^t) - \frac{1}{G} \sum_{i \in \mathcal{G}} \nabla f_i(x_i^t) \right\|^2 \\
& \quad + \gamma \left\| \nabla \hat{f}(\bar{x}^t) - \nabla f_1(\bar{x}^t) \right\|^2 + \gamma \left\| \nabla f_1(\bar{x}^t) - \nabla f(\bar{x}^t) \right\|^2 \\
& \quad + \frac{L\gamma^2}{2} \mathbb{E} \left\| \frac{1}{G} \sum_{i \in \mathcal{G}} g_i^t \right\|^2 \\
& \stackrel{(\text{Lemma } C.1)}{\leq} \mathbb{E} \hat{f}(\bar{x}^t) - \frac{\gamma}{2} \|\nabla f(\bar{x}^t)\|^2 + \frac{\gamma}{2} \left\| \nabla f(\bar{x}^t) - \frac{1}{G} \sum_{i \in \mathcal{G}} \nabla f_i(x_i^t) \right\|^2 \\
& \quad + \gamma \left\| \nabla f_1(\bar{x}^t) - \nabla f(\bar{x}^t) \right\|^2 + \frac{L\gamma^2}{2} \mathbb{E} \left\| \frac{1}{G} \sum_{i \in \mathcal{G}} g_i^t \right\|^2 + \gamma \zeta(N) \\
& \stackrel{(\text{CS})}{\leq} \mathbb{E} \hat{f}(\bar{x}^t) - \frac{\gamma}{2} \|\nabla f(\bar{x}^t)\|^2 + \frac{\gamma}{2} \left\| \nabla f(\bar{x}^t) - \frac{1}{G} \sum_{i \in \mathcal{G}} \nabla f_i(x_i^t) \right\|^2 \\
& \quad + \gamma \left\| \nabla f_1(\bar{x}^t) - \nabla f(\bar{x}^t) \right\|^2 + \frac{3L\gamma^2}{2} \mathbb{E} \left\| \frac{1}{G} \sum_{i \in \mathcal{G}} g_i^t - \frac{1}{G} \sum_{i \in \mathcal{G}} \nabla f_i(x_i^t) \right\|^2 \\
& \quad + \frac{3L\gamma^2}{2} \mathbb{E} \left\| \frac{1}{G} \sum_{i \in \mathcal{G}} \nabla f_i(x_i^t) - \nabla f(\bar{x}^t) \right\|^2 + \frac{3L\gamma^2}{2} \mathbb{E} \|\nabla f(\bar{x}^t)\|^2 + \gamma \zeta(N).
\end{aligned}$$

Now we use Assumption 3.3 with the fact that $\mathbb{E} g_i^t = \nabla f_i(x^t)$ and $\mathbb{E} \langle \nabla f_i(x^t) - g_i^t, \nabla f_j(x^t) - g_j^t \rangle = 0$ to bound $\mathbb{E} \left\| \frac{1}{G} \sum_{i \in \mathcal{G}} (g_i^t - \nabla f_i(x_i^t)) \right\|^2 \leq \frac{\sigma^2}{G}$. Taking expectation again, we move to

$$\begin{aligned}
\mathbb{E} \hat{f}(\bar{x}^{t+1}) & \leq \mathbb{E} \hat{f}(\bar{x}^t) - \frac{\gamma}{2} (1 - 3L\gamma) \mathbb{E} \|\nabla f(\bar{x}^t)\|^2 \\
& \quad + \frac{\gamma}{2} (1 + 3L\gamma) \mathbb{E} \left\| \frac{1}{G} \sum_{i \in \mathcal{G}} \nabla f_i(x_i^t) - \nabla f(\bar{x}^t) \right\|^2 \\
& \quad + \gamma \mathbb{E} \left\| \nabla f_1(\bar{x}^t) - \nabla f(\bar{x}^t) \right\|^2 + \frac{3L\gamma^2}{2G} \sigma^2 + \gamma \zeta(N) \\
& \stackrel{(\text{CS})}{\leq} \mathbb{E} \hat{f}(\bar{x}^t) - \frac{\gamma}{2} (1 - 3L\gamma) \mathbb{E} \|\nabla f(\bar{x}^t)\|^2 \\
& \quad + \gamma (1 + 3L\gamma) \mathbb{E} \left\| \frac{1}{G} \sum_{i \in \mathcal{G}} \nabla f_i(x_i^t) - \frac{1}{G} \sum_{i \in \mathcal{G}} \nabla f_i(\bar{x}^t) \right\|^2 \\
& \quad + \gamma (1 + 3L\gamma) \mathbb{E} \left\| \frac{1}{G} \sum_{i \in \mathcal{G}} \nabla f_i(\bar{x}^t) - \nabla f(\bar{x}^t) \right\|^2 + \gamma \mathbb{E} \left\| \nabla f_1(\bar{x}^t) - \nabla f(\bar{x}^t) \right\|^2 \\
& \quad + \frac{3L\gamma^2}{2G} \sigma^2 + \gamma \zeta(N)
\end{aligned}$$

$$\begin{aligned}
&\stackrel{(\text{CS})}{\leq} \mathbb{E} \hat{f}(\bar{x}^t) - \frac{\gamma}{2} (1 - 3L\gamma) \mathbb{E} \|\nabla f(\bar{x}^t)\|^2 \\
&\quad + \frac{\gamma(1 + 3L\gamma)}{G} \sum_{i \in \mathcal{G}} \mathbb{E} \|\nabla f_i(x_i^t) - \nabla f_i(\bar{x}^t)\|^2 \\
&\quad + \frac{\gamma(1 + 3L\gamma)}{G} \sum_{i \in \mathcal{G}} \mathbb{E} \|\nabla f_i(\bar{x}^t) - \nabla f(\bar{x}^t)\|^2 + \gamma \mathbb{E} \|\nabla f_1(\bar{x}^t) - \nabla f(\bar{x}^t)\|^2 \\
&\quad + \frac{3L\gamma^2}{2G} \sigma^2 + \gamma \zeta(N).
\end{aligned}$$

Using Assumption 3.4 to bound $\|\nabla f_i(\bar{x}^t) - \nabla f(\bar{x}^t)\|^2 \leq \delta_1 + \delta_2 \|\nabla f(\bar{x}^t)\|^2$ for all $i \in \mathcal{G}$ we get

$$\begin{aligned}
\mathbb{E} \hat{f}(\bar{x}^{t+1}) &\leq \mathbb{E} \hat{f}(\bar{x}^t) - \frac{\gamma}{2} ((1 - 4\delta_2) - 3L\gamma(1 + 2\delta_2)) \mathbb{E} \|\nabla f(\bar{x}^t)\|^2 \\
&\quad + \frac{\gamma(1 + 3L\gamma)}{G} \sum_{i \in \mathcal{G}} \mathbb{E} \|\nabla f_i(x_i^t) - \nabla f_i(\bar{x}^t)\|^2 + \frac{3L\gamma^2}{2G} \sigma^2 \\
&\quad + \gamma(2 + 3L\gamma)\delta_1 + \gamma \zeta(N) \\
&\stackrel{(\text{Lip})}{\leq} \mathbb{E} \hat{f}(\bar{x}^t) - \frac{\gamma}{2} ((1 - 4\delta_2) - 3L\gamma(1 + 2\delta_2)) \mathbb{E} \|\nabla f(\bar{x}^t)\|^2 \\
&\quad + L^2\gamma(1 + 3L\gamma) \frac{1}{G} \sum_{i \in \mathcal{G}} \mathbb{E} \|x_i^t - \bar{x}^t\|^2 \\
&\quad + \frac{3L\gamma^2}{2G} \sigma^2 + \gamma(2 + 3L\gamma)\delta_1 + \gamma \zeta(N).
\end{aligned} \tag{11}$$

Now we want to give the estimate for iterations $t \neq t_{k,l}$. The update rule combined with (Lip) gives

$$\hat{f}(\bar{x}^{t+1}) = \hat{f} \left[\frac{1}{G} \sum_{i=1}^n x_i^t - \frac{\gamma}{G} \sum_{i=1}^n g_i^t \right] \leq \hat{f} \left[\frac{1}{G} \sum_{i=1}^n x_i^t - \frac{\gamma}{G} \sum_{i=1}^n g_i^t \right].$$

Mention, this estimate is coincide with the (10). Thus, proceeding analogically to the $t = t_{k,l}$ case, we obtain (11). In that way, (11) delivers the result of the lemma. \square

Now we pass to the main theorem of this section.

Theorem G.3. *Under Assumptions 3.1, 3.2(b), 3.3, 3.4 with $\delta_2 \leq \frac{1}{8}$, 3.5, for solving the problem (1), for Algorithm 7 with $\gamma \leq \frac{1}{25(l-1)L}$, the following holds:*

$$\begin{aligned}
\frac{1}{T} \sum_{t=0}^{T-1} \mathbb{E} \|\nabla f(\bar{x}^t)\|^2 &\leq \frac{5\mathbb{E} [\hat{f}(x^0) - \hat{f}(\hat{x}^*)]}{\gamma T} + 20L^2\gamma^2(l-1)\sigma^2 + \frac{8L\gamma}{G} \sigma^2 \\
&\quad + 13\delta_1 + 30L\gamma(l-1)\delta_1 + 5\zeta(N).
\end{aligned}$$

Proof. To begin with, we combine the result of Lemma G.2 with result of Lemma G.1 to obtain

$$\begin{aligned}
\mathbb{E} \hat{f}(\bar{x}^{t+1}) &\leq \mathbb{E} \hat{f}(\bar{x}^t) - \frac{\gamma}{2} ((1 - 4\delta_2) - 3L\gamma(1 + 2\delta_2)) \mathbb{E} \|\nabla f(\bar{x}^t)\|^2 \\
&\quad + \frac{9\delta_2 L\gamma^2(1 + 3L\gamma)}{2} \sum_{j=t_{k,l}}^{t-1} \mathbb{E} \|\nabla f(\bar{x}^j)\|^2 + \frac{9\delta_1 L\gamma^2(1 + 3L\gamma)(l-1)}{2} \\
&\quad + 3L^2\gamma^3(1 + 3L\gamma)\sigma^2(l-1) + \frac{3L\gamma^2}{2G} \sigma^2 \\
&\quad + \gamma(2 + 3L\gamma)\delta_1 + \gamma \zeta(N).
\end{aligned}$$

Summing over all iterations and using $\sum_{t=0}^{T-1} \sum_{j=t_{k,l}}^{t-1} \mathbb{E} \|\nabla f(\bar{x}^j)\|^2 \leq (l-1) \sum_{t=0}^{T-1} \mathbb{E} \|\nabla f(\bar{x}^t)\|^2$,

$$E \left[\hat{f}(x^T) - \hat{f}(x^0) \right]$$

$$\begin{aligned}
&\leq -\frac{\gamma}{2} ((1 - 4\delta_2) - 3L\gamma(1 + 2\delta_2)) \sum_{t=0}^{T-1} \mathbb{E} \|\nabla f(\bar{x}^t)\|^2 \\
&\quad + \frac{9\delta_2 L\gamma^2(1 + 3L\gamma)(l-1)}{2} \sum_{t=0}^{T-1} \mathbb{E} \|\nabla f(\bar{x}^t)\|^2 + \frac{9\delta_1 L\gamma^2(1 + 3L\gamma)(l-1)T}{2} \\
&\quad + 3L^2\gamma^3(1 + 3L\gamma)\sigma^2(l-1)T + \frac{3L\gamma^2 T}{2G}\sigma^2 + \gamma(2 + 3L\gamma)\delta_1 T + \gamma\zeta(N)T \\
&= -\frac{\gamma}{2} (1 - 4\delta_2 - 3L\gamma(1 + 2\delta_2) - 9L\gamma\delta_2(1 + 3L\gamma)(l-1)) \sum_{t=0}^{T-1} \mathbb{E} \|\nabla f(\bar{x}^t)\|^2 \\
&\quad + 3L^2\gamma^3(1 + 3L\gamma)\sigma^2(l-1)T + \frac{3L\gamma^2 T}{2G}\sigma^2 + \frac{9\delta_1 L\gamma^2(1 + 3L\gamma)(l-1)T}{2} \\
&\quad + \gamma(2 + 3L\gamma)\delta_1 T + \gamma\zeta(N)T.
\end{aligned}$$

Now we want to estimate the coefficient before the $\sum_{t=0}^{T-1} \mathbb{E} \|\nabla f(\bar{x}^t)\|^2$ term. Let us take $\delta_2 \leq \frac{1}{8}$ and $\gamma \leq \frac{1}{25(l-1)L}$ (it is the smallest γ from all we choose before, thus, all previous transitions holds true). Thus,

$$\begin{aligned}
1 - 4\delta_2 - 3L\gamma(1 + 2\delta_2) - 9L\gamma\delta_2(1 + 3L\gamma)(l-1) &\geq \frac{1}{2} - \frac{15}{4}L\gamma \\
&\quad - \frac{9}{8}L\gamma \left(1 + \frac{3}{25(l-1)}\right)(l-1) \\
&\stackrel{l \geq 2}{\geq} \frac{1}{2} - \frac{15}{4}L\gamma - \frac{63}{50}L\gamma(l-1) \\
&\geq \frac{1}{2} - \frac{3}{20} - \frac{63}{1250} \geq \frac{1}{5}
\end{aligned}$$

In that way,

$$\begin{aligned}
\frac{\gamma}{5} \sum_{t=0}^{T-1} \mathbb{E} \|\nabla f(\bar{x}^t)\|^2 &\leq \mathbb{E} [\hat{f}(x^0) - \hat{f}(\hat{x}^*)] + 4L^2\gamma^3(l-1)\sigma^2 T + \frac{3L\gamma^2 T}{2G}\sigma^2 \\
&\quad + \frac{5}{2}\gamma\delta_1 T + 6L\gamma^2\delta_1(l-1)T + \gamma\zeta(N), \\
\frac{1}{T} \sum_{t=0}^{T-1} \mathbb{E} \|\nabla f(\bar{x}^t)\|^2 &\leq \frac{5\mathbb{E} [\hat{f}(x^0) - \hat{f}(\hat{x}^*)]}{\gamma T} + 20L^2\gamma^2(l-1)\sigma^2 + \frac{8L\gamma}{G}\sigma^2 \\
&\quad + 13\delta_1 + 30L\gamma(l-1)\delta_1 + 5\zeta(N),
\end{aligned}$$

that ends the proof of the theorem. \square

Remark G.4. In this remark we want to explain why $\frac{1}{T} \sum_{t=0}^{T-1} \mathbb{E} \left\| \nabla f \left(\frac{1}{G} \sum_{i \in \mathcal{G}} x_i^t \right) \right\|^2$, that we choose as a criterion in Theorem G.3 is consistent. When we consider iterations, when Algorithm 7 performs aggregation, we assign weights of honest devices, i.e. devices, which send honest stochastic gradient g with $\mathbb{E}[g] = \nabla f(x)$ equal to $\frac{1}{G}$, and weights of other devices (who acts as Byzantine) is equal to 0. And this layout gives an estimate that is an upper bound of true ω realization (10). In other words, we say, that if algorithm at each aggregation round take average of points from devices, which all previous local round act like honest it would not be better than for convergence, than real iteration of the algorithm. In such a way, we are not interesting in the points of devices, who perform even one Byzantine-like iteration in the local round. Now it is clear why we have to weaken the assumption about at least one honest device at each iteration, not necessary the same: we request at least one honest device at each local round, not necessary the same in different rounds.

Corollary G.5. *Under the assumptions of Theorem G.3, for solving the problem (1), after T iterations of Algorithm 7 with*

$\gamma \leq \min \left\{ \frac{1}{25(l-1)L}, \frac{\sqrt{5\mathbb{E}[\hat{f}(x^0) - \hat{f}(\hat{x}^*)]G}}{\sigma\sqrt{9LT}} \right\}$, the following holds:

$$\frac{1}{T} \sum_{t=0}^{T-1} \mathbb{E} \|\nabla f(\bar{x}^t)\|^2 = \mathcal{O} \left(\frac{\mathbb{E} [\hat{f}(x^0) - \hat{f}(\hat{x}^*)] lL}{T} + \frac{\sigma \sqrt{\mathbb{E} [\hat{f}(x^0) - \hat{f}(\hat{x}^*)] L}}{\sqrt{TG}} + \delta_1 + \zeta(N) \right).$$

We note that we do not provide the version for the first of our algorithms, `Bant` in this and the following sections. The reason is that its examination completely replicates the implementation of the technique discussed in this section for the proofs presented in Section D. We consider it unnecessary to repeat this procedure; however, we are confident in the practical applicability of the technique to both of our methods: `Bant` and `AutoBant`.

H Partial participation

In the previous section, we discussed an important regime in distributed systems known as the local approach. Another widely used scenario in distributed learning is partial participation, which can be advantageous in various practical setups (Yang, Fang, and Liu 2021; Wang and Ji 2022; Li et al. 2022). In this section, we extend our `AutoBant` algorithm to support partial participation in federated learning. Below, we provide a formal description of the `AutoBant` with `PARTIAL PARTICIPATION` method (Algorithm 8).

Algorithm 8 `AutoBant` with `PARTIAL PARTICIPATION`

```

1: Input: Starting point  $x^0 \in \mathbb{R}^d$ 
2: Parameters: Stepsize  $\gamma > 0$ , error accuracy  $\delta$ 
3: for  $t = 0, 1, 2, \dots, T - 1$  do
4:   Define a set of active workers  $\mathcal{W}(t) = \mathcal{G}(t) \cup \mathcal{B}(t)$ ;  $n(t) = |\mathcal{W}(t)|$ 
5:   Server sends  $x^t$  to each worker from  $\mathcal{W}(t)$ 
6:   for all workers  $i \in \mathcal{W}(t)$  in parallel do
7:     Generate  $\xi_i^t$  independently
8:     Compute stochastic gradient  $g_i^t = g_i(x^t, \xi_i^t)$ 
9:     Send  $g_i^t$  to server
10:  end for
11:   $\omega^t \approx \arg \min_{\omega \in \Delta_1^{n(t)}} \hat{f} \left( x^t - \gamma \sum_{i \in \mathcal{W}(t)} \omega_i g_i^t \right)$ 
12:   $x^{t+1} = x^t - \gamma \sum_{i \in \mathcal{W}(t)} \omega_i^t g_i^t$ 
13: end for
14: Output:  $\frac{1}{T} \sum_{t=0}^{T-1} x^t$ 

```

The key change is that at each iteration we have a set $\mathcal{W}(t)$, which is a subset of the full list of accessible devices. In that way, we impose a stricter assumption compared to the regular training regime, namely, we require the presence of at least one honest device (including server) in each of the $\mathcal{W}(t)$ sets.

Now we present the main theorem of this section.

Theorem H.1. *Under Assumptions 3.1, 3.2(c), 3.3, 3.4 with $\delta_2 \leq 0.25$, 3.5, for solving the problem (1), after T iteration of Algorithm 2 in partial participation scenario with $\gamma \leq \frac{1}{15L}$, it implies*

$$\frac{1}{T} \sum_{t=0}^{T-1} \mathbb{E} \|\nabla f(x^t)\|^2 \leq \frac{4\mathbb{E} [\hat{f}(x^0) - \hat{f}(\hat{x}^*)]}{\gamma T} + 3\delta_1 + \frac{6L\gamma}{\tilde{G}} \sigma^2 + 4\zeta(N),$$

where $\tilde{G} = \min_{t \leq T} G(t)$.

Proof. The iterative update formula for x^{t+1} is given by

$$x^{t+1} = x^t - \gamma \sum_{i \in \mathcal{W}(t)} \left(\arg \min_{\omega \in \Delta_1^n} \hat{f} \left[x^t - \gamma \sum_{i \in \mathcal{W}(t)} \omega_i g_i^t \right] \right) g_i^t,$$

which leads to an upper bound on $\hat{f}(x^{t+1})$:

$$\begin{aligned}
\hat{f}(x^{t+1}) &= \min_{\omega \in \Delta_1^n} \hat{f} \left[x^t - \gamma \sum_{i \in \mathcal{W}(t)} \omega_i g_i^t \right] \\
&\leq \hat{f} \left[x^t - \frac{\gamma}{G(t)} \sum_{i \in \mathcal{G}(t)} g_i^t \right] \\
&\stackrel{(\text{Lip})}{\leq} \hat{f}(x^t) - \left\langle \nabla \hat{f}(x^t), \frac{\gamma}{G(t)} \sum_{i \in \mathcal{G}(t)} g_i^t \right\rangle + \frac{L\gamma^2}{2} \left\| \frac{1}{G(t)} \sum_{i \in \mathcal{G}(t)} g_i^t \right\|^2.
\end{aligned}$$

Taking the expectation,

$$\begin{aligned}
\mathbb{E}\hat{f}(x^{t+1}) &\leq \mathbb{E}\hat{f}(x^t) - \left\langle \nabla \hat{f}(x^t), \frac{\gamma}{G(t)} \sum_{i \in \mathcal{G}(t)} \nabla f_i(x^t) \right\rangle \\
&\quad + \frac{L\gamma^2}{2} \mathbb{E} \left\| \frac{1}{G(t)} \sum_{i \in \mathcal{G}(t)} g_i^t \right\|^2 \\
&\stackrel{(\text{Lemma C.2})}{\leq} \mathbb{E}\hat{f}(x^t) + \gamma\zeta(N) - \frac{\gamma}{2} \|\nabla f(x)\|^2 \\
&\quad + \frac{3\gamma}{2} (\delta_1 + \delta_2 \|\nabla f(x^t)\|^2) + \frac{L\gamma^2}{2} \mathbb{E} \left\| \frac{1}{G(t)} \sum_{i \in \mathcal{G}(t)} g_i^t \right\|^2 \\
&\stackrel{(\text{CS})}{\leq} \mathbb{E}\hat{f}(x^t) + \gamma\zeta(N) - \frac{\gamma}{2} \|\nabla f(x)\|^2 + \frac{3\gamma}{2} (\delta_1 + \delta_2 \|\nabla f(x^t)\|^2) \\
&\quad + \frac{3L\gamma^2}{2} \left\| \frac{1}{G(t)} \sum_{i \in \mathcal{G}(t)} (\nabla f(x^t) - \nabla f_i(x^t)) \right\|^2 \\
&\quad + \frac{3L\gamma^2}{2} \mathbb{E} \left\| \frac{1}{G(t)} \sum_{i \in \mathcal{G}(t)} (\nabla f_i(x^t) - g_i^t) \right\|^2 \\
&\quad + \frac{3L\gamma^2}{2} \left\| \frac{1}{G(t)} \sum_{i \in \mathcal{G}(t)} \nabla f(x^t) \right\|^2.
\end{aligned}$$

Due to the fact that $\mathbb{E}g_i^t = \nabla f_i(x^t)$ and $\mathbb{E}\langle \nabla f_i(x^t) - g_i^t, \nabla f_j(x^t) - g_j^t \rangle = 0$,

$$\begin{aligned}
\mathbb{E}\hat{f}(x^{t+1}) &\stackrel{(\text{CS})}{\leq} \mathbb{E}\hat{f}(x^t) + \gamma\zeta(N) - \frac{\gamma}{2} \|\nabla f(x)\|^2 + \frac{3\gamma}{2} (\delta_1 + \delta_2 \|\nabla f(x^t)\|^2) \\
&\quad + \frac{3L\gamma^2}{2} \left(\frac{1}{G(t)} \sum_{i \in \mathcal{G}(t)} \|\nabla f(x^t) - f_i(x^t)\|^2 \right. \\
&\quad \left. + \frac{1}{(G(t))^2} \sum_{i \in \mathcal{G}(t)} \mathbb{E} \|\nabla f_i(x^t) - g_i^t\|^2 \right) + \frac{3L\gamma^2}{2} \|\nabla f(x^t)\|^2 \\
&\stackrel{(\text{Ass. 3.3,3.4})}{\leq} \mathbb{E}\hat{f}(x^t) + \gamma\zeta(N) - \frac{\gamma}{2} \|\nabla f(x)\|^2 + \frac{3\gamma}{2} (\delta_1 + \delta_2 \|\nabla f(x^t)\|^2) \\
&\quad + \frac{3L\gamma^2}{2} \left(\delta_1 + \delta_2 \|\nabla f(x^t)\|^2 + \frac{\sigma^2}{G(t)} \right) + \frac{3L\gamma^2}{2} \|\nabla f(x^t)\|^2 \\
&= \mathbb{E}[\hat{f}(x^t)] - \frac{\gamma}{2} [1 - 3L\gamma - (3 + 3L\gamma)\delta_2] \|\nabla f(x^t)\|^2 \\
&\quad + \frac{2\gamma}{2} (1 + 3L\gamma)\delta_1 + \frac{3L\gamma^2}{2G(t)} \sigma^2 + \gamma\zeta(N).
\end{aligned}$$

We first fix $\delta_2 \leq \frac{1}{12}$. Finally, by choosing $\gamma \leq \frac{1}{13L} \leq \frac{1}{12L(1+\delta_2)}$, utilizing $G(t) \geq \min_{t \leq T} G(t) = \tilde{G}$ and summing over the iterations, we obtain the constraint in Theorem:

$$\frac{1}{T} \sum_{t=0}^{T-1} \mathbb{E} \|\nabla f(x^t)\|^2 \leq \frac{4\mathbb{E} [\hat{f}(x^0) - \hat{f}(\hat{x}^*)]}{\gamma T} + 3\delta_1 + \frac{6L\gamma}{\tilde{G}} \sigma^2 + 4\zeta(N).$$

□

Corollary H.2. Under the assumptions of Theorem H.1, for solving the problem (1), after T iterations with $\gamma \leq \min \left\{ \frac{1}{13L}, \frac{\sqrt{2\mathbb{E}[\hat{f}(x^0) - \hat{f}(\hat{x}^*)] \tilde{G}}}{\sigma\sqrt{3LT}} \right\}$, the following holds:

$$\frac{1}{T} \sum_{t=0}^{T-1} \mathbb{E} \|\nabla f(x^t)\|^2 = \mathcal{O} \left(\frac{\mathbb{E} [\hat{f}(x^0) - \hat{f}(\hat{x}^*)] L}{T} + \frac{\sigma \sqrt{\mathbb{E} [\hat{f}(x^0) - \hat{f}(\hat{x}^*)] L}}{\sqrt{T \tilde{G}}} + \delta_1 + \zeta(N) \right).$$

Remark H.3. We adopted our method to the scenario of partial participation. It is natural that it requires stronger assumption: we need at least one honest client from that taking participation at each iteration, but not always the same.

I SimBant

We also propose another method for dealing with Byzantine attacks - *SimBant*. Here we use the concept of the trial function in a different way: the key is that we look not at the loss function \hat{f} , as in Algorithms 1, 2, but at the output of the model m on the trial data \hat{D} . In particular, the calculation of trust scores w_i is now based on how the outputs of the model parameters obtained on the server (a guaranteed honest device, without losing generality, we can assume that it has index 1) and on the device are similar to each other. The server is validated in pairs with each device and the trust scores are calculated for each device relative to the prediction classes based on how similar they are between the server and the device. And only on the basis of the trust scores, we give a weights to devices' trained models and calculate the new state of the general model. Let us denote by g^t the model that the server sends to the devices at step t , $g_i^t, i \in \{2, \dots, n\}$ - devices' trained models, g_1^t the trained server model. Then the trust score for i -th device is function $\alpha_i \rightarrow \text{sim}(m(x^t - \gamma g_i^t, \hat{D}), m(x^t - \gamma g_1^t, \hat{D}))$, which measures the similarity of predictions of server and device models, where $x^t - \gamma g_i^t$ and $x^t - \gamma g_1^t$ are new parameters on the i -th device and the server, respectively, *sim* is responsible for the measure of the similarity of the outputs. We do not provide the theory for this method but validate it in practice (see Section 6).

Algorithm 9 *SimBant*

```

1: Input: Starting point  $x^0 \in \mathbb{R}^d$ 
2: Parameters: Step size  $\gamma > 0$ , error accuracy  $\delta$ 
3: for  $t = 0, 1, 2, \dots, T - 1$  do
4:   Server sends  $x^t$  to each worker
5:   for all workers  $i = 1, 2, \dots, n$  in parallel do
6:     Generate  $\xi_i^t$  independently
7:     Compute stochastic gradient  $g_i^t = g_i(x^t, \xi_i^t)$ 
8:     Send  $g_i^t$  to server
9:   end for
10:   $\omega_i^t = (1 - \beta)\omega_i^{t-1} + \beta \frac{\text{sim}(m(x^t - \gamma g_i^t, \hat{D}), m(x^t - \gamma g_1^t, \hat{D}))}{\sum_{j=1}^n \text{sim}(m(x^t - \gamma g_j^t, \hat{D}), m(x^t - \gamma g_1^t, \hat{D}))}$ 
11:   $x^{t+1} = x^t - \gamma \sum_{i=1}^n \omega_i^t g_i^t$ 
12: end for
13: Output:  $\frac{1}{T} \sum_{t=0}^{T-1} x^t$ 

```
